

2008

Recent Sedimentation Patterns and Facies Distribution on the Waipaoa River Shelf, N.Z

Lila Eve Rose

College of William and Mary - Virginia Institute of Marine Science

Follow this and additional works at: <https://scholarworks.wm.edu/etd>



Part of the [Geology Commons](#), [Geomorphology Commons](#), and the [Oceanography Commons](#)

Recommended Citation

Rose, Lila Eve, "Recent Sedimentation Patterns and Facies Distribution on the Waipaoa River Shelf, N.Z" (2008). *Dissertations, Theses, and Masters Projects*. Paper 1539617878.

<https://dx.doi.org/doi:10.25773/v5-f7v2-th07>

This Thesis is brought to you for free and open access by the Theses, Dissertations, & Master Projects at W&M ScholarWorks. It has been accepted for inclusion in Dissertations, Theses, and Masters Projects by an authorized administrator of W&M ScholarWorks. For more information, please contact scholarworks@wm.edu.

Recent Sedimentation Patterns and Facies Distribution on the Waipaoa River Shelf, N.Z.

A Thesis

Presented to

The Faculty of the School of Marine Science

The College of William and Mary in Virginia

In Partial Fulfillment

Of the Requirements for the Degree of

Master of Science

by

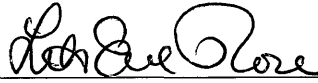
Lila Eve Rose

2008

APPROVAL SHEET


This thesis is submitted in partial fulfillment of
The requirements for the degree of

Master of Arts

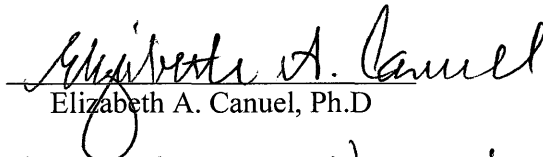


Lila Eve Rose

Approved, May 2008



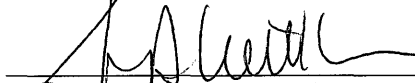
Steven A. Kuehl, Ph.D.
Committee Chairman/ Advisor



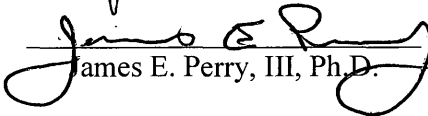
Elizabeth A. Canuel, Ph.D.



Courtney K. Harris, Ph.D.



John D. Milliman, Ph.D.



James E. Perry, III, Ph.D.

TABLE OF CONTENTS

	Page
ACKNOWLEDGMENTS.....	iv
LIST OF FIGURES.....	v
LIST OF TABLES.....	vi
ABSTRACT.....	vii
1.0 Introduction.....	2
1.1 Background.....	4
2.0 Methods.....	8
2.1 Sampling plan.....	8
2.2 X-radiography.....	9
2.3 Bulk Density.....	10
2.4 ⁷ Be.....	10
3.0 Results.....	12
3.1 Sedimentary Structures.....	12
3.2 Bulk Density.....	13
3.3 ⁷ Be.....	14
4.0 Discussion.....	16
4.1 Facies Descriptions.....	16
4.1.1 Interbedded/laminated muds and sands (ILMS) facies.....	16
4.1.2 Mixed layers and mottles (MLM) facies.....	17
4.1.3 Mottled mud (MM) facies.....	20
4.2 Facies distribution on the shelf.....	21
4.3 Facies comparison with other continental shelves.....	22
4.4 ⁷ Be activity and sediment dispersal.....	25
4.5 ⁷ Be inventory measurements.....	26
4.6 Sedimentation Patterns on the shelf.....	29
5.0 Conclusion.....	33
REFERENCES.....	34
APPENDIX A: Box and Kasten Core Information.....	69
APPENDIX B: Box core X-radiographs, Facies Classifications and Bulk Density Measurements.....	73
APPENDIX C: Box Core ⁷ Be Data.....	94
VITA.....	100

ACKNOWLEDGEMENTS

I'd like to thank, first and foremost, my advisor, Dr. Steven Kuehl, who has been the most positive guide, both academically and spiritually. His thoughtful questions, attention to detail and tirelessly inquisitive nature have made him a great role model and an inspiration. I have been very fortunate to travel the globe several times with him, catch a ride on his bike and learn about important food groups, like flat whites, dark chocolate and sushi. Steve puts the ohm into VIMS. Thanks to my committee members, Drs. Liz Canuel, Courtney Harris, John Milliman, and Jim Perry for their time, support, great advice and questions.

This work would not have been possible without funding from the NSF Margins S2S program and the countless individuals and colleagues involved therein. A big thanks to the crew of the *R/V Kilo Moana*. Thanks for the help and support of the Radiosotope Geochronology lab, especially Linda Meneghini. Thanks are also extended to the wonderful VIMS Physical Sciences staff, especially Cindy Hornsby, Beth Marshall and Cynthia Harris, who have provided invaluable administrative support and advice.

My interest in science can only be attributed to two people: my parents. They've instilled in me a love of the natural world and have provided unflagging support and encouragement. No one has my back like my fantastic sister, Katie. The love of my family is unparalleled.

I would be remiss without mentioning the influence of both Sylvia Stein and Dr. H. Allen Curran in the development of my interest in science. They each had a most unique and stimulating way of teaching and insisted, although quite the experts in their respective fields, that they were always students of science.

And of course, none of this would be possible without the love, quick wits, advice and random trips with my dearest girl friends, Heidi "One Word: Murchison" Wadman, Megan "Partner-in-Crime" Ridley-Lane and Lisa "Lord Have Mercy" Mijzlik.

Life is far richer with Pat "That's-How-I-Roll" Dickhudt's scientific and emotional support, and the friendship of the other man-ranch dudes, J.Paul "Masa Master" Reinheimer and Andrew "Tunes" Wozniak, as well as my rad bad friends, Lynn "Fan of the Bassist" Killberg-Thoreson, Jennifer "Mrs. Awesomest" Larkum and Emily "Mrs. Greenwood" Yam.

Thanks to a host of other great friends, including Lindsey Kraatz, Karen Gardner, Annie Miller, Andrij Horodysky, Cielomar Rodriguez-Calderon, Ginny Lascara and Bob Middleton, Mitch Birdsong, Jake Boyd, Jennifer Miselis, and Dan Dutton.

Finally, a multitude of (mostly furry) four-legged comrades have also enriched life as a grad student – Izzy, the most marvelous mutt, Action Jackson, Matilda, Barli and Hildie, Tima, Perrin, Blackbeard, Jiatze, Othello, White Kitty, and Frolly.

LIST OF FIGURES

1. New Zealand and Waipaoa River Location Map.....	38
2. Box Core Location Map.....	40
3. Waipaoa Discharge at Kanakanaia.....	42
4. Facies Classifications.....	44
A) Interbedded/Laminated Muds and sands	
B) Mixed Layer and Mottles	
C) Mottled Mud	
D) Shell hash, pebbles, rubble	
5. Regional Facies Map.....	49
6. Bulk Density Profiles Overlain onto X-radiographs.....	51
7. Spatial Distribution of Bulk Densities.....	53
A) Average bulk density of each core.	
B) Average bulk density from the surface to 5cm depth of each core	
8. Bulk Density, ⁷ Be Inventories and ²¹⁰ Pb Accumulation Rate Results and Standard Deviations by Shelf Region.....	56
A) Bulk Density	
B) ⁷ Be and ²¹⁰ Pb	
9. ⁷ Be Concentration Maps.....	58
A) Surface Specific Activity	
B) Inventory	
C) Average surface-5cm bulk density with ⁷ Be contours overlain	
10. Sedimentation Patterns.....	61
A) Spatial distribution of facies with characteristic ²¹⁰ Pb profiles	
B) Bulk density contours overlain ²¹⁰ Pb accumulation rates	
C) ⁷ Be Inventory contour map overlain on ²¹⁰ Pb accumulation rate map	
11. Theoretical Schematic of Parameters on the Shelf Along Transect A-A'.....	65

LIST OF TABLES

1. T-test results (P-values) of parameters by shelf region.....67
 - A) Mean bulk density (g cc^{-1})
 - B) Mean surface to 5cm interval bulk density (g cc^{-1})
 - C) ^7Be Inventories (dpm cm^{-2})
 - D) ^{210}Pb accumulation rates (cm y^{-1})

ABSTRACT

Modern sediment dispersal and accumulation on the continental shelf off the Waipaoa River, NZ, is investigated using X-radiographic, radioisotopic and physical property analyses of nearly 200 box and kasten cores collected in January 2005 aboard the *R/V Kilo Moana*. The high-yield, small mountainous Waipaoa River empties onto a tectonically active, narrow margin and represents an important analog for shelf sedimentation in similar environments worldwide. X-radiographs and bulk density measurements from a multi-sensor core logger show three distinct facies on the shelf where physical and/or biological factors dominate strata formation. Spatial distribution of these facies delineates a radial pattern with distance from the river mouth from areas dominated by layers and laminations on the innershelf to mottled muds on the outer shelf. Analysis of short-lived ^7Be ($t_{1/2} = 53$ days) reveals a broad spatial distribution across- and along-shelf in surface sediments, suggesting rapid transport from the Waipaoa source. Beryllium-7 inventories are consistent with centennial scale trends observed by other workers using longer-lived ^{210}Pb analyses, with highest inventories in recently identified depocenters located landward of two shelf anticlines. Box core bulk density analyses show lower than average bulk densities within these depocenters, and higher than average bulk density on the inner shelf and between the depocenters. This confirms rapid deposition of low-density muds in the depocenters, with higher bulk density, possibly reworked sediments remaining off the mouth of Poverty Bay and between the depocenters. Based on this single observational period, there appears to be no fundamental difference between seasonal and longer-term accumulation patterns on the shelf.

Recent Sedimentation Patterns and Facies Distribution on the Waipaoa River Shelf, N.Z.

1.0 Introduction

One of the fundamental objectives of marine sedimentology is the interpretation of stratigraphic sequences in order to discern Earth processes and history. Processes governing siliciclastic sedimentation on continental shelves involve tectonic, climatological, physical, biologic, geochemical and morphodynamic factors that interact along a spectrum of space and time scales, and ultimately control shelf stratigraphy and the rock record. Until recently, attention was focused on large river systems located on passive margins, which presented shelf accumulations often exhibiting clinoform geometry. This archetypal river system is characterized by a vast catchment area, low sediment yield and suspended sediment concentration entering the coastal ocean onto wide continental shelves. Examples include the Amazon, Po, Mississippi, Ganges-Brahmaputra, and Yangtze Rivers, among many others. A recent paradigm shift has illuminated the disproportionate impact of small, mountainous riverine systems in supplying sediment to the global ocean, conservatively estimated at an annual flux of 20BT (Milliman and Syvitski, 1992; Mulder and Syvitski, 1995; Syvitski et al., 2005).

Small mountainous rivers are typically characterized by steep gradients, high sediment yields, large loads (relative to catchment area and river discharge), and are often located on tectonically active margins whose catchments are strongly impacted by regional precipitation, and periodic wet storm events (Milliman and Syvitski, 1992; Mulder and Syvitski, 1995; Walsh and Nittrouer, 2005). Wet storms, as defined by

Wheatcroft (2000), are storm events with concomitant rain on land and elevated wave action on the continental shelf. Ongoing work on shelves off small mountainous rivers (e.g. Eel, Columbia, Waipua) has begun to effectively quantify sediment budgets and describe the geological and geochemical character of strata on adjacent continental shelves (Sommerfield and Nittrouer, 1999; Blair et al., 2004; Crockett and Nittrouer, 2004; Brackley, 2006; Nittrouer et al., 2007; Wadman and McNinch, 2008; Miller and Kuehl, submitted).

The Waipaoa River, located on the tectonically active East Cape of the North Island, New Zealand and adjacent continental shelf is an excellent example of a small, steep, high-yield mountainous river system (Figure 1). As such, it is an excellent location to investigate the dynamic changes in sediment transfer from land to sea with reference to global climate change, anthropogenic influences and tectonic forces, and was chosen as a study location in the Margins Source-to-Sink (S2S) program (MARGINS, 2003). Accumulation rates on the order of 1 cm yr^{-1} on the Waipaoa shelf (Orpin et al., 2006; Miller and Kuehl, submitted) suggest the shelf strata might contain an unprecedented high-resolution record of Holocene sedimentation.

This paper documents recent sedimentation on the shelf off the Waipaoa River, with a focus on seasonal to decadal timescales, as part of a collaborative effort to characterize sediment transport, deposition, and burial from the source waters of the Waipaoa to the continental shelf and slope. The objective of this study is to characterize recent sediment distribution and modern strata on the Waipaoa shelf using X-radiograph and radioisotopic analyses. Spatial distribution of sedimentation patterns and facies

from X-radiographs, ^7Be , and sediment bulk density measurements from nearly 200 sediment cores serve as the basis for this study. This work complements previous shelf core investigations (e.g., Brackley, 2006) and concurrent geophysical, textural and sediment budget analyses (Wood, 2006; Gerber et al., submitted; Miller and Kuehl, submitted).

1.1 Background

The Waipaoa River drains a small catchment (2205km^2) along the actively deforming Hikurangi Margin, between the Pacific and Australian Plates (Figure 1). Although its annual average sediment yield is $\sim 6800\text{t km}^{-2}\text{ yr}^{-1}$, annual sediment delivery to the marine environment by the Waipaoa varies widely, being dependant on the magnitude and frequency of storm events (Hicks et al., 2004). Tectonism causes regional uplift in the catchment's headwaters of up to 4mm yr^{-1} with concomitant subsidence along the coastal Poverty Bay Flats. Over 95% of sediment with provenance on the East Cape of New Zealand derives from soft, fine-grained rocks, including fissile Cretaceous to Paleocene mudstone and argillite in the headwaters of the Waipaoa to Tertiary siltstone and mudstone in the lower basin (Foster and Carter, 1997; Page et al. 2001, Hicks et al., 2004). Gully erosion within the catchment is the main modern erosional regime, and frequent landsliding occurs during extreme rainfall events (Foster and Carter, 1997).

Imprinted upon the natural geomorphologic catchment characteristics is a long history of human disturbance. Polynesian settlers to the East Cape (ca. 700y Bp) initiated widespread and aggressive burning of indigenous forest (Wilmshurst, 1997; Wilmshurst et al., 1997). Further land-use changes, post European arrival, included continued

deforestation and conversion of scrubland to pasture, destabilizing the landscape and causing common mass failures. The result is increased erosion rates up to 6 times greater than pre-European settlement (Page et al., 1994a; b; Wilmshurst, 1997; Wilmshurst et al., 1997; Eden and Page, 1998; Tate et al., 2000; Page et al., 2000; Page et al., 2001). A cascade of poorly quantified biogeochemical effects, including erosion and vegetation regime shifts, soil carbon sequestration fluctuations, runoff and suspended sediment volume changes, and impacts on local fauna have resulted from these anthropogenic disruptions (e.g., Page et al., 2001). Due to a combination of highly erodible lithologies within the catchment, increased erosion due to land use practices, and an annual average rainfall between 1 and 2.5 meters, the Waipaoa River supplies an average total annual sediment load of between $13\text{-}15 \times 10^6 \text{ t yr}^{-1}$ to the ocean (Griffiths, 1982; Foster and Carter, 1997). Significant storm events, associated with mass wasting and flushing of stored catchment sediments, such as the 100-year Cyclone Bola, can increase the annual load considerably (Page et al., 1994 a; b; Brackley, 2006). New Zealand regional climate responds significantly to changes in El Niño-Southern Oscillation (ENSO; Gomez et al., 2004). During Southern Oscillation Index (SOI) positive (La Niña) years, New Zealand experiences higher than average rainfall and frequency of cyclonic landfall, and warmer than average temperatures. In SOI negative years (El Niño), lower than average rainfall, cooler temperatures and fewer cyclones are experienced (Eden and Page, 1998; Gomez et al., 2004).

Previous investigations on the Waipaoa shelf identified increased modern sedimentation rates and a fining upwards signature in cores, interpreted to be a result of increased agricultural pressures and erosion within the catchment and Holocene climate

change (Foster and Carter, 1997; Wilmshurst, 1997; Gomez et al., 2004). Waipaoa effluent enters the shelf environment via hypopycnal flow during fair weather conditions and is speculated to be transported via hyperpycnal flow during intense wet storm events with a recurrence interval on the order of 40 years (Foster and Carter, 1997; Hicks et al., 2000). A single depocenter or “mid-shelf mud belt” of accumulating sediments, morphologically controlled by a synclinal basin on the shelf, was identified using seismic reflection studies and analysis of surface sediments (Foster and Carter, 1997; Orpin et al., 2006). Mud dispersion on the shelf is thought to be controlled primarily by wind and associated currents and sediment supply (Foster and Carter, 1997). It was speculated that relatively little sediment input by the Waipaoa escaped to the outer shelf and beyond because of the tectonic barrier created by shelf break anticlines, resulting in a seemingly “closed” system (Foster and Carter, 1997; Brackley, 2006; Orpin et al., 2006). This interpretation has been revised based on high-resolution seismic and ^{210}Pb analyses from the January 2005 *R/V Kilo Moana* cruise, with the identification of two discrete mid-shelf depocenters (Figure 2) separated by a region of little net accumulation (the bypassing region) as well as a third depocenter at the shelf break (Kuehl et al., 2006; Gerber et al., submitted; Miller and Kuehl, submitted). Foster and Carter (1997) documented nearshore sands grading into a mudbelt on the inner and middle shelf. This is augmented by an investigation of surficial sediments which classified several facies based on grain size modalities and also recognized the three distinct depocenters (Wood and Carter, submitted).

Local circulation within Poverty Bay and on the shelf is not well understood; however, it is known that Waipaoa effluent enters Poverty Bay (Figure 1) and under

typical conditions is entrained into an anticlockwise gyre before being transported to the shelf (e.g., Stephens et al., 2001; Brackley, 2006; Wood, 2006). The extension of the Wairarapa Coastal Current around the Mahia Peninsula creates a mean ambient current flow to the northeast along the shelf, and this is intensified by storm swell from the south (Chiswell, 2000; Stephens et al., 2001; Wood, 2006). At the shelf break, seaward of the Ariel and Lachlan anticlines, the warm, saline East Cape Current travels south (Carter et al., 1996; Foster and Carter, 1997; Chiswell, 2005).

2.0 Methods

2.1 Sampling plan

A suite of 87 box cores (max length 61cm; Appendix A) and 85 kasten cores were collected in a dense grid on the shelf adjacent to the Waipaoa River, N.Z. aboard the *R/V Kilo Moana*, January 2005 (Figure 2, 3). Box cores were used to evaluate the spatial and temporal distribution of sediment characteristics on the continental shelf. Box cores were collected between ~26 to ~75 meter water depths, with a few at deeper sites, seaward of the two anticlines. Box cores typically retrieve up to 0.5m of sediment and preserve the sediment-water interface.

Kasten cores (max length 270cm; Appendix A) were retrieved for radioisotopic and sediment budget analyses by Miller and Kuehl (submitted). Kasten cores are large cross-section (12cm X 12cm) gravity cores that provide up to 3 meters of sediment. Box cores were generally collected at the same site as kasten core retrieval to obtain both a well-preserved interface and the longer term stratigraphy at one location. Sediment accumulation rates derived from ^{210}Pb geochronology (Miller and Kuehl, submitted) were used to define specific regions for ease of comparison with other geochemical and physical property analyses in this study. These areas include the northern and southern depocenters, bypassing and shelf regions (Figure 2). Depocenters were defined as regions with accumulations of $> 0.5\text{cm yr}^{-1}$. For the southern depocenter this includes the following box cores: B22, B32, B33, B34, B46, B47, B52, B54A, B59, B60, B61, B63;

for the northern depocenter: B4, B5, B9, B15, B16, B17, B18, B78, B79, B80, B84, B85 (Figure 2). The bypassing region was delineated as the area between the two shelf depocenters (B1, B2, B3, B6, B19, B20, B21, B23, B24, B25, B26, B27, B28, B29, B31, B35, B37, B40; Figure 2). Shelf break cores include all cores taken at or near the shelf break, excluding canyon head and anticline cores (B30, B41, B71, B72, B73, B76, B82; Figure 2).

On board the *R/V Kilo Moana*, box and kasten core subsamples (2cm-thick slices) were extruded for post-cruise geochemical and textural analyses, and accompanying subsamples were also removed for X-radiography (from box and kasten cores) and Multi-Sensor Core Logging (MSCL) of physical properties (box cores). Kastan core radioisotopic and X-radiographic analyses are used for comparative purposes in this study to augment box core analyses.

2.2 X-radiography

Digital X-radiograph negative images were collected from each box and kasten core section (2.5cm-thick rectangular subcores; Appendix B). Digital X-radiography provides a nearly instantaneous reference for sedimentary structures within a core. Using Varian Paxscan[®] Imaging software (VIVA), each image was adjusted for optimal balance and contrast, and full cores were mosaiced together using Adobe Photoshop[®]. Digital X-radiographs were characterized by the degree of bioturbation along with identification of primary and secondary sedimentary structures. Based on these observations, facies distributions on the shelf were classified.

2.3 Bulk Density

On-board processing of box cores included use of a Geotek® Multi-Sensor Core Logger (MSCL) to record continuous down-core physical properties including gamma attenuation, p-wave velocity, magnetic susceptibility (SI) and derived acoustic impedance. MSCL measurements were made at centimeter and half-centimeter intervals. Sub-samples were taken every 20cm for laboratory bulk density measurements and were used to ground-truth the MSCL bulk density and porosity logs. Gamma ray attenuation through each core is measured and wet bulk density is calculated using the equation:

$$\rho = 1/\mu d * \ln(I_0/I) \quad \text{eq. 1}$$

where: ρ = sediment bulk density, μ = the Compton attenuation coefficient, d = the sediment thickness, I_0 = the gamma source intensity, I = the measured intensity through the sample. Calibration of gamma attenuation was performed using a reference core comprised of a core liner, water and various thicknesses of a standard reference material. Geotek® software also calculates fractional porosity. Dry bulk density was calculated from the fractional porosity measurements by subtracting the fractional porosity from the density of seawater and multiplying this value by an assumed grain density of 2.65g cc⁻¹ (quartz) and an assumed water density of 1.025g cc⁻¹. All bulk density measurements reported are dry bulk density.

2.4 ⁷Be

Analyses for ⁷Be ($t_{1/2}$ = 53 days) were performed immediately upon conclusion of the cruise (Appendix C). ⁷Be is a cosmogenic radionuclide that decays by beta emissions and is useful in determining short term deposition rates (on the order of months/seasons)

(e.g., Sommerfield et al., 1999). Surface sediment samples (from 0-1 cm depth) from each box core were prepared for gamma spectroscopy analyses on three LEGe (Low Energy planar intrinsic Germanium) detectors. Samples were homogenized and wet-packed into Petri dishes and counted for 90,000 seconds. Specific activity (dpm g^{-1}) was calculated using the ^7Be peak intensity at 477 keV. Detector efficiency was determined by calibration with a mixed gamma standard. If ^7Be was detected, samples were prepared, in discrete centimeter intervals of depth into core, until no activity was detected. A total of 202 samples were analyzed.

3.0 Results

3.1 Sedimentary Structures

X-radiographs show a variety of sedimentary structures (Figure 4) including prominent layering and laminations, a range of layer contacts from sharp to wavy, cross-bedding and ripples as well as burrows. X-radiographs also show relative changes in sediment bulk density downcore. High bulk density sediment, such as pebbles, shell hash and sands reduce X-ray penetration and result in light greys on the X-radiograph negative (Figure 4). Low bulk densities are seen as dark grey or black on the X-radiograph and include watery silts and muds (Figure 4). The extent of bedding preserved was assessed qualitatively for each core, to visually distinguish percent core dominated by layers and laminations. Degree of bioturbation was also assessed qualitatively for each core, visually accounting for burrow frequency and mottling, as well-bioturbated sediments can often be hard to distinguish from unbioturbated homogenous pelagic sediments. Secondary sedimentary structures were also observed, including dewatering structures. Cores were categorized according to the dominant primary sedimentary structures and degree of bioturbation revealed by X-radiographs and facies were classified as follows: (1) interlaminated muds and sands facies (ILMS), (2) mixed layers and mottles facies (MLM), and (3) mottled muds (MM) facies (Figures 4A, B, C). These characteristics were used to develop a regional facies map (Figure 5).

3.2 Bulk density

Dry bulk density measurements (calculated using the fractional porosity measurements generated by the gamma attenuation from the Multi-Sensor Core Logger) for every box core were averaged. Mean bulk density for shelf cores was $1.21 \text{ g cc}^{-1} \pm 0.22$. Conservative mean bulk density measurements for each core were obtained by removing the top 10 centimeters of data, which corresponds with the maximum depth of a surface mixed layer (Miller and Kuehl, submitted), in order to eliminate the influence of any low density surface layer or core disturbance, and these results were compared with the whole core means. The average bulk density of cores with the upper 10 centimeters removed was $1.22 \text{ g cc}^{-1} \pm 0.19$. There is no significant difference between these two measures of bulk density. The average bulk density for each core from the surface to 5 centimeters depth was also found, in order to compare with ^7Be measurements (see below, *Section 3.3*) which found the typical depth of ^7Be penetration to be 4-5cm. Mean bulk density of cores from the surface to 5cm interval was $1.12 \text{ g cc}^{-1} \pm 0.25$. To visually ground-truth X-radiographs, bulk density profiles were overlain onto them (Figure 6). Generally, the bulk density profiles were in agreement with X-radiographs (i.e. higher bulk density corresponded to lighter grey on the X-radiographs).

Distribution maps of average core bulk density (Figure 7A) and average bulk density between the surface and 5cm interval (Figure 7B) reveal two central locations of low bulk density on the shelf roughly consistent with the location of the northern and southern depocenters and high mud accumulation. Bulk density measurements presented in Figure 7 represent the average over the length of each core (~37cm). Distribution of bulk density from the surface to 5-cm interval has a similar geometry to that of the

average bulk densities (Figure 7), although the surface-5cm averages had generally lower bulk densities, especially within the depocenters. The highest bulk densities occur: 1) flanking the anticlines, associated with pebbles, gravel and shell hash found in these areas (Figures 1, 4D); and 2) offshore of the mouth of Poverty Bay associated with the interbedded/laminated muds and sands facies, especially the physically laminated sands endmember (Figure 4A).

Mean bulk density and mean bulk density from the surface to 5cm interval were plotted by shelf location - northern and southern depocenters, and bypassing and shelf regions (Figure 8). These location designations were based on previous accumulation rate data derived from ^{210}Pb geochronology (Miller and Kuehl, submitted; *Section 2.1*). Unpaired t-tests found significant differences ($P < .05$) in our measured parameters (mean bulk density and mean bulk density from the surface to 5cm interval) between the southern depocenter and the bypassing region, the northern depocenter and bypassing region, the northern depocenter and shelf and the bypassing region and shelf (Table 1A, B).

3.3 ^7Be

Spatial analysis of ^7Be ($t_{1/2} = 53$ days) activity concentrations from surface samples at each box core location reveals a generally broad distribution across and along shelf, with highest activities in the southern depocenter (Figure 9A). Average surface sample activity of ^7Be was $0.54 \pm 0.50\text{dpm g}^{-1}$ and ranged from no activity adjacent to Poverty Bay and flanking the landward side of Lachlan anticline, to $2.71 \pm 0.03\text{dpm g}^{-1}$ in the southern depocenter (Figure 9A; Appendix C). Activities exceeded 0.50dpm g^{-1} in

40% of all surface shelf sediments analyzed. Several shelf break cores also have high ^7Be surface sample activities. ^7Be was detected down to 5cm depth in some locations. Inventory calculations reveal regions of ^7Be accumulation in the southern and northern depocenters (Figure 9B). The average ^7Be inventory for the southern and northern depocenters, the shelf break and the bypassing regions are, respectively, $1.38 \pm 0.96\text{dpm cm}^{-2}$, $1.15 \pm 0.93\text{dpm cm}^{-2}$, $0.53 \pm 0.62\text{dpm cm}^{-2}$, and $0.59 \pm 0.47\text{dpm cm}^{-2}$ (Figure 8). T-tests show that there is a significant difference ($P < .05$) in ^7Be inventory between the southern depocenter and the bypassing region, the southern depocenter and the shelf break and the northern depocenter and the bypassing region (Table 1C).

4.0 Discussion

4.1 Facies Descriptions

Three main facies were identified on the shelf based on the sedimentary structure and degree of bioturbation revealed by X-radiographs (Figure 4). These facies include: 1) interbedded/laminated muds and sands (ILMS) facies (Figure 4A; • - labeled cores in Appendix 2), 2) mottled mud (MM) facies (Figure 4C; •• - labeled cores in Appendix 2), and 3) a combination of these two end members, the mixed layers and mottles (MLM) facies (Figure 4B; ••• - labeled cores in Appendix 2). The ILMS are clearly the result of physical processes affecting emplacement on the sea-bed and syn- and post-depositional processes such as soft sediment deformation and winnowing. The MM facies is indicative of near complete destruction of any physical structure by biologic agents. Cores within the MLM facies displayed both physical and biologic structures (burrows, tubes), often with partially intact layers disrupted by burrowing (Figure 4B, ex. B26). Examples of distinct stratigraphy that diverged from the three main facies identified included sites that had predominantly shell hash or pebbles (•••• - labeled cores in Appendix 2; Figure 4D).

4.1.1 Interbedded/laminated muds and sands (ILMS) facies

The interbedded/laminated muds and sands facies on the inner shelf (centered around 30-40m water depth, never >50m isobath), seaward of Poverty Bay, is comprised

of physically laminated sands nearshore that grade into interbedded sands and muds (Figure 4A, 5). X-radiographs within the ILMS revealed considerable variability. For example, cores closest to Poverty bay display finely laminated and crossbedded sands with climbing ripples (Figure 4A; B1), indicative of energetic physical processes while others have alternate units of laminated sand and mud (Figure 4A; B6, B24). Occasional rhythmic interbedding of muds and sands is also observed, some with distinct high-density layers punctuating the more subtle layering (Figure 4A; B20).

The distribution of the interbedded/laminated sands and muds facies above fair-weather wave base on the shelf indicate that physical processes dominate preservation of strata. High shear stresses hinder fine sediment from settling and benthic infaunal communities from forming in the shallow and energetic inner shelf. Sandy deposits are commonly reworked by waves and/or currents, evidenced by climbing ripples and crossbeds. This innershelf region corresponds with the area of fair-weather mud-resuspension and other authors have found increased surface sand fractions here (Foster and Carter, 1997; Brackley, 2006; Wood and Carter, submitted). Some sand may be derived from *in situ* weathering of anticlinal rock exposure and shedding, and be transported landward during energetic storm events (Wood, 2006).

4.1.2 Mixed layers and mottles (MLM) facies

The interbedded/laminated muds and sands facies quickly grades into the mixed layers and mottles facies (Figure 4B, 5) with distance away from the river mouth, both across shelf and along shelf (~45m water depth). This is likely due to the dynamic balance between sediment supply, storm activated wave base and benthic community

vigor. Sandier, high density layers in this facies reflect higher shear stresses due to currents and increased wave energies (Figure 4B, B61). Primary structures, such as fine crossbeds and ripples, along with high bulk densities indicate that physical reworking can play a major role by winnowing sediment and removing fines (Figure 4B, B19, B61). However, these layers are partially destroyed by burrows and intermixed with muddier, bioturbated sediment, emplaced during comparatively quiescent periods (Figure 4B, B26). Preserved layers of mud become more common with increased depth and distance from the mouth of Poverty Bay. The limited presence of large burrows within these cores corroborates that depth decreases the degree of wave reworking and increases the ability to preserve layers and sustain benthos. The mixed layers and mottles facies is thus interpreted to be a transitional depositional environment on the shelf that exists both within and outside of the depocenters along the inner to middle shelf.

The transitional environment characteristic of the MLM facies allows for some, usually high-density, layers to be wholly or partially preserved (Figure 4B, B61), especially on the inner mid-shelf. Other units within this facies are nearly obliterated by bioturbation. It is likely that during the stormier winter months, large magnitude floods with overwhelming sediment delivery emplace event layers on the shelf. This was seen with the unit deposited by Cyclone Bola in 1988 on the inner shelf (Brackley, 2006). A geochemically distinct storm sequence was observed here, with increased clay content, percent organic carbon, and a terrestrial $\delta^{13}\text{C}$ signature (Brackley, 2006). Benthic communities were also found to be significantly depleted in both quantity and diversity in this flood deposit (Foster and Carter, 1997; Brackley, 2006). This is akin to strata

observed on the Eel margin during extraordinary wet event sedimentation (Leithold and Hope, 1999; Wheatcroft and Borgeld, 2000; Nittrouer et al., 2007).

The nature of the MLM facies - alternating layers and mottled muds - indicates a threshold exists below which sediment from the Waipaoa, (probably during low-flow summer months and perhaps during normal hypopycnal pelagic sedimentation) is not preserved due to biological mixing. During periods of increased sediment discharge (e.g., during winter, when storm frequency and intensity increase; Griffiths, 1982; Page et al., 2001; Hicks et al., 2004), strata are likely emplaced on the shelf within the MLM facies.

The MLM facies is interpreted to be where event layers are potentially (and/or partially) preserved, and transit time and dissipation time of a layer or signal are in constant flux. The transit time of a layer refers to the time it takes to move from the mixed layer (where it is subjected to destruction by various physical and biological agents) to the zone of preservation and the dissipation time of an event bed is the amount of time necessary to completely destroy the bed (Wheatcroft and Drake, 2003; Wheatcroft et al., 2007). X-radiographs from this facies reveal layers preserved within strata on the shelf, suggesting that the dissipation time of a signal on the shelf is likely longer for the Waipaoa than the Eel (~2 yrs; Wheatcroft and Drake, 2003; Nittrouer et al., 2007), and exceeds the transit time in some locations. The greatest potential for preservation would likely be for wet storm event layers emplaced within the MLM facies in the depocenters, where Miller and Kuehl (submitted) record the highest shelf accumulation rates.

4.1.3 *Mottled mud (MM) facies*

The mottled mud facies (Figure 4C, 5) is indicative of strong bioturbation/reworking of sediment resulting in the loss of visible primary sedimentary structures. Burrow remnants indicate intense bioturbation in these core locations. In contrast to the ILMS, the mottled mud facies found throughout the outer shelf reveals that no layered strata is preserved below the mixed layer due to secondary processes (Nittrouer and Sternberg, 1981; Wheatcroft and Drake, 2003). According to Wood (2006), only under extreme conditions is mud resuspended deeper than 50 meters and the near absence of physical disturbance makes this environment ideal for a healthy benthic community. Evidence of these organisms include burrows and tubes, which create the “mottled” character of this facies. It is also likely that layer-producing sedimentation on the shelf is modulated by energy reduction associated with increasing depth and distance from the river mouth, and in some cases, increased sedimentation rates (Miller and Kuehl, submitted). However, geochemical results indicate that extremely large, episodic floods or storms, like the 100-year Cyclone Bola (1988), remain identifiable by grain size and stable isotopes even if not visually detectable in X-radiographs (Brackley, 2006; Rose, unpublished results). The MM facies extends onto the inner shelf (<50m water depth, Figure 5), both north and south of the river mouth. This suggests the facies is limited by sediment supply and accumulation in these locations and event beds are destroyed by bioturbation before they can be preserved by burial.

4.2 Facies distribution on the shelf

A distribution map of the three facies (Figure 5) reveals a broad, fan-like geometry radiating out from the mouth of Poverty Bay across and along the shelf. The ILMS facies extends along the inner shelf for ~20 km, adjacent to the mouth of Poverty Bay (Figure 5, blue). This region quickly grades into the narrow and elongate MLM facies, along the midshelf, which fingers to the north and south (Figure 5, green). The MLM grades into the MM facies (Figure 5, yellow), which occupies the largest area across shelf, beginning at ~50m water depth in the south and ~60m water depth in the north. Northwest or southeast along the shelf and away from Poverty Bay, the regions dominated by ILMS or MLM quickly grade into the mottled mud facies. Small pockets of shell hash and well rounded pebble rubbles that flank the landward sides of both anticlines are likely the result of *in situ* shedding of emergent, highly fissile Cretaceous to Paleocene mudrock at these locations (Figure 1, 4D).

All transitions between facies are gradational, although the switch from the ILMS into the MLM or MM is more abrupt than that of the MLM into the MM facies (Figure 5). Facies distributions on the shelf are not exclusively constrained by bathymetry, but rather are influenced by distance from the Waipaoa River mouth, water depth and associated reduction in sediment supply. Sediment accumulation rate may also be a major influence on the radiating pattern of shelf sediment facies identified, with supply limiting the development of strata on the shelf. We suggest that dissipation time on the Waipaoa shelf must vary widely, dependant on location according to the different facies on the shelf. Strata, especially those emplaced by event sedimentation, are preserved in

specific locations, influenced by sediment supply and water depth. This is supported by ^{210}Pb accumulation rates reported by Miller and Kuehl (submitted).

Bulk density measurements complement X-radiographs by providing a quantitative dimension to the visual analyses of X-rays. As such, bulk density core profiles can be overlain onto their corresponding X-radiograph to highlight the correlation between X-ray transparent layers and low density material (dark grey and black) and opaque layers with high density sediment (light grey; Figure 6). Described facies on the shelf can thus be identified by their bulk density profiles. The ILMS facies displays a characteristic and consistent high bulk density core profile within individual cores (Figure 6, B6), but is very variable between cores, depending on the nature of the laminations – for example, physically laminated sands vs. rhythmically laminated muds and sands (Figure 4; B1 vs. B20). The ILMS usually has high amplitude variations downcore. The MM facies has a highly recognizable bulk density profile, characterized by low amplitude variations/fluctuations with depth and often lower than average bulk densities (Figure 6; B85). The MLM facies is similar in profile to the ILMS facies, but is more variable within a core – characteristic intermediate density fluctuations punctuated by brief higher density layers (Figure 6; B24).

4.3 Facies comparison with other continental shelves

The distribution observed of Waipaoa shelf facies is comparable to others described on active margin shelves with small mountainous river delivery. The small, mountainous Eel River is an excellent analogue to the Waipaoa River shelf, as it drains a small catchment (9000 km²), and its flow is episodic and seasonally driven (Sommerfield

and Nittrouer, 1999). The Waipaoa and Eel have comparable sediment loads, 15Mt yr^{-1} and $15\text{-}24\text{Mt yr}^{-1}$, respectively (Wheatcroft and Borgeld, 2000; Wheatcroft and Drake, 2003). On the inner Eel shelf, sand deposits dominate, and are more extensive than those offshore of the Waipaoa, presumably because of shelf morphology and higher wave energy (Crockett and Nittrouer, 2004). The Eel mid-shelf mud deposit located between 50 and 100 meters on the shelf is interpreted to result from episodic flood sedimentation. Energetic hydrodynamic factors on the shelf act in concert to destroy much of the physical sedimentary structure emplaced by storm events and seasonal sedimentation, as the transit time exceeds the dissipation time of all but the thickest layers on the shelf (Wheatcroft and Drake, 2003; Nittrouer et al., 2007). Some of these signals are preserved, resulting in a facies not unlike the mixed layers and mottles observed on the Waipaoa shelf. On the U.S. Washington Margin as well, physically laminated sediments characterize innershelf stratigraphy of the upper 50cm of seabed and grade into intermixed mud and sand and bioturbated sediments (Nittrouer and Sternberg, 1981). These patterns are interpreted to be caused by fluctuations in sediment supply, decreased influence of mixing with increased water depth and accumulation rate. Key differences between the Waipaoa and these and other small mountainous rivers that influence shelf deposits include the tectonic shelter provided by the uplifting anticlines that buffer southern swell and currents and act as geomorphic traps to sedimentation. Also, the Waipaoa is hypothesized to produce hyperpycnal plumes an order of magnitude less frequently than other East Cape Rivers of New Zealand (e.g., Waiapu and Uawa Rivers, Hicks et al., 2004).

The facies present on the Waipaoa shelf and their distribution are different from those observed on many passive margin shelves because of a number of physical, hydrodynamic and geochemical factors. On the Amazon shelf, for example, the physically stratified sand facies are found nearshore and the interbedded mud and sand facies described for the Amazon consists of thick mud layers and numerous discrete thin sand beds (Kuehl et al., 1986). On the Waipaoa shelf, the single facies, interbedded/laminated muds and sands, comprising both physically stratified sands through interbedded muds and sands, is seen as a continuum across-shelf, influenced by increasing depth and decreasing wave energy and sediment supply. Crossbedded and laminated sandy deposits located just offshore of Poverty Bay (ex. B1, B2, B6, Appendix 2) are similar to the physically stratified sand facies of the Amazon. In contrast, there is a clear difference between the interbedded mud and sand facies described for the Amazon and the Waipaoa. There is less difference in the thicknesses of the interbedded sand and mud layers on the Waipaoa shelf than the Amazon shelf. For example, the Waipaoa ILMS cores often have equally thick or more thick, high bulk density (sandy) units relative to muddy units (Appendix B), while Amazon shelf cores display relatively thin sandy units (on the order of 0.5-1.0cm) within thicker (5-10cm) mud beds (Kuehl et al., 1986; 1995). Most Waipaoa ILMS cores also show evidence of some bioturbation, while Amazon interbedded mud and sand has little to no bioturbation except at its seaward boundary (Kuehl et al., 1986). No Waipaoa analogue exists for either the proximal-shelf sandy silt or faintly laminated mud facies described for the Amazon clinoform. However, it is important to realize the progression of facies on the narrow, tectonically active Waipaoa shelf may be similar to those of much larger river passive margin shelves,

but the disparate scales of these systems engender different facies identification.

Although transitions from facies across shelf may parallel each other due to the ranking of similar processes in their operation on the shelf (sediment supply, wave energy, water depth) there are clear departures. These include considerable differences in climate, shelf width (Waipaoa = narrow; Amazon = wide) and suspended sediment types, delivery, discharge (Waipaoa = low; Amazon = high), accumulation rates and transport mechanisms. These system characteristics are influenced by dynamic variations in sediment supply, transport and tectonic forces between these continental shelf environments (Milliman and Syvitski, 1992; Walsh and Nittrouer, 2005). The morphology of continental shelf deposits on passive vs. active margins can also be quite different – e.g. subaqueous delta clinoform geometry observed on passive margins is absent on the Waipaoa shelf.

4.4 ⁷Be activity and sediment dispersal

Surface ⁷Be activities, exceeding 0.5 dpm g⁻¹ in 40% of all surface sediments, were widespread, detected along and across the continental shelf, including the shelf-break (Figure 9A). ⁷Be is found as distant from the Waipaoa as the heads of canyons incising the shelf-break (J.P. Walsh and C. Alexander, pers. comm.). As ⁷Be is thought to derive primarily from riverine input (e.g., Sommerfield et al., 1999), its distribution provides evidence that Waipaoa river sediment is broadcast throughout the study area over short time scales and that some sediment rapidly bypasses the anticlines and is transported to the outer shelf and slope. The only locations where surface activities were not detectable included the landward flank of the Lachlan anticline, where surface

sediments are coarse (Figure 4D), and directly at the mouth of Poverty Bay, where surface sediments are reworked and mainly sandy (ILMS facies; Figure 4A). There may also be an associated grain size effect with increased energy, where ^7Be -bearing particles such as clay and silt are preferentially removed by wave reworking, especially in the inner shelf region, which is above fair-weather wave base.

^7Be distribution maps show the highest surface activities are located in the depocenters landward of the Ariel and Lachlan Anticlines (Figure 9A), with higher activities in the southern depocenter (e.g. 2.71dpm g^{-1} vs. 1.38dpm g^{-1} in the northern depocenter). This suggests that even during low-flow conditions, at the time of sampling, in January 2005 (austral summer; Figure 3), Waipaoa effluent was actively being transported to shelf depocenters. The shelf-break cores with elevated surface ^7Be activities suggest that even under low-flow conditions, surface sediments have been recently deposited. Deposition at the shelf break is likely derived from Waipaoa River that bypassed the anticlines, or sediment that was transported around the promontory of the Mahia Peninsula via the Wairarapa Current or by the southward flowing East Cape Current. We favor the former idea, as it is unlikely that high accumulation rates on the shelf break could be solely supported by lateral input of sediments delivered from sources outside the Waipaoa sedimentary system via surface currents.

4.5 ^7Be Inventory measurements

^7Be inventory measurements (activity integrated over depth) are important because they allow us to determine if: 1) sediments are rapidly accumulating; 2) distribution of surface sediment ^7Be activities are representative of instantaneous

deposition or are fairly steady (over month-seasonal timescales); and 3) reworking and downward diffusion by physical or biological agents is present. In contrast to the relatively evenly distributed ^7Be surface activity (aside from the amplification in the southern depocenter) ^7Be inventories clearly reveal highest accumulations to be within the southern and northern depocenters, with modest accumulation outside the depocenters (Figure 8B, 9B). The southern depocenter has a central focus of high inventories in the same location as high ^7Be activities in surface sediments (Figure 9A, B; between 40-50m water depth). A broad, wedge shaped area emanating from southern depocenter, also has high inventories; this area is sheltered by the Mahia peninsula (Figure 9B) and may be subject to less intense wave reworking, which may increase deposition.

The northern and southern depocenters are similar in terms of physical sedimentary characteristics and ^7Be inventory spatial distributions. Differences between the inventories of the northern and southern depocenter are not statistically significant (as well as differences between ^{210}Pb accumulation rates; Table 1C, D), although the highest measured ^7Be inventory (B84, 2.88 dpm g^{-2} ; Appendix C) is seen in the northern depocenter, suggesting more rapid river effluent transport to this depocenter. The locus of highest ^7Be activity in the northern depocenter is also closer to shore than that of the southern depocenter, although water depths are similar (Figure 9B). Mean northern inventory and range is smaller ($1.15 \text{ dpm cm}^{-2} \pm 0.93$ and $0.00 \text{ dpm cm}^{-2} - 2.88 \text{ dpm cm}^{-2}$, respectively) than the respective mean and range ($1.38 \text{ dpm cm}^{-2} \pm 0.96$ and $0.25 \text{ dpm cm}^{-2} - 2.84 \text{ dpm cm}^{-2}$) of the southern depocenter (Figure 8B, Appendix C). The areas directly offshore of Poverty Bay and along the bypassing region and the landward flank of the Lachlan Anticline are notably devoid of ^7Be activity (Figure 9B). The zone directly

seaward of Poverty Bay is interpreted to be highly reworked (ILMS; Figure 4A), is comprised largely of sandy sediments, and is characterized by high bulk density (average of surface-5cm depth for each core) sediments (Figure 9C).

Inventory (and surface) activities of ^7Be at the shelf break are relatively low (compared to depocenters) where low bulk density material is found (Figure 8, 9C). In comparison, ^{210}Pb accumulation rates are low as well ($< 0.5 \text{ cm yr}^{-1}$, Figure 8B), however the shelf break region is interpreted as a secondary zone of deposition on the centennial timescale (Miller and Kuehl, submitted). Thus, low ^7Be inventories on the shelf break might be due to longer sediment transit times to this location coupled with slower accumulation rates.

Shelf circulation may bring an influx of sediment to other locations seasonally, but this study did not re-occupy core sites on a seasonal basis to test this idea. However, sample collection was during the austral summer, which has characteristically reduced wet storm frequency and severity, as well as less energetic wave action (dry storms). Discharge measurements at Kanakanaia gauging station show the Waipaoa was experiencing low-flow conditions prior to and during sampling, with the most recent storm and associated high discharge in October 2004 (Figure 3). ^7Be inventories reported here are consequently considered to be “conservative” values, representing a period of low ^7Be input. During austral winter, with higher river discharge, ^7Be would likely be found at higher activities broadcast throughout the shelf. Although the timescale represented by ^7Be is a few months at maximum, the spatial depositional patterns compare favorably with Holocene deposition interpreted from seismic studies and with ^{210}Pb accumulation rates, suggesting sediment accumulation patterns, though

affected by different transport and depositional mechanisms on these timescales, are fundamentally the same (Kuehl et al., 2006; Orpin et al., 2006; Gerber et al., submitted).

4.6 Sedimentation Patterns on the shelf

Two patterns of sedimentation, described by various radioisotopic and physical properties of recent shelf sediment shed light on modern-day transport and accumulation on the Waipaoa margin. The first is the radial distribution of facies emanating from the mouth of Poverty Bay (Figure 5). The second is the location of two depocenters landward of the outershelf anticlines (Figures 7, 8, 9). ^{210}Pb ($t_{1/2} = 22.3\text{yrs}$) activity profiles and geochronology for 85 kasten cores retrieved during the same cruise are reported in Miller and Kuehl (submitted) augment this study's findings.

The type and occurrence of characteristic ^{210}Pb activity profiles correspond well with the radial distribution pattern of facies (Figure 10A). All kasten cores found to have low, uniform activity profiles are located within the ILMS facies (Figure 10A, grey circles). Miller and Kuehl (submitted) interpret this activity profile as being indicative of intense physical reworking that would presumably homogenize sediments while removing fines, which are likely to have the highest activities, and produce little net accumulation. Most interestingly, kasten cores with non-steady state activity profiles are found almost exclusively within the MLM facies (Figure 10A, red diamonds). Seven out of 11 of these cores overlap with exact locations of box cores reported in this study. These data suggest that the MLM facies is located in a region where event layers are often preserved, which can cause non-steady-state activity profiles. Steady-state ^{210}Pb profiles (log decrease of excess ^{210}Pb activity; Figure 10A, grey pluses) are located within

the MM facies, primarily deeper than fair weather wave base, where sediment accumulation is often high and sediment supply and bioturbation are more consistent.

In contrast, bulk density, ^7Be inventories and ^{210}Pb accumulation rates delineate clear centers of sediment accumulation on the shelf, disconnected from the facies distribution (Figure 10B, C). Spatial analyses of ^{210}Pb accumulation from Kasten cores on the shelf confirm the two foci of accumulation on the centennial-year time-scale (Figure 8B). ^{210}Pb accumulation rates are highest in the depocenters (Miller and Kuehl, submitted; Figure 10B), as are ^7Be inventories with the maximum overlap between ^7Be inventories and ^{210}Pb accumulation rates in the southern depocenter (Figure 8B, 10C). Bulk density measurements represent an intermediate timescale between ^7Be ($t_{1/2} = 53$ d) and ^{210}Pb ($t_{1/2} = 22.3$ yr), as box cores average ~ 37 cm in length filling in information on decadal to multi-decadal timescales. Spatial deposition of averages of surface-5cm depth bulk density compare favorably with ^7Be inventories (Figure 9C). The surface-5cm averages were used to compare with ^7Be because the inventory measurements went as deep as 5cm. Higher than average bulk densities are usually associated with very low ^7Be inventories (Figure 9C). Lowest bulk densities are associated with areas with the highest ^7Be activity inventories and fall almost entirely within the MM facies. For example, low bulk densities and high ^7Be inventory activities are found on the northwestern flank of the southern depocenter, where non-steady ^{210}Pb accumulation and the interbedded/laminated muds and sands facies indicates event deposition dominates (Figures 9C, 10C).

Interestingly, multiple facies are found within the depocenters. This suggests that on the first order, accumulation rate is not the overriding control. This “disconnect” in

spatial distribution is possibly due to differences in transport to, and depositional regimes on, the Waipaoa continental shelf as well as post-depositional processes. Depo-center muds, with high clay contents, may consolidate on short timescales (days to weeks) as evidenced by analytical modeling for the Eel shelf (Scully et al., 2002). This inhibits resuspension and fosters continued bioturbation. Preliminary stable carbon isotopic carbon analyses of box cores show there is no $\delta^{13}\text{C}$ overlap between the two depocenters, with the northern depocenter being more terrestrially influenced (Rose, unpublished results), confirming Wood's (2006) suggestion that, based on grain size modalities, the northern and southern depocenters are isolated from each other.

It is also interesting to note that multiple types of ^{210}Pb activity profiles can be found within the depocenters (Figure 10A). Non-steady state profiles correspond with cores on the landward flanks of the two depocenters within the MLM facies, while steady state cores are located in the centers of the depocenters (MM facies) where highest accumulations are found. Steady-state profiles are also characteristic of areas of lower accumulation on the midshelf between the two depocenters (Miller and Kuehl, submitted) indicating that along-shelf variation in accumulation rate does not necessarily translate into differences in profile characteristics. Wood (2006) suggests that surface sediment (taken from splits of box cores from this study) grain-size distributions are most influenced by bathymetric and wave base controls, as well as the relative amount of cohesive sediments. This could also explain the occurrence of multiple facies and ^{210}Pb activity profiles along shelf and within depocenters.

A transect from near the mouth of Poverty Bay, northeast along shelf (Figure 11) clearly shows all three facies are present, although the change in water depth (from 40 to

60 meters over approximately 22 kilometers) is very gradual. Traditionally sediment supply is regarded as having first order control on facies distribution, however, a convergence of other factors are clearly important in producing the observed sedimentation patterns and strata formation on the Waipaoa shelf. As physical disturbance to the seabed via wave resuspension and winnowing drops, biological mixing intensity increases (Figure 11). This is seen clearly in the progression from ILMS to MLM and finally the MM facies along shelf (Figure 4, 11). Sediment accumulation rates (Miller and Kuehl, submitted) increase to a maximum ~ 1.25 cm yr⁻¹, where the transect enters the northern depocenter. Wood (2006) found that surface sand content decreased from a high of $\sim 55\%$ at A to A' while surface mud (silt + clay) increased along A – A' (surface samples taken from splits of box cores from this study). We hypothesize that the dynamic interplay between sediment supply, distance from source, grain size, biological mixing activity and physical disturbance determine the facies progression and by extension the dissipation time of a signal on the shelf at any location (Figure 11; Wheatcroft et al., 2007).

Similar controls are likely responsible for the location of the MLM facies and non-steady state profiles in the northern end of the southern depocenter (Figure 10A) overlaps with Wood's (2006) sandy clayey silt facies (scZ2), for example. Higher sand content in this area (closer to shore) may aid in the rapid cohesion of mud layers (McCave, 1984; Wood, 2006). Deeper in the depocenter (~ 50 m water depth), the MM facies and steady state profiles dominate (partial overlap with Wood (2006)'s cZ2 facies), presumably due to a combination of reduction in wave energy, benthic community and reduced sand content.

5.0 Conclusions

X-radiographic, radioisotopic and physical properties analysis of nearly 200 box and kasten cores collected in January 2005 aboard the *R/V Kilo Moana* show distinct trends in sediment dispersal and accumulation on the continental shelf off the Waipaoa River, NZ.

- 1) Three distinct facies are radially distributed across and along shelf with increasing distance from the Waipaoa River mouth: 1) interbedded/laminated muds and sands (ILMS); 2) mixed layers and mottles (MLM); and 3) mottled muds (MM) facies.
- 2) ^7Be is widespread throughout surface sediments in the study area indicating rapid seaward transport of Waipaoa effluent. ^7Be inventories indicate accumulation occurs predominantly within two depocenters located landward of the Ariel and Lachlan anticlines.
- 3) Bulk density measurements have similar patterns to those of ^7Be inventory distributions along and across shelf. Accumulation rates revealed from spatial analyses of longer-lived ^{210}Pb in Kastan cores (Miller and Kuehl, submitted), which are highest in the depocenters and on the shelf break, confirm this pattern.
- 4) Characteristic ^{210}Pb activity profiles are distinctly partitioned by facies. Low, uniform activities are found exclusively with the ILMS, non-steady state activity profiles are found in the MLM facies and largely steady-state accumulation is observed in the MM facies.

REFERENCES

- Blair, N.E., Leithold, E.L., Aller, R.C. (2004) From bedrock to burial: the evolution of particulate organic carbon across coupled watershed-continental margin systems. *Marine Chemistry*, 92: 141-156.
- Brackley, H.L. (2006) Land to ocean transfer of erosion-related organic carbon, Waipaoa sedimentary system, East Coast, New Zealand. Unpublished Ph.D. Thesis, Victoria University of Wellington. 129 pp plus appendices.
- Carter, L., Carter, R.M., McCave, I.N., Gamble, J. (1996) Regional sediment recycling in the abyssal Southwest Pacific Ocean. *Geology*, 24 (8): 735-738.
- Chiswell, S.M. (2000) The Wairarapa Coastal Current. *New Zealand Journal of Marine and Freshwater Research*, 34: 303-315.
- Chiswell, S.M. (2005) Mean and variability in the Wairarapa and Hikurangi Eddies, New Zealand. *New Zealand Journal of Marine and Freshwater Research*, 39: 121-134.
- Crockett, J.S. & Nittrouer, C.A. (2004) The sandy inner shelf as a repository for muddy sediment: an example from Northern California. *Continental Shelf Research*, 24 (1): 55-73.
- Eden, D.N. and Page, M.J. (1998) Palaeoclimatic implications of a storm erosion record from late Holocene lake sediments, North Island, New Zealand. *Palaeogeography, Palaeoclimatology, Palaeoecology*, 139: 37-58.
- Foster, G. and Carter, L. (1997) Mud sedimentation on the continental shelf at an accretionary margin – Poverty Bay, New Zealand. *New Zealand Journal of Geology and Geophysics*, 40: 157-173.
- Gerber, T., Pratson, L., Kuehl, S., Walsh, J.P., Alexander, C., Palmer, A. (Submitted) The influence of post-glacial sea level rise and tectonics on sediment storage along the high-sediment supply Waipaoa continental shelf. *Marine Geology*.
- Gomez, B., Carter, L., Trustrum, N.A., Palmer, A.S., Roberts, A.P. (2004) El Nino – Southern Oscillation signal associated with middle Holocene climate change in intercorrelated terrestrial and marine sediment cores, North Island, New Zealand. *Geology*, 32 (8): 653-656.
- Griffiths, G.A. (1982) Spatial and temporal variability in suspended sediment yields of North Island basins, New Zealand. *Water Resources Bulletin*, 8 (4): 575-583.

Hicks, D.M., Gomez, B., Trustrum, N.A. (2000) Erosion thresholds and suspended sediment yields, Waipaoa River Basin, New Zealand. *Water Resources Research*, 36 (4): 1129-1142.

Hicks, D.M., Gomez, B., Trustrum, N.A. (2004) Event suspended sediment characteristics and the generation of hyperpycnal plumes at river mouths: East Coast Continental Margin, North Island, New Zealand. *The Journal of Geology*, 112: 471-485.

Kuehl, S.A., Nittrouer, C.A., DeMaster, D.J. (1986) Distribution of sedimentary structures in the Amazon subaqueous delta. *Continental Shelf Research*, 6: 311-336.

Kuehl, S.A., Alexander, C., Carter, L., Gerald, L., Gerber, T., Harris, C., McNinch, J., Orpin, A., Pratson, L., Syvitski, J., Walsh, J.P. (2006) Understanding sediment transfer from land to ocean. *Eos*, 87 (29): 281, 286.

Kuehl, S.A., Pacioni, T.D., Rine, J.M. (1995) Seabed dynamics of the inner Amazon continental shelf: temporal and spatial variability of surficial strata. *Marine Geology*, 125: 283-302.

Leithold, E.L. and Hope, R.S. (1999) Deposition and modification of a flood layer on the northern California shelf: lessons from and about the fate of terrestrial particulate organic carbon. *Marine Geology*, 154: 183-195.

MARGINS Office. (2003) Source-to-Sink. In NSF MARGINS Program Science Plans 2004. Lamont-Doherty Earth Observatory of Columbia University, New York, September 2003.

McCave, I.N. (1984) Erosion, transport and deposition of fine-grained marine sediments. pp. 35-69 in Stow, D.A.V., Piper, D.J.W., (eds). *Fine-Grained Sediments: Deep Water Processes and Facies*. Blackwell Scientific Publications, Oxford. 659 pp.

Miller, A.J. and S.A. Kuehl. (*Submitted*) A sediment budget for recent shelf sedimentation off the Waipaoa River, NZ. *Marine Geology*.

Milliman, J. and Syvitski, J.P.M. (1992) Geomorphic/tectonic control of sediment discharge to the ocean: the importance of small mountainous rivers. *The Journal of Geology*, 100: 525-544.

Mulder, T. and Syvitski, J.P.M. (1995) Turbidity currents generated at river mouths during exceptional discharges to the world oceans. *The Journal of Geology*, 103: 285-299.

Nittrouer, C.A., Austin, J.A., Field, M.E., Kravitz, J.H., Syvitski, J.P.M., Wiberg, P.L. (2007). Writing a Rosetta stone: insights into continental-margin sedimentary processes

and strata. In C. Nittrouer, J. Austin, M. Field, J. Kravitz, J. Syvitski and P. Wiberg (eds.), *Continental Margin Sedimentation* (pp 1-48). Hoboken, N.J.: Wiley-Blackwell.

Nittrouer, C.A. and R.W. Sternberg. (1981) The formation of sedimentary strata in an allochthonous shelf environment: The Washington continental shelf. *Marine Geology*, 42: 201-232.

Orpin, A.R., Alexander, C., Carter, L., Kuehl, S., Walsh, J.P. (2006) Temporal and spatial complexity in post-glacial sedimentation on the tectonically active, Poverty Bay continental margin of New Zealand. *Continental Shelf Research*, 26: 2205-2224.

Page, M.J., Trustrum, N.A. & DeRose, R.C. (1994 a) A high resolution record of storm induced erosion from lake sediments, New Zealand. *Journal of Paleolimnology*, 11 (3): 333-348.

Page, MJ, Trustrum, NA & Dymond, JR (1994 b) Sediment budget to assess the geomorphic effect of a cyclonic storm, New Zealand. *Geomorphology*, 9 (3): 169-188.

Page, M.J., Trustrum, N.A. & Gomez, B. (2000) Implications of a century of anthropogenic erosion for future land use in the Gisborne-East Coast region of New Zealand. *New Zealand Geographer*, 56 (2): 13-24.

Page, M.J., Trustrum, N.A., Brackley, H.L., Gomez, B., Kasai, M., Marutani, T. (2001) Waipaoa River (North Island, New Zealand). pp. 86-101. In: Marutani T., Brierley, G.J., Trustrum, N.A., Page, M.J., (eds). Source-to-Sink Sedimentary Cascades in Pacific Rim Geo-Systems. Matsumoto Sabo Work Office, Ministry of Land, Infrastructure and Transport, Japan.

Scully, M.E., Friedrichs, C.T. and L.D. Wright. (2002) Application of an analytical model of critically stratified gravity-driven sediment transport and deposition to observations from the Eel River continental shelf, Northern California. *Continental Shelf Research*, 22: 1951-1974.

Sommerfield, C.K. and C.A. Nittrouer. (1999) Modern accumulation rates and a sediment budget for the Eel shelf: a flood-dominated depositional environment. *Marine Geology*, 154: 227-241.

Sommerfield, C.K., Nittrouer, C.A. and C.R. Alexander. (1999) ^7Be as a tracer of flood sedimentation on the northern California continental margin. *Continental Shelf Research*, 19: 335-361.

Stephens, S.A., Bell, R.G., Black, K.P. (2001) Complex circulation in a coastal embayment: shelf-current, wind and density-driven circulation in Poverty Bay, New Zealand. *Journal of Coastal Research*, 34: 45-59.

Syvitski, J.P.M., Vorosmarty, C.J., Kettner, A.J., Green, P.G. (2005) Impact of humans on the flux of terrestrial sediment to the global coastal ocean. *Science*, 308: 376-380.

Tate, K.R., Scott, N.A., Parshotam, A., Brown, L., Wilde, R.H., Giltrap, D.J., Trustrum, N.A., Gomez, B. and Ross, D.J. (2000) A multi-scale analysis of a terrestrial carbon budget: Is New Zealand a source or sink of carbon? *Agriculture, Ecosystems and Environment*, 82: 229-246.

Wadman, H.M. and J.E. McNinch. (2008) Stratigraphic spatial variation on the inner shelf of a high-yield river, Waipua River, New Zealand: Implications for fine-sediment dispersal and preservation. *Continental Shelf Research*, 28 (7): 865-886.

Walsh, J.P. and C.A. Nittrouer. (2005) Understanding the distal delta: Controls on the fate of fine-grained sediments in fluvial dispersal systems. Unpublished manuscript. 16pp plus figures.

Wheatcroft, R.A. (2000) Oceanic flood sedimentation: a new perspective. *Continental Shelf Research*, 20: 2059-2066.

Wheatcroft, R.A. and J.C. Borgeld. (2000) Oceanic flood deposits on the northern California shelf: large-scale distribution and small-scale physical properties. *Continental Shelf Research*, 20: 2163-2190.

Wheatcroft, R.A. and Drake, D.E. (2003) Post-depositional alteration and preservation of sedimentary event layers on continental margins, I. The role of episodic sedimentation. *Marine Geology*, 199: 123-137.

Wheatcroft, R.A., Wiberg, P. L., Alexander, C.R., Bentley, S.J., Drake, D.E., Harris, C.K., Ogston A.S. (2007) Post-depositional alteration and preservation of sedimentary strata. In C. Nittrouer, J. Austin, M. Field, J. Kravitz, J. Syvitski and P. Wiberg (eds.), *Continental Margin Sedimentation* (pp 101-155). Hoboken, N.J.: Wiley-Blackwell.

Wilmshurst, J.M. (1997) The impact of human settlement on vegetation and soil stability in Hawke's Bay New Zealand. *New Zealand Journal of Botany*, 35: 97-111.

Wilmshurst, J.M., McGlone, M.S., Partridge, T.R. (1997) A late Holocene history of natural disturbance in lowland podocarp/hardwood forest, Hawke's Bay, New Zealand. *New Zealand Journal of Botany*, 35: 79-96.

Wood, M.P. (2006) Sedimentation on a high input continental shelf at the active Hikurangi margin, Poverty Bay, New Zealand. Unpublished M.S. thesis, Victoria University of Wellington. 141 pp plus appendices.

Wood, M.P. and L. Carter. (*Submitted*) Modern depositional framework of the high discharge Waipaoa continental shelf. *Marine Geology*.

Figure 1. New Zealand and Waipaoa River Location Map

New Zealand with East Coast, North Island enlarged to show Waipaoa River catchment (blue outline), catchment sediment yields (modified from Hicks et al., 2004) and adjacent continental shelf. Arrow indicates approximate location of Kanakania gauging station. Study area is enlarged with bathymetry indicated in meters (modified from NIWA). Dashed bold line indicates the shelf break at 150m water depth. Ariel (north) and Lachlan (south) Anticlines are designated with rectangles. PB = Poverty Bay, MR = Monowai Rocks, MP = Mahia Peninsula.

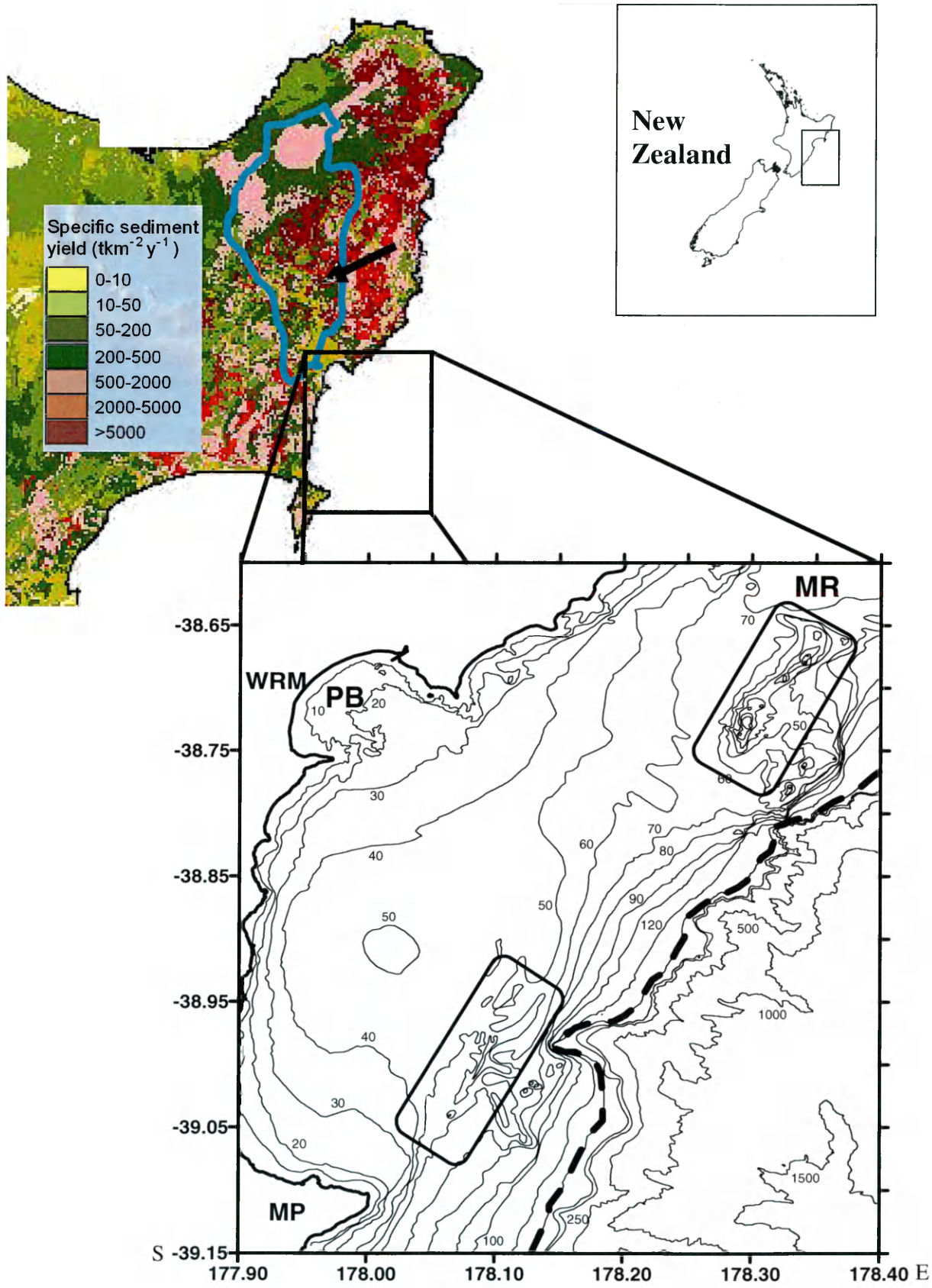


Figure 2. Box Core Location Map

Locations of 87 box cores collected on the continental shelf off the Waipaoa in January, 2005 aboard the *R/V Kilo Moana*. Locations of cores are denoted by black squares and bold labels (ex. **B1**) are core names. Shaded regions delineate southern and northern depocenters defined by ^{210}Pb accumulation rate data from Miller and Kuehl (submitted). These are regions with $> 0.5 \text{ cm yr}^{-1}$ accumulation. For the southern depocenter, the following box cores fall within these bounds: B22, B32, B33, B34, B46, B47, B52, B54A, B59, B60, B61, B63. For the northern depocenter: B4, B5, B9, B15, B16, B17, B18, B78, B79, B80, B84, B85. Other shelf regions to note are the bypassing region, delineated as cores between the two shelf depocenters: B1, B2, B3, B6, B19, B20, B21, B23, B24, B25, B26, B27, B28, B29, B31, B35, B37, B40 and shelf break cores, which include all cores taken at or near the shelf break, excluding canyon head and anticline cores: B30, B41, B71, B72, B73, B76, B82. Dashed line indicates shelf break at 150m. WRM = Waipaoa River Mouth.

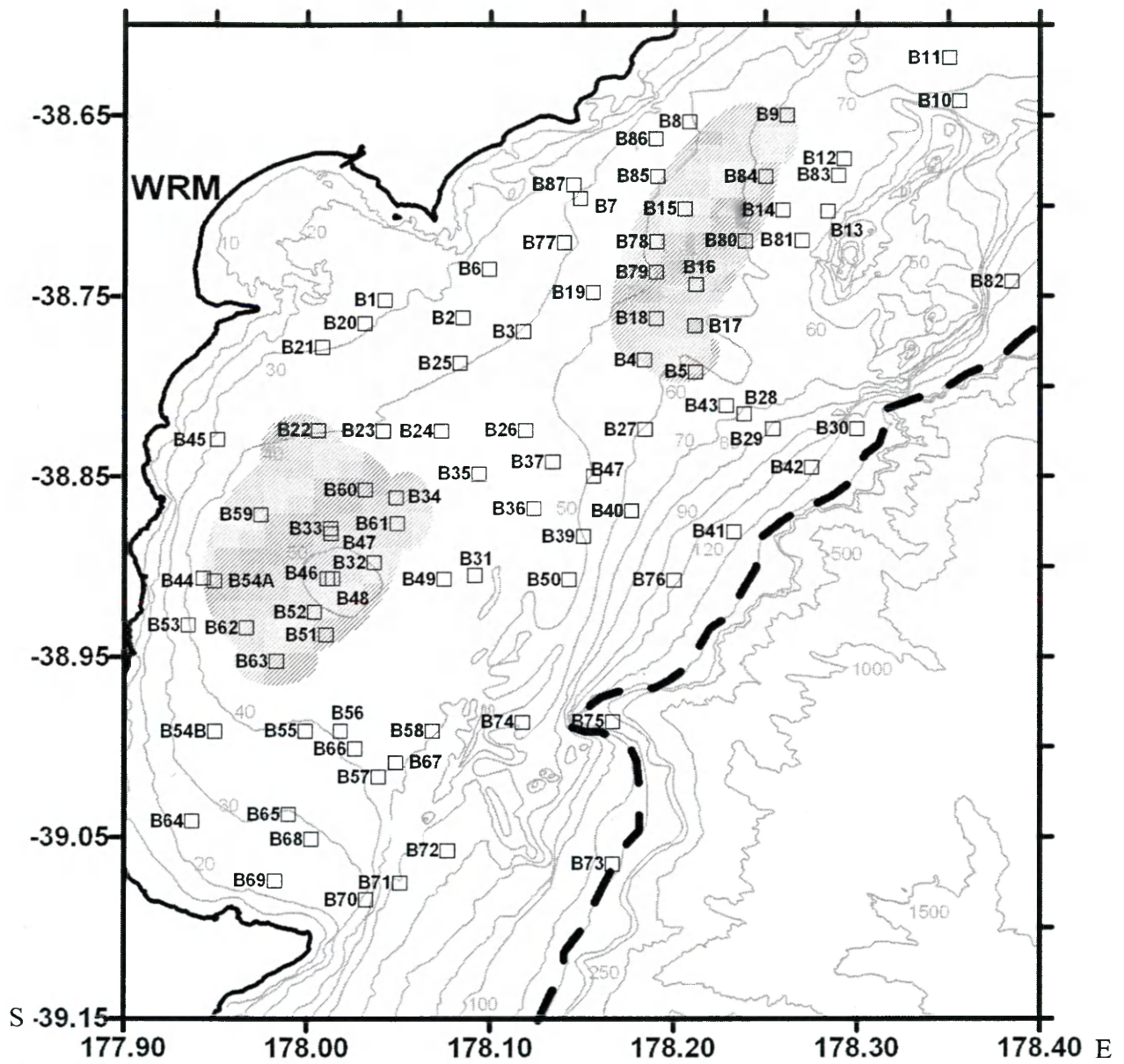


Figure 3. Waipaoa discharge at Kanakanaia from January 1, 2004 to February 28, 2005. Bold rectangle indicates time of cruise. Note that there was a roughly 3-month period where no high discharge events were recorded prior to the cruise.

Figure 3

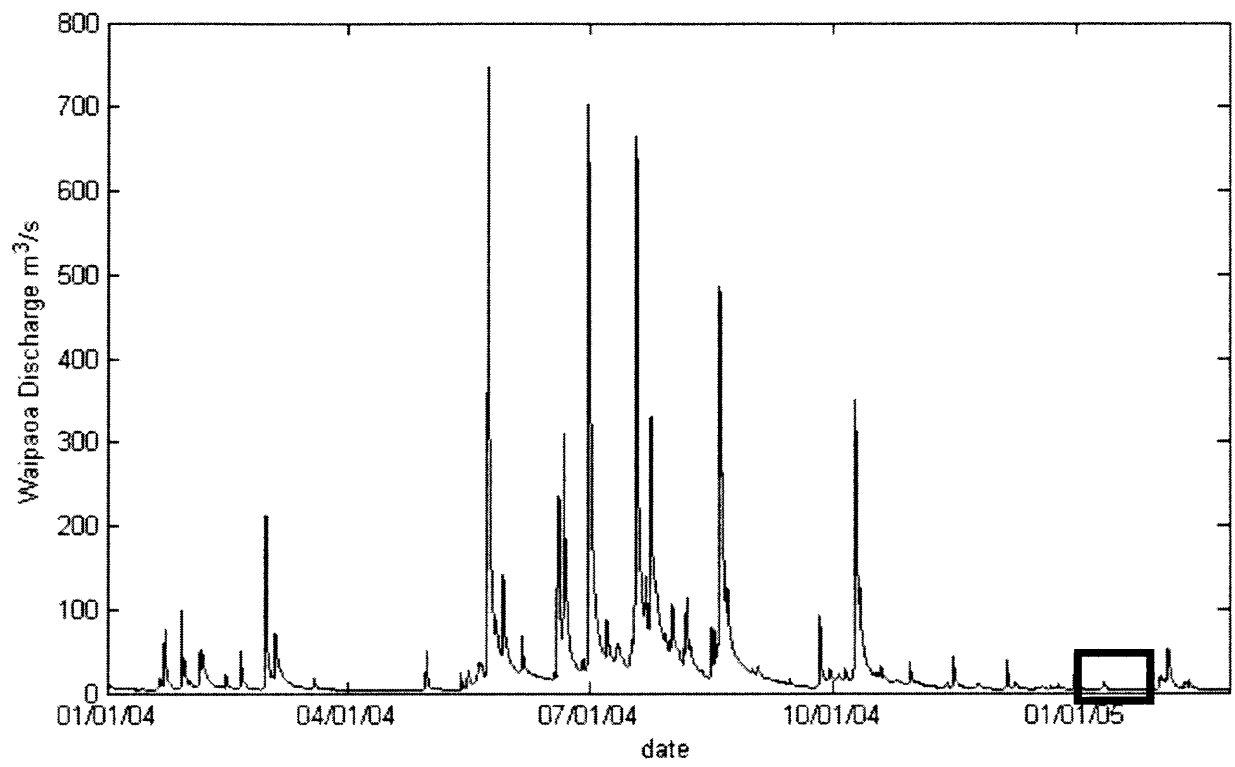
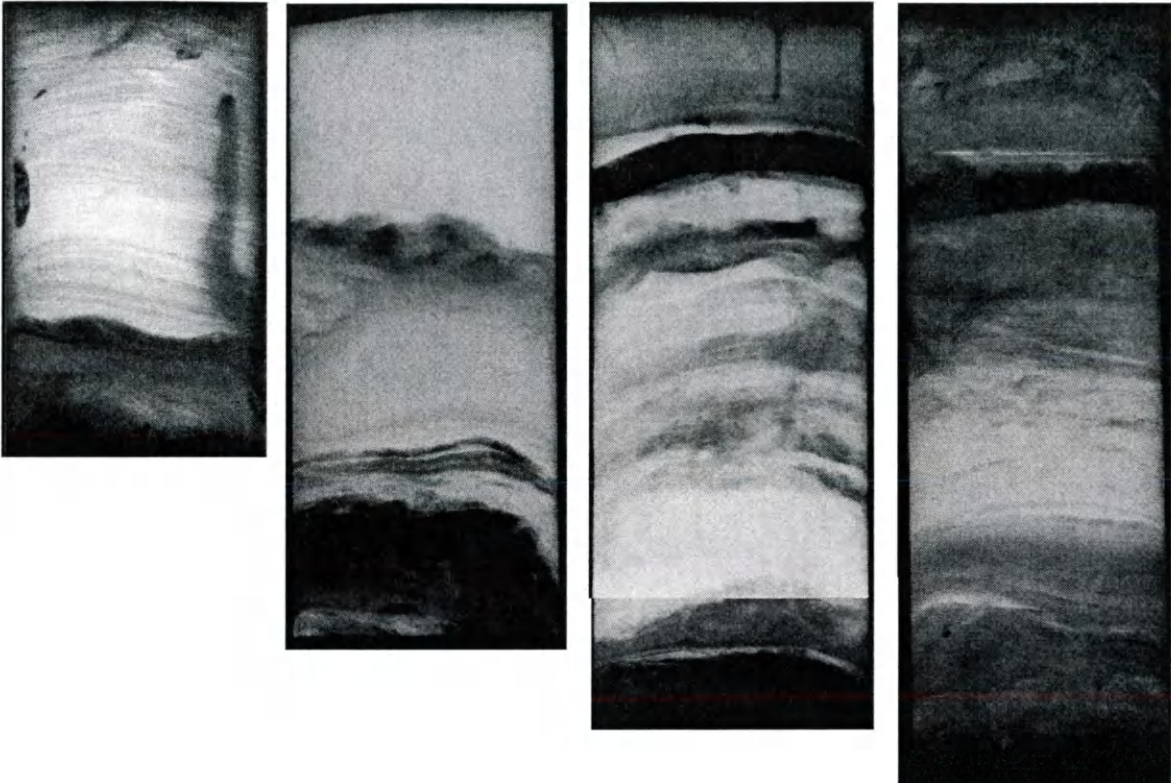


Figure 4. Facies Classifications

X-radiographic examples of facies from box cores on the Waipaoa shelf. These images are X-ray negatives: lighter greys = higher bulk density; darker greys = lower bulk density. The width of each X-radiograph represents 10cm. X-radiographs are labeled with corresponding box core number.

- A) A range of X-ray examples showing the diversity within the interbedded/laminated muds and sands (ILMS) facies, ranging from physically laminated sands on the right to interbedded mud and sands on the left.
- B) Examples of the mixed layers and mottles (MLM) facies.
- C) Examples of the mottled muds (MM) facies.
- D) Examples of shell hash and pebble rubble.

Figure 4A



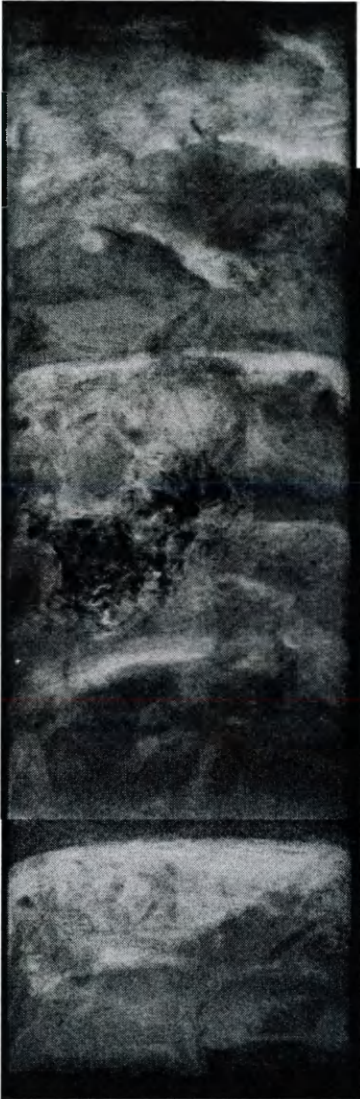
B1

B6

B20

B24

Figure 4B



B26

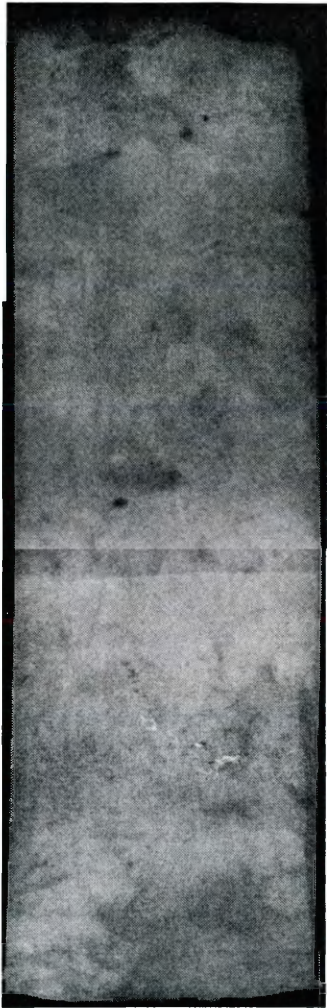


B19

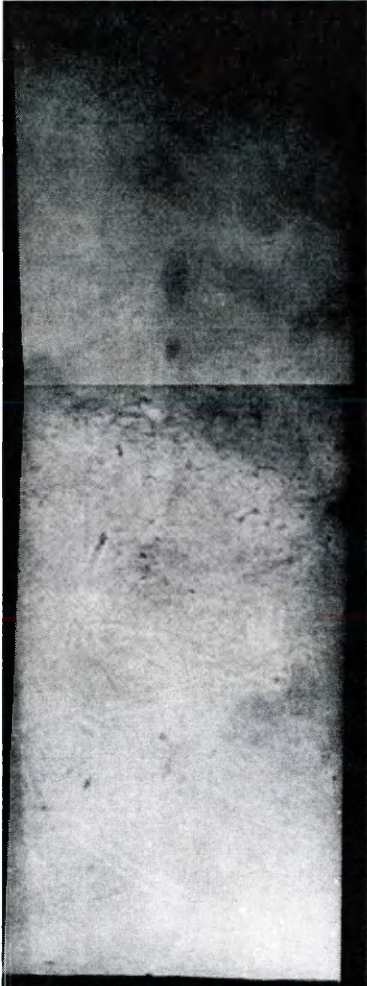


B61

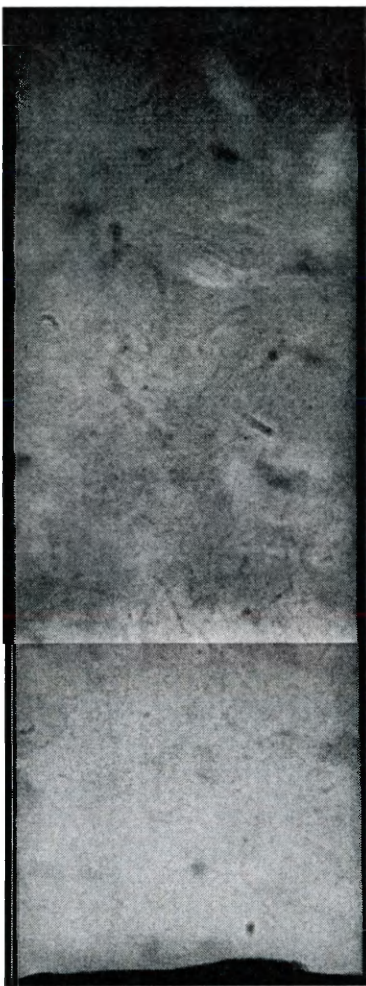
Figure 4C



B85



B63

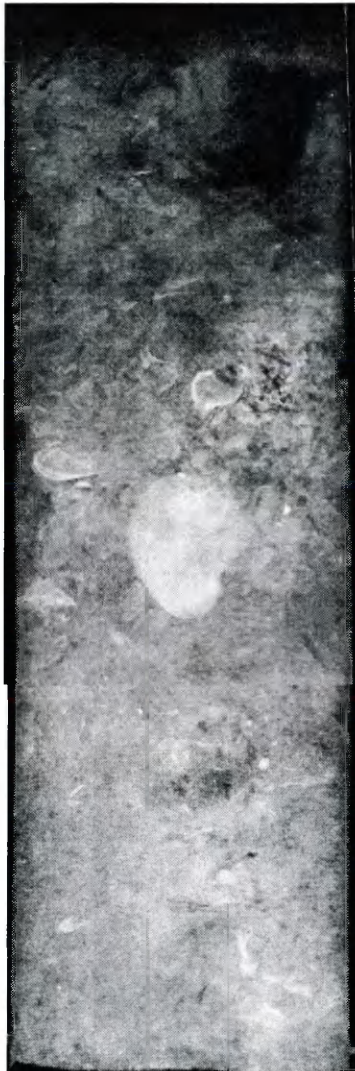


B46

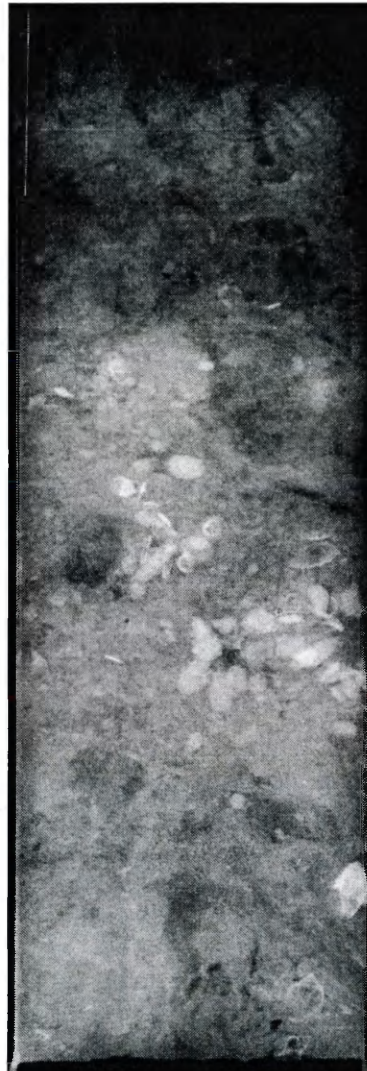
Figure 4D



B13



B57



B40

Figure 5. Regional Facies Map

Spatial distribution of facies on Waipaoa continental shelf with X-radiographic examples. A = core B20; B = core B26; C = core B46. Location of letter on map is approximate location of core on shelf. Blue = interbedded/laminated sands and muds (ILMS); Green = mixed layers and mottles (MLM); Yellow = mottled muds (MM). The dashed line at 150m indicates the shelf break. WRM = Waipaoa River Mouth.

Figure 5

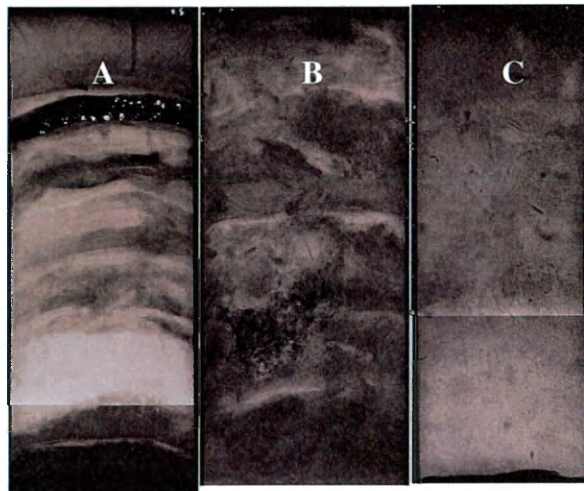
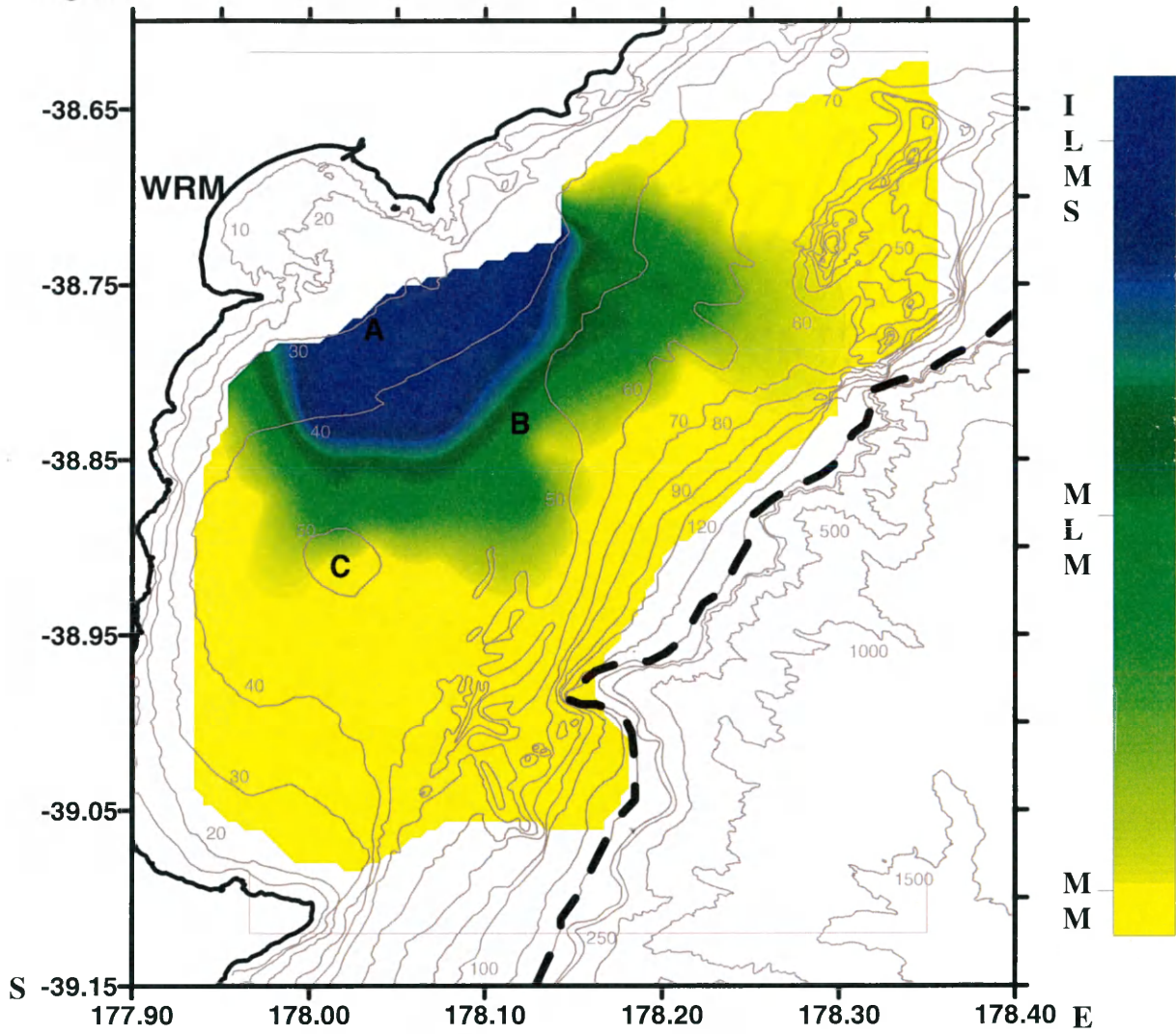
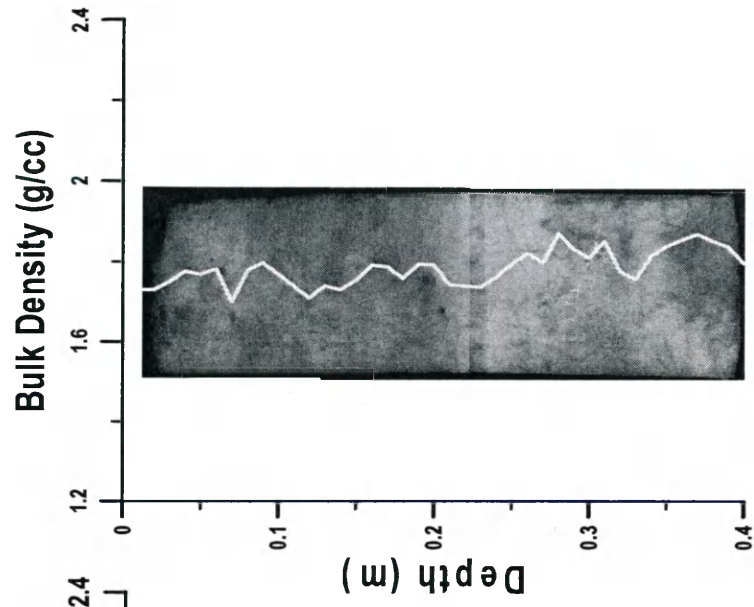
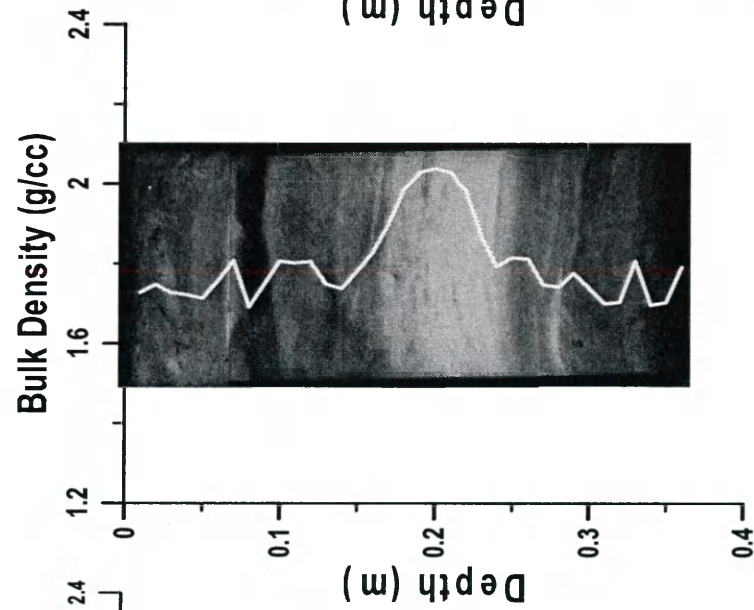


Figure 6. Bulk Density Profiles overlain onto X-radiographs

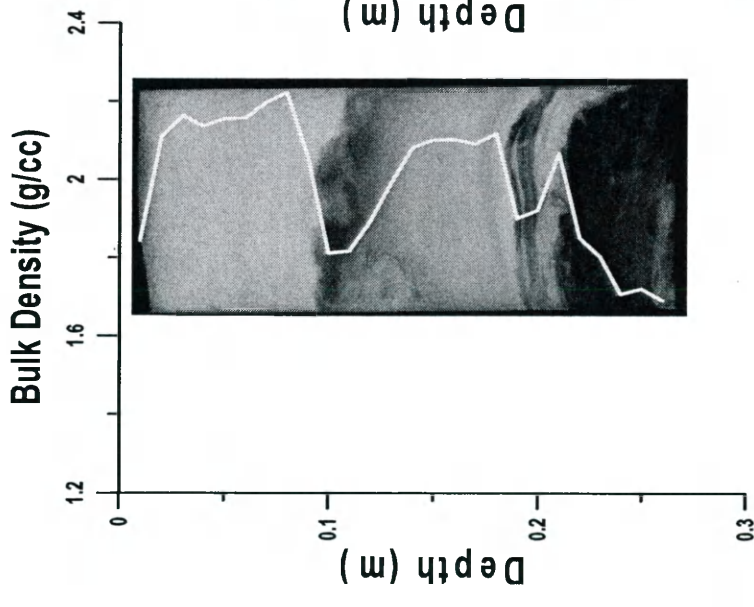
Examples of X-radiographs from each facies classification with measured multi-sensor core logger (MSCL) bulk density profiles overlain. B6 = interbedded/laminated muds and sands (ILMS); B24 = mixed layers and mottles (MLM); B85 = mottled mud (MM).



B85



B24



B6

Figure 7. Spatial Distribution of Bulk Densities

Spatial distribution of average (whole core) sediment dry bulk densities (g cc^{-1}) along and across the continental shelf. The dashed line at 150m indicates the shelf break. WRM = Waipaoa River Mouth.

- A) Average bulk density of each core.
- B) Average bulk density from the surface to 5cm depth of each core.

Figure 7A

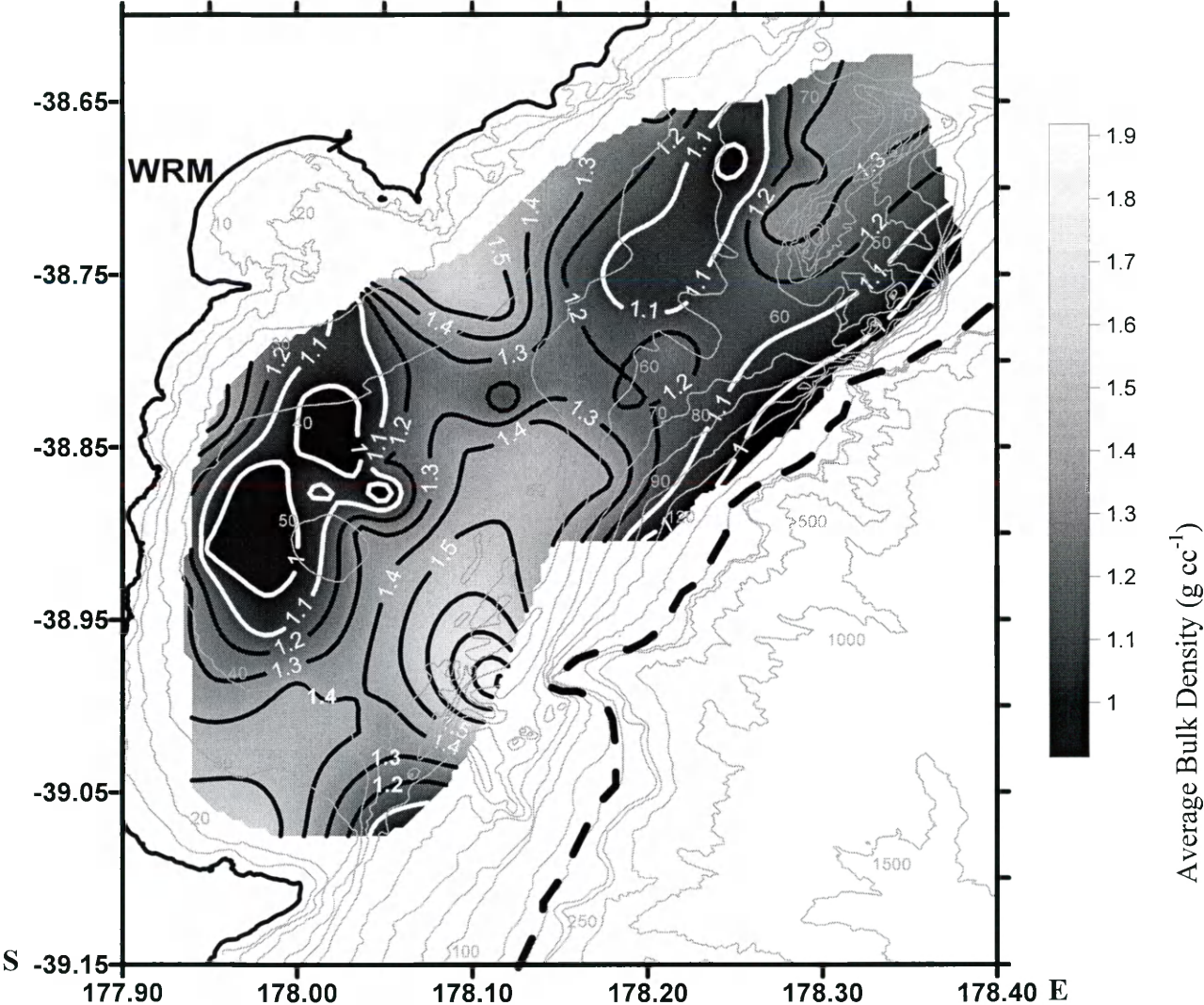


Figure 7B

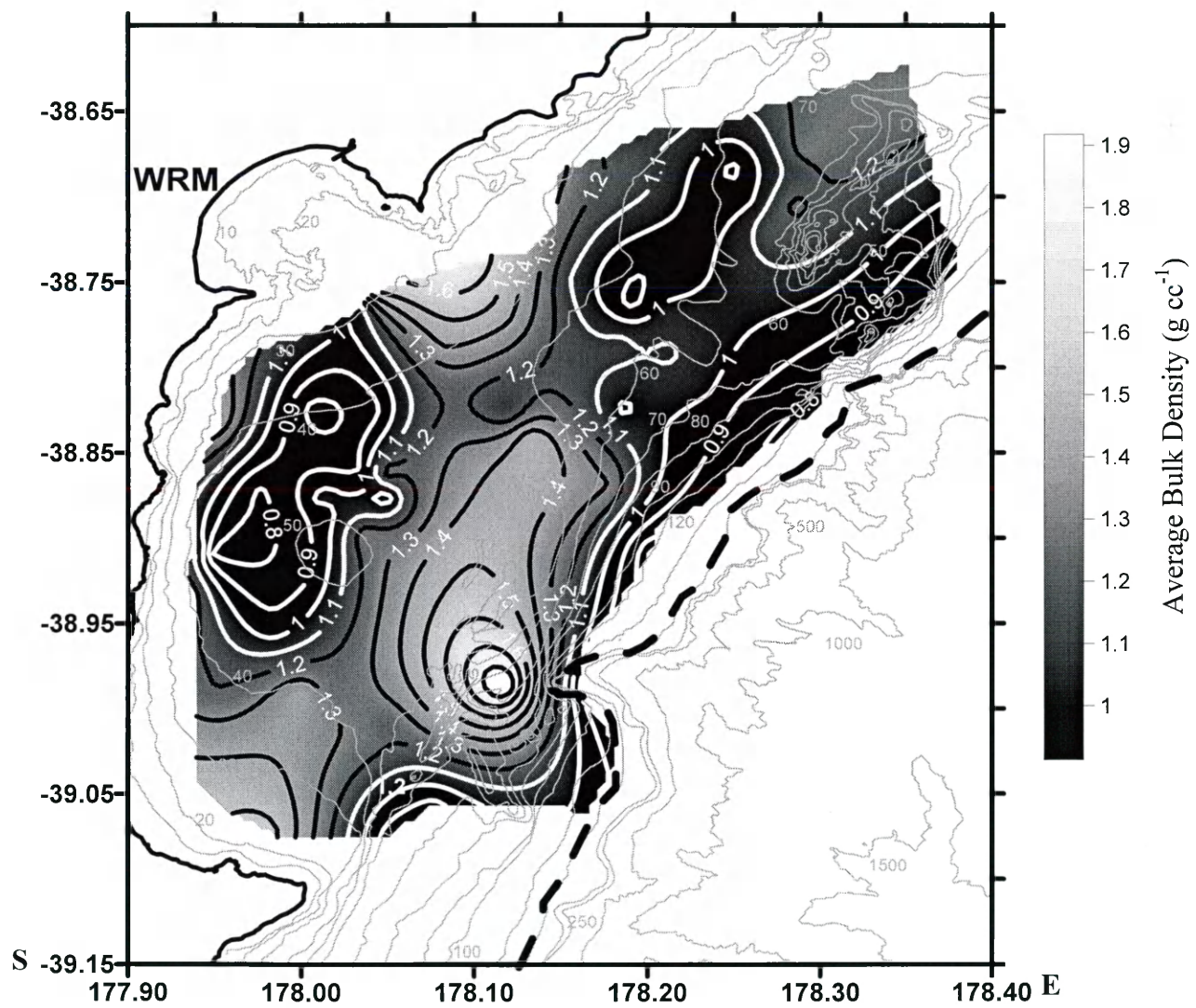


Figure 8. Bulk Density, ^7Be and ^{210}Pb

Bulk density (g cc^{-1} ; average and surface to 5cm interval) and ^7Be inventories and ^{210}Pb accumulation rate results and standard deviations by shelf region. Shelf regions (southern and northern depocenters, bypassing and shelf break areas) are defined by ^{210}Pb accumulation rate data from Miller and Kuehl (submitted). See *Section 2.1* and Figure 2 for lists of box cores within each region.

- A) Bulk density average and bulk density from the surface to 0-5cm interval average by shelf region (g cc^{-1}).
- B) ^7Be inventory (dpm cm^{-2}) and ^{210}Pb (cm yr^{-1}) by shelf region.

Figure 8

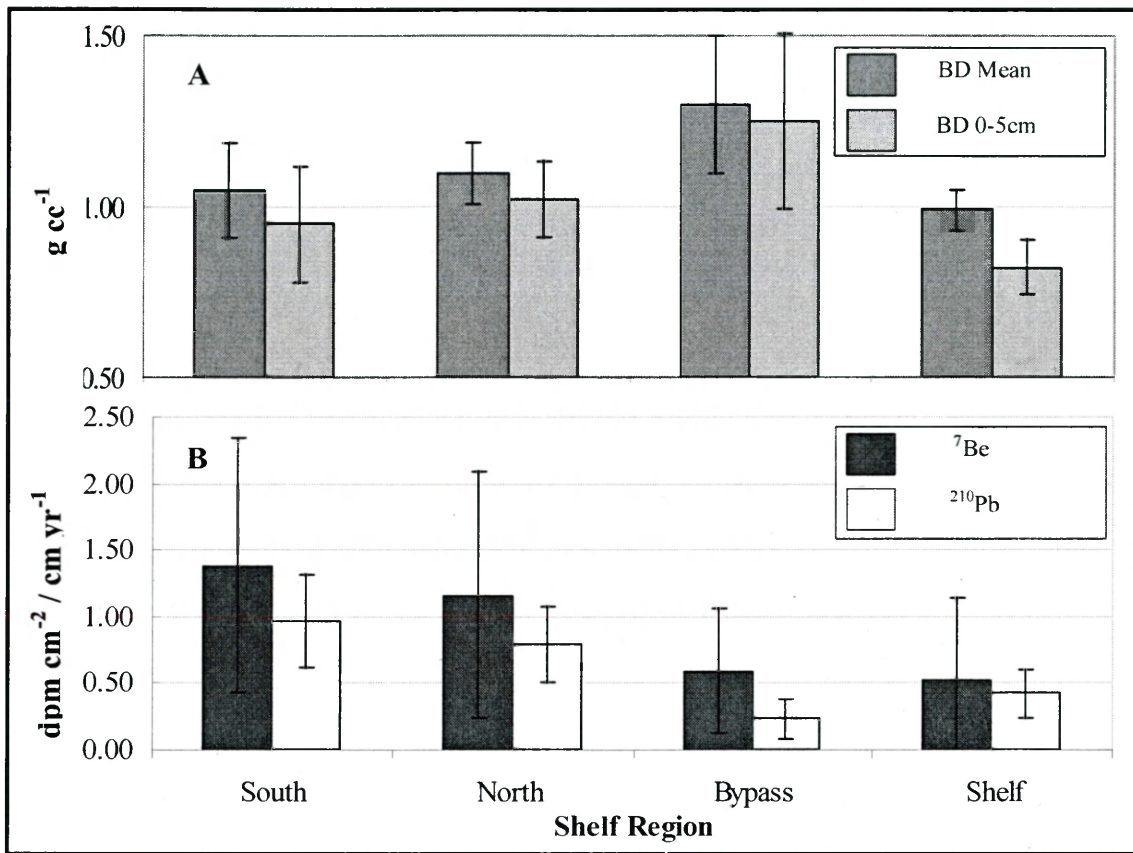


Figure 9. ^7Be Concentration Maps

Spatial distribution of ^7Be surface specific activities (dpm g^{-1}) and inventories (dpm cm^2), which show integration of activity through depth, on the continental shelf. Scale and color bar are the same for each map. The dashed line at 150m indicates the shelf break. WRM = Waipaoa River Mouth.

- A) Surface (0-1cm) specific activity (dpm g^{-1}).
- B) ^7Be inventories (dpm cm^{-2}).
- C) Average surface-5cm bulk density (g cc^{-1}) with ^7Be inventory (dpm cm^{-2}) contours overlain.

Figure 9

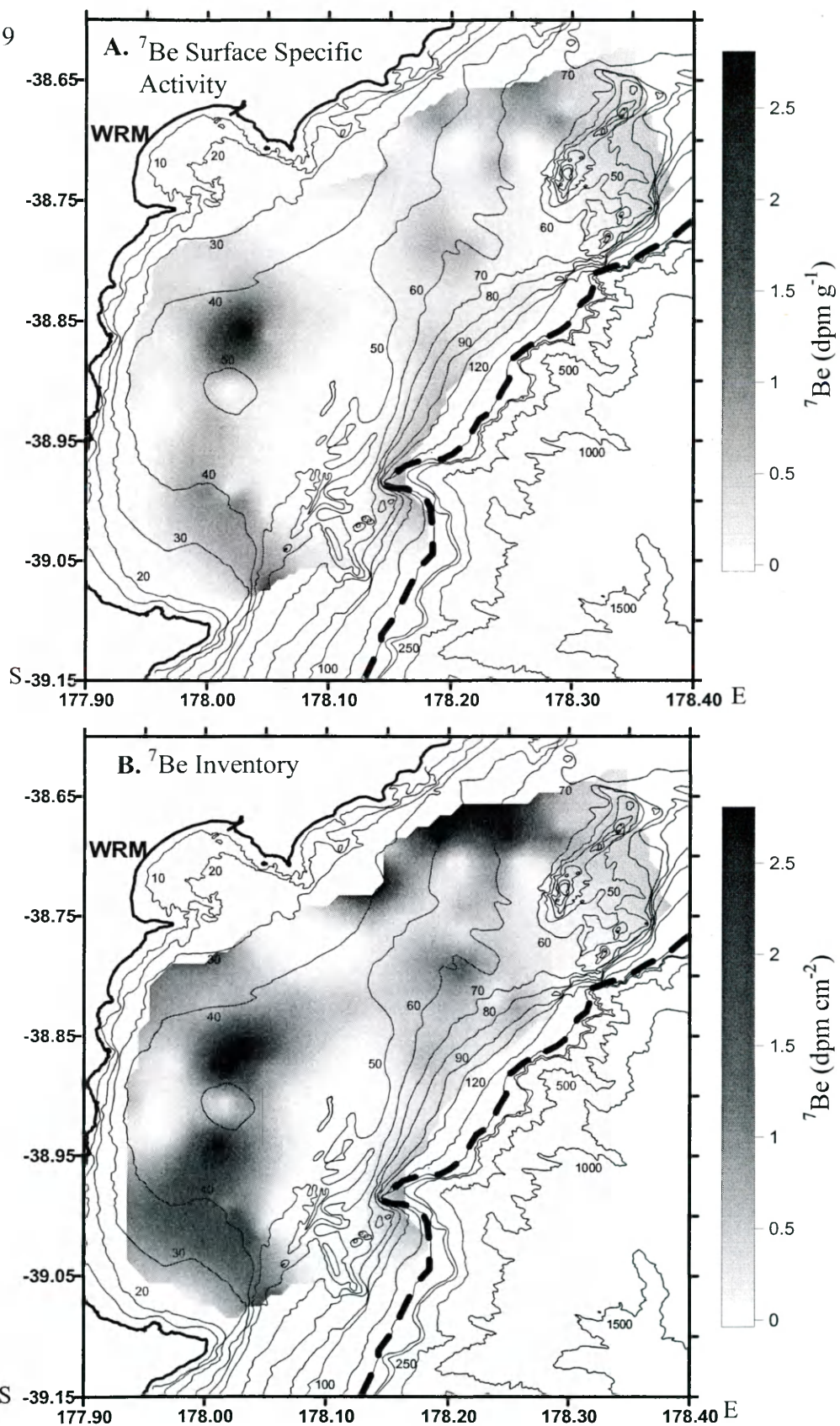


Figure 9C. Surface to 5cm average bulk density with ^7Be inventory contours.

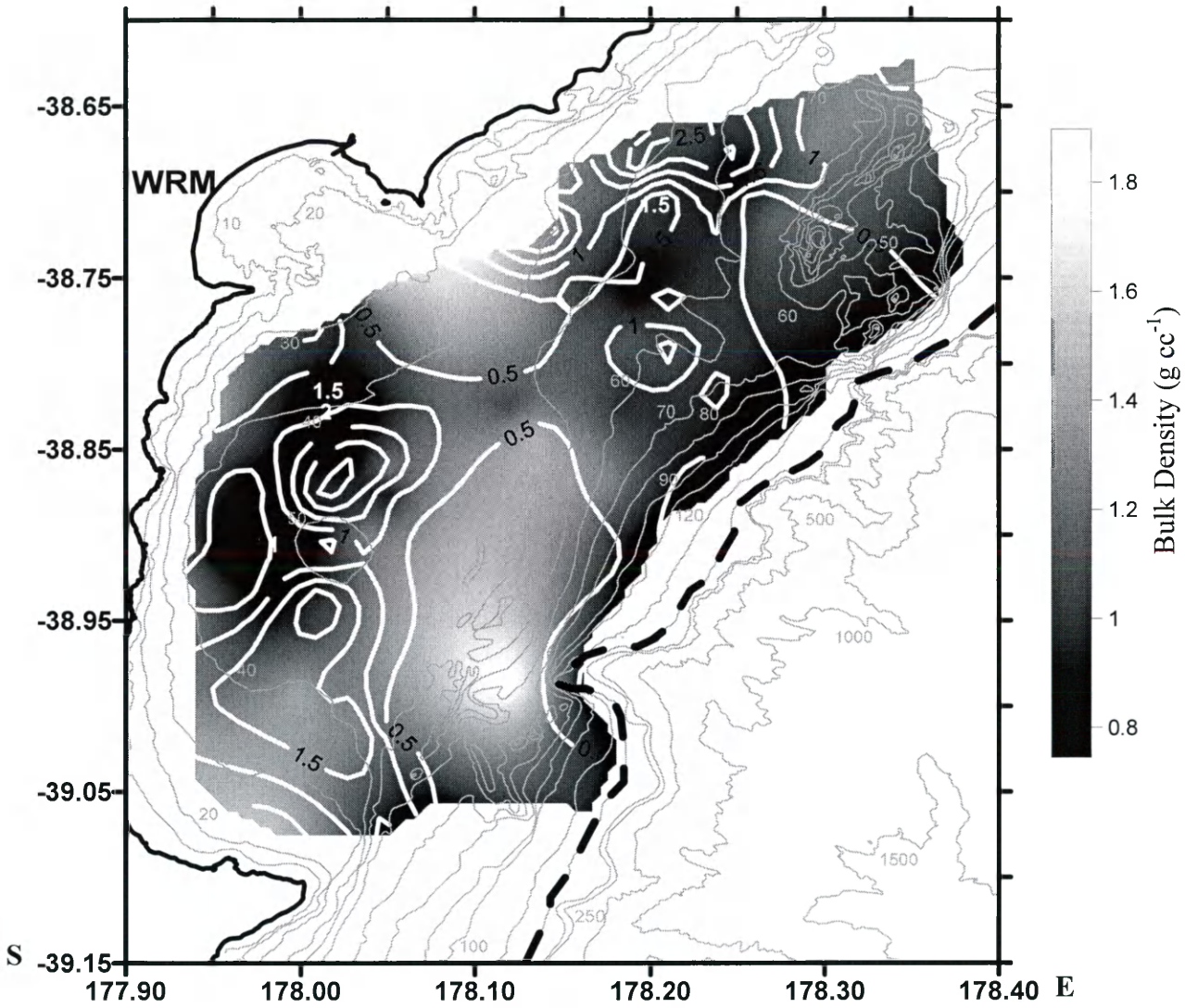


Figure 10. Sedimentation Patterns

- A) Spatial distribution of facies with characteristic ^{210}Pb activity profiles from Kasten Cores overlain.
- B) ^{210}Pb accumulation rates (cm y^{-1}) overlain with average bulk density (g cc^{-1}) contours.
- C) ^{210}Pb accumulation rates (cm y^{-1}) overlain with ^7Be inventory (dpm cm^{-2}) contours.

Figure 10A. Facies with characteristic ^{210}Pb activity profiles overlain.

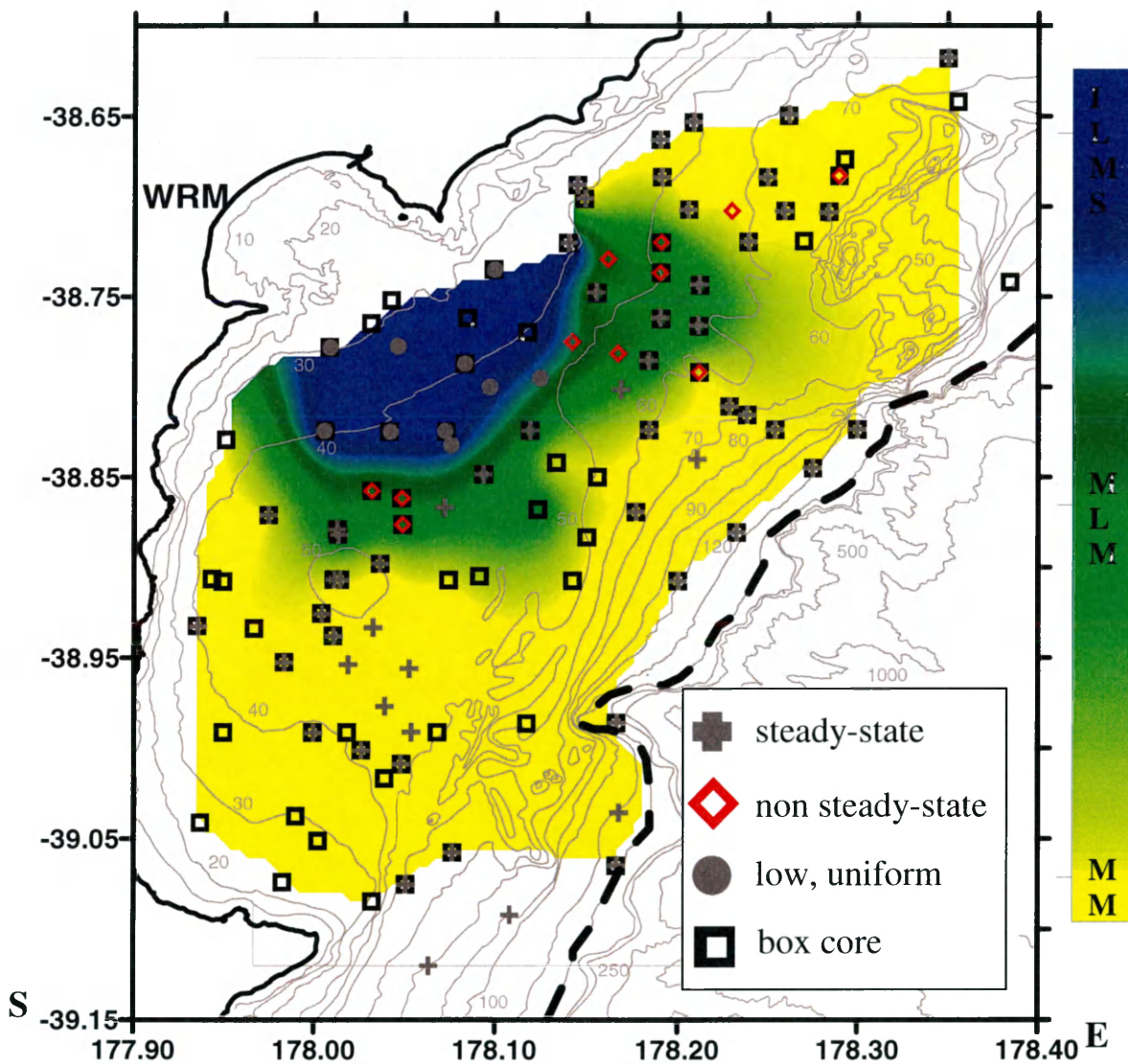


Figure 10B: Bulk density (contours) vs. ^{210}Pb accumulation rates.

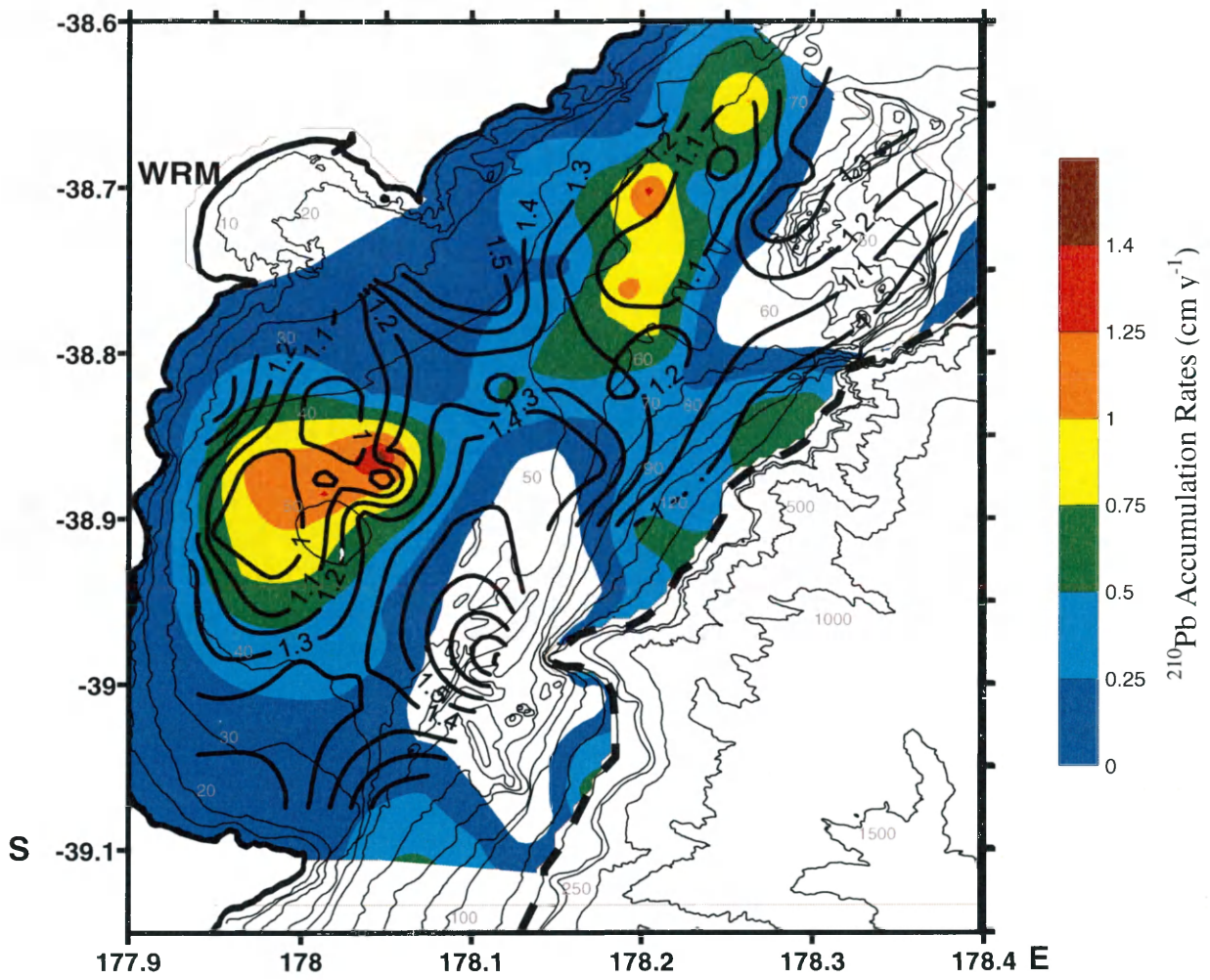


Figure 10C: ^7Be inventory (contours) vs. ^{210}Pb accumulation rates.

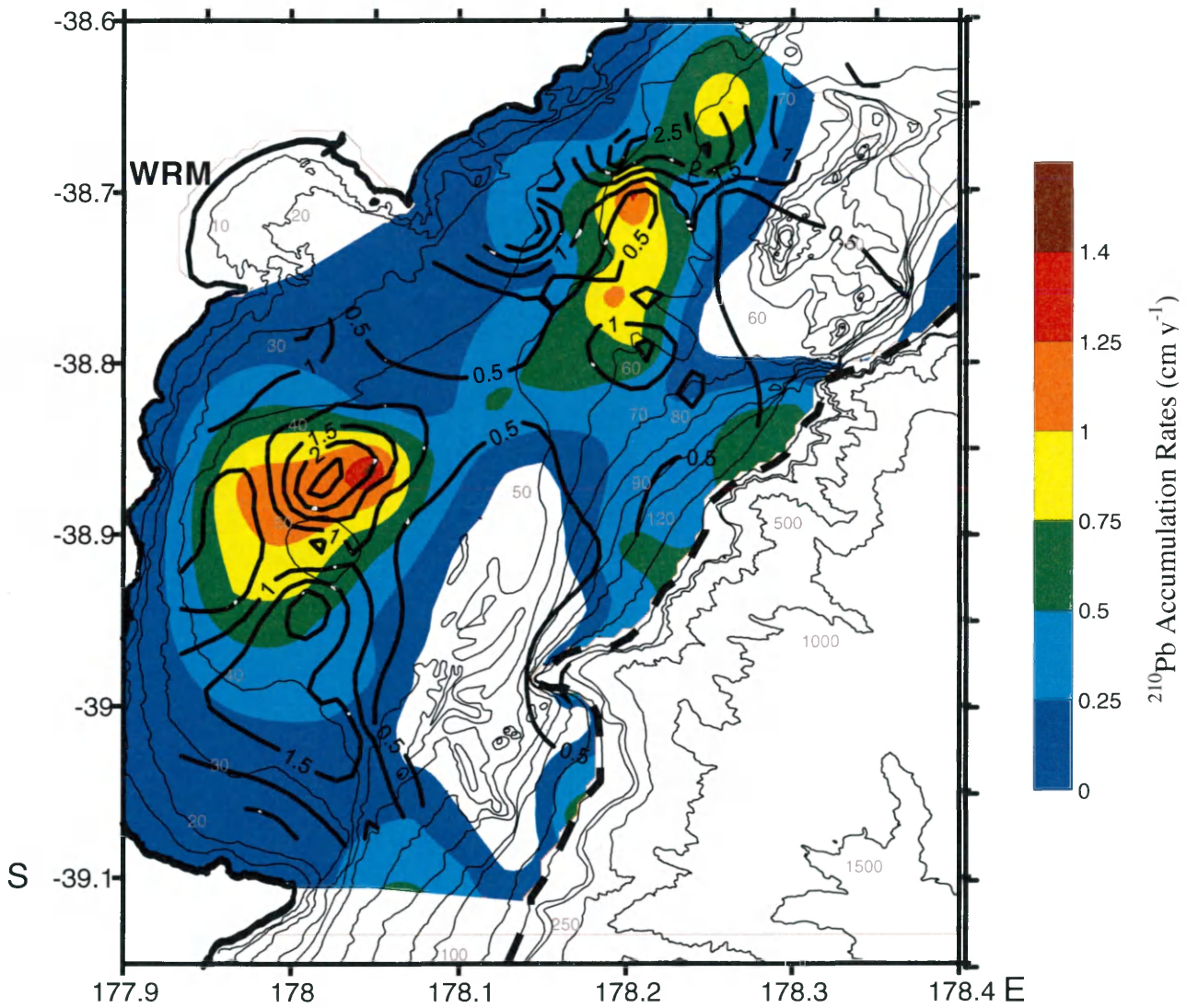


Figure 11. Theoretical schematic showing various parameters on the shelf along shore-parallel transect A-A'

Parameters are as follows:

Percent sand and mud based on surface sample splits of each box core from Wood (2006).

Physical Disturbance and Biological Mixing Intensity based on X-radiographic and facies analyses along with water depth and distance from river mouth.

Accumulation Rate based on ^{210}Pb geochronology (Miller and Kuehl, submitted) of Kasten cores located on the A-A' transect.

Dissipation Time based on the hypothetical time for a deposited layer to be destroyed, after Wheatcroft et al. (2007).

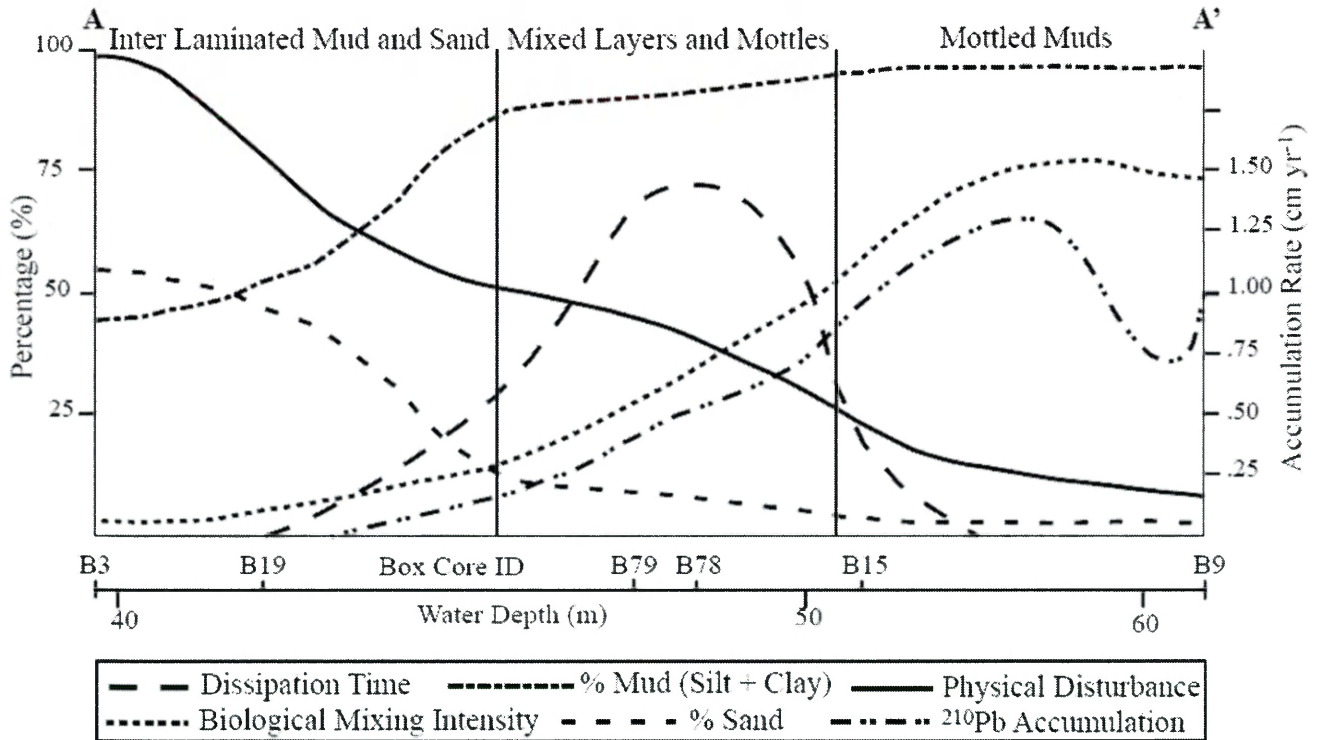
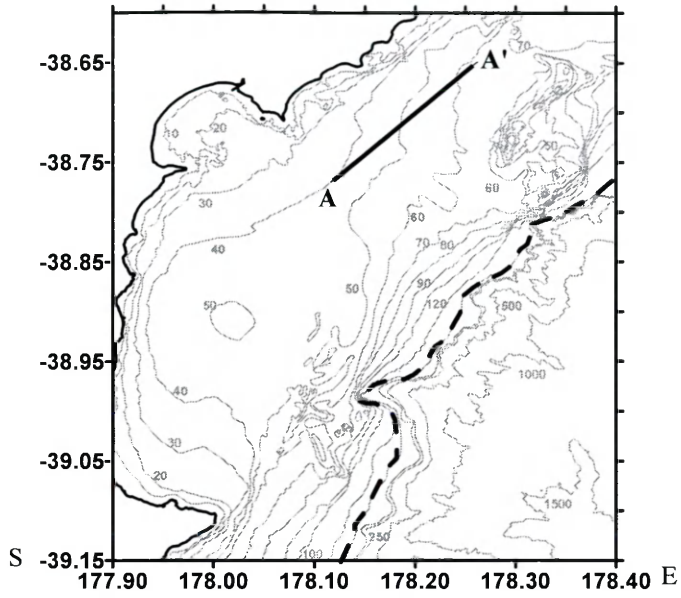


Table 1.

T-test results (P-values) to test the differences in parameters between subenvironments on the shelf. Significant results ($P < .05$) are indicated by an asterisk (*). Shelf regions (southern and northern depocenters, bypassing and shelf break areas) are defined by ^{210}Pb accumulation rate data from Miller and Kuehl (submitted). See *Section 2.1* and Figure 2 for lists of box cores within each region.

- A) Mean bulk density (g cc^{-1})
- B) Mean surface to 5cm interval bulk density (g cc^{-1})
- C) ^7Be Inventories (dpm cm^{-2})
- D) ^{210}Pb accumulation rates (cm y^{-1})

A. Mean BD

	South	North	Bypass
North	0.25		
Bypass	0.00*	0.00*	
Shelf	0.29	0.01*	0.00*

C. ^7Be

	South	North	Bypass
North	0.57		
Bypass	0.01*	0.03*	
Shelf	0.05*	0.14	0.83

B. BD Surface-5cm

	South	North	Bypass
North	0.26		
Bypass	0.00*	0.01*	
Shelf	0.07	0.00*	0.00*

D. ^{210}Pb

	South	North	Bypass
North	0.21		
Bypass	0.00*	0.00*	
Shelf	0.00*	0.01*	0.03*

APPENDIX A

Kasten and Box Core Information

Core	Latitude (S)	Longitude (E)	Water Depth (m)	Date Collected
B1	38 45.1335	178 2.553	27	01.15.04
B2	38 45.727	178 5.072	32	"
B3	38 46.186	178 7.056	38	"
B4	38 47.125	178 11.039	54	"
B5	38 47.517	178 12.708	59	"
B6	38 44.110	178 5.939	33	"
B7	38 41.758	178 8.907	40	01.16.05
B8	38 39.211	178 12.498	49	"
B9	38 38.993	178 15.688	61	"
B10	38 38.523	178 21.338	67	"
B11	38 37.088	178 21.006	75	"
B12	38 40.438	178 17.563	64	"
B13	38 42.184	178 17.040	62	"
B14	38 42.156	178 15.574	62	"
B15	38 42.110	178 12.353	52	"
B16	38 44.627	178 12.720	55	"
B17	38 45.982	178 12.693	57	"
B18	38 45.738	178 11.430	53	"
B19	38 44.889	178 9.327	45	"
B20	38 45.907	178 1.883	29	"
B21	38 46.701	178 0.491	31	"
B22	38 49.468	178 0.361	42	01.17.05
B23	38 49.484	178 2.493	43	"
B24	38 49.489	178 4.375	46	"
B25	38 47.234	178 4.988	38	"
B26	38 49.461	178 7.138	48	"
B27	38 49.438	178 11.053	59	"
B28	38 48.927	178 14.308	70	"
B29	38 49.422	178 15.244	79	"
B30	38 49.413	178 17.991	123	"
B31	38 54.297	178 5.486	41	01.19.05
B32	38 53.880	178 2.191	52	"
B33	38 52.741	178 0.762	49	"
B34	38 51.702	178 2.907	49	"
B35	38 50.912	178 5.617	49	"
B36	38 52.077	178 7.404	41	"
B37	38 50.516	178 8.006	44	"
B38	38 50.994	178 9.347	49	"
B39	38 52.998	178 9.011	47	"
B40	38 52.156	178 10.621	62	"
B41	38 52.842	178 13.964	107	"
B42	38 50.705	178 16.510	112	"
B43	38 48.650	178 13.714	65	"
B44	38 54.394	177 56.589	43	01.20.05

Core	Latitude (S)	Longitude (E)	Water Depth (m)	Date Collected
B45	38 49.769	177 57.046	32	"
B46	38 54.404	178 0.652	49	"
B47	38 52.908	178 0.786	48	"
B48	38 54.407	178 0.847	49	"
B49	38 54.423	178 4.467	45	01.21.05
B50	38 54.442	178 8.543	46	"
B51	38 56.280	178 0.629	49	"
B52	38 55.532	178 0.239	50	"
B53	38 55.950	177 56.098	39	"
B54A	38 54.478	177 56.952	46	"
B54B	38 59.486	177 56.971	39	"
B55	38 59.484	177 59.949	41	"
B56	38 59.483	178 1.097	43	"
B57	39 1.009	178 2.351	45	"
B58	38 59.479	178 4.102	50	"
B59	38 52.271	177 58.476	56	01.22.05
B60	38 51.460	178 1.907	47	"
B61	38 52.575	178 2.948	49	"
B62	38 56.038	177 57.991	47	"
B63	38 57.158	177 58.996	47	"
B64	39 2.480	177 56.214	27	"
B65	39 2.260	177 59.389	32	"
B66	39 0.077	178 1.572	43	"
B67	39 0.534	178 2.912	49	"
B68	39 3.087	178 0.137	29	"
B69	39 4.448	177 58.944	26	"
B70	39 5.086	178 1.937	40	"
B71	39 4.524	178 3.059	62	"
B72	39 3.463	178 4.607	67	"
B73	39 3.898	178 9.990	129	01.23.05
B74	38 59.183	178 7.038	63	"
B75	38 59.170	178 9.990	254	"
B76	38 54.457	178 12.003	95	"
B77	38 43.233	178 8.376	38	01.26.05
B78	38 43.205	178 11.437	50	"
B79	38 44.212	178 11.428	51	"
B80	38 43.176	178 14.344	59	"
B81	38 43.158	178 16.192	62	"
B82	38 44.526	178 23.068	111	"
B83	38 40.991	178 17.376	64	"
B84	38 41.035	178 14.992	61	"
B85	38 41.029	178 11.464	46	"
B86	38 39.787	178 11.410	45	"
B87	38 41.300	178 8.682	37	"
K1	38 47.517	178 12.710	59	01.15.05
K2	38 47.1255	178 11.0412	54	"
K6	38 38.521	178 21.398	68	"
K7	38 38.945	178 15.709	61	"

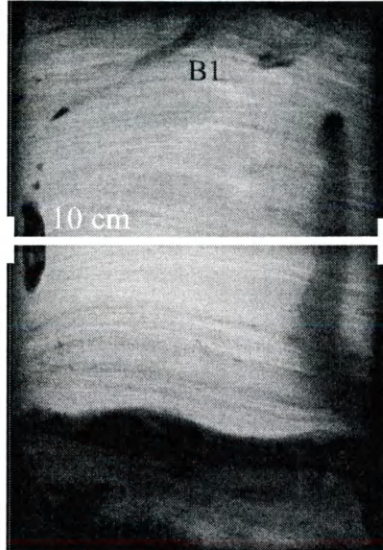
Core	Latitude (S)	Longitude (E)	Water Depth (m)	Date Collected
K8	38 39.191	178 12.518	48	"
K9	38 41.742	178 8.939	38	"
K10	38 44.118	178 5.975	31	01.16.05
K11	38 37.061	178 21.018	76	"
K11	38 37.060	178 21.018	76	"
K12	38 42.211	178 17.025	63	"
K13	38 42.156	178 15.556	62	"
K13	38 42.156	178 15.556	62	"
K14	38 42.117	178 12.336	52	"
K15	38 44.606	178 12.720	55	"
K16	38 45.961	178 12.687	56	"
K17	38 45.713	178 11.423	52	"
K18	38 44.874	178 9.322	44	"
K19	38 49.413	178 17.991	123	01.17.05
K20	38 49.420	178 15.247	79	"
K21	38 48.930	178 14.304	70	"
K21a	38 48.930	178 14.304	70	"
K21b	38 48.931	178 14.304	70	"
K22	38 49.438	178 11.055	60	"
K23	38 49.455	178 7.147	48	01.18.05
K24	38 47.232	178 4.989	38	"
K25	38 49.468	178 4.342	46	"
K26	38 49.499	178 2.525	43	"
K27	38 49.464	178 0.327	41	"
K28	38 46.702	178 0.518	30	"
K29	38 45.923	178 1.916	28	"
K30	38 48.651	178 13.715	65	01.20.05
K31	38 50.701	178 16.499	112	"
K32	38 52.840	178 13.960	109	"
K33	38 52.158	178 10.623	64	"
K34	38 50.913	178 5.611	48	"
K35	38 51.704	178 2.920	48	"
K36	38 52.741	178 0.759	48	"
K37	38 53.883	178 2.182	49	"
K38	38 54.296	178 5.484	40	"
K39	38 59.479	178 4.102	50	01.21.05
K40	39 0.972	178 2.361	45	"
K41	38 59.490	178 1.118	43	"
K42	38 59.498	177 59.972	41	"
K43	38 59.490	177 56.973	38	"
K44	38 55.970	177 56.126	38	"
K45	38 55.553	178 0.254	50	"
K46	38 56.295	178 0.649	49	"
K47	38 54.416	178 0.860	50	"
K48	38 52.922	178 0.807	49	"
K49	38 54.408	178 0.669	50	"
K50	38 49.773	177 57.039	33	"
K51	38 54.390	177 56.572	43	"

Core	Latitude (S)	Longitude (E)	Water Depth (m)	Date Collected
K52	38 54.455	178 12.001	95	1.23.05
K53	38 59.167	178 10.001	256	"
K54	39 3.899	178 9.998	130	"
K55	39 3.464	178 4.608	70	"
K56	39 4.523	178 3.060	62	"
K57	39 0.530	178 2.890	50	"
K58	39 0.086	178 1.580	43	"
K59	38 57.165	177 59.000	46	"
K60	38 56.046	177 57.996	46	"
K61	39 7.221	178 3.816	79	"
K62	39 5.537	178 6.495	91	"
K63	39 2.155	178 10.087	119	"
K64	38 57.372	178 3.161	47	01.24.05
K65	38 56.007	178 1.957	49	"
K66	38 52.578	178 2.934	49	"
K67	38 52.271	177 58.478	47	"
K68	38 51.459	178 1.910	48	"
K69	38 49.947	178 4.536	47	"
K70	38 46.657	178 2.764	32	"
K70	38 46.657	178 2.764	32	"
K71	38 49.367	178 5.587	47	"
K72	38 48.016	178 5.816	43	"
K72	38 48.012	178 5.816	43	"
K73	38 46.515	178 8.532	50	"
K74	38 46.905	178 10.039	51	"
K74	38 46.899	178 10.045	50	"
K75	38 48.099	178 10.142	53	"
K76	38 50.418	178 12.662	72	"
K77	38 41.299	178 8.681	37	01.26.05
K78	38 39.786	178 11.410	46	"
K79	38 41.029	178 11.460	47	"
K80	38 41.036	178 14.991	61	"
K81	38 40.987	178 17.382	65	"
K82	38 43.174	178 14.348	59	"
K83	38 42.157	178 13.819	57	01.27.05
K84	38 43.202	178 11.453	50	"
K85	38 44.211	178 11.427	50	"
K86	38 43.766	178 9.718	43	"
K86	38 43.766	178 9.718	43	"
K87	38 43.226	178 8.408	38	"
K87	38 43.226	178 8.408	38	"
K88	38 52.812	178 6.030	42	01.28.05
K89	38 52.018	178 4.315	49	"
K90	38 47.725	178 7.488	45	"
K91	38 47.866	177 58.995	33	"
K92	38 57.242	178 1.129	47	"
K93	38 58.624	178 2.350	47	"
K94	38 59.480	178 3.230	49	"

APPENDIX B

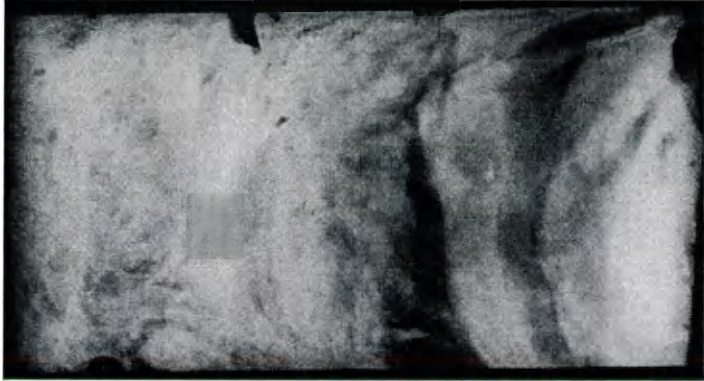
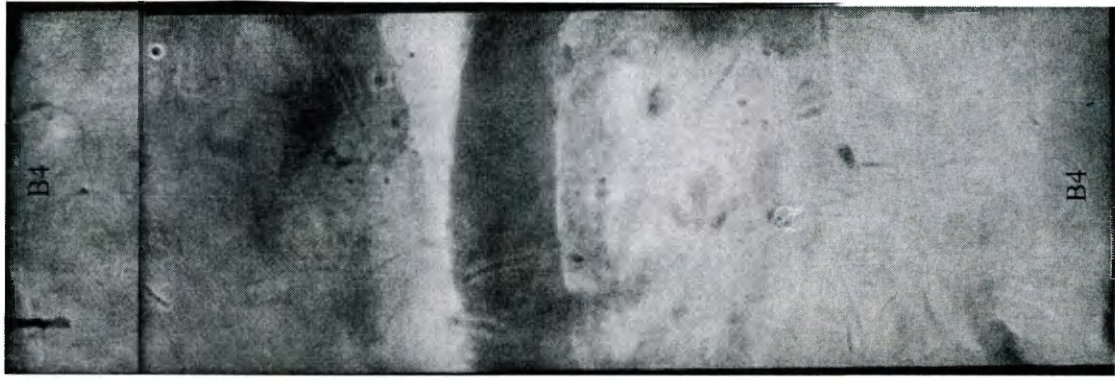
Box core X-radiographs and Facies Classifications

Key to X-radiographs:



X-radiograph negative –
light = high density; dark =
low density sediments.

- B1 ● } Box Core ID # / Symbol indicates facies classification / Notes
- – Interbedded / Laminated Muds and Sands (ILMS)
 - – Mottled Mud (MM)
 - – Mixed Layers and Mottles (MLM)
 - – Shell Hash / Pebbles
 - - Undetermined

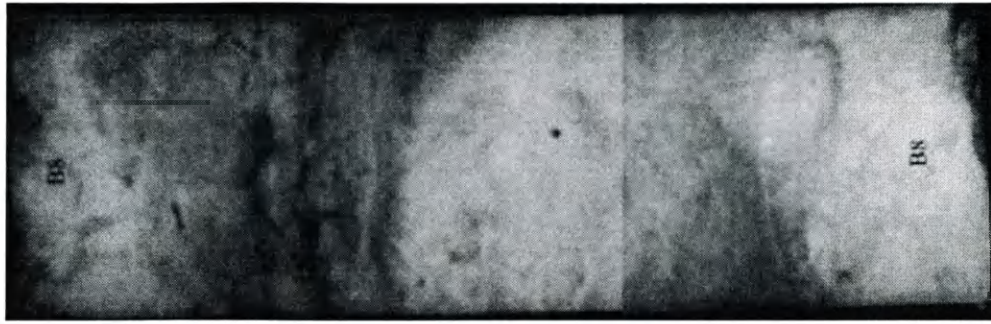


B4●●●●

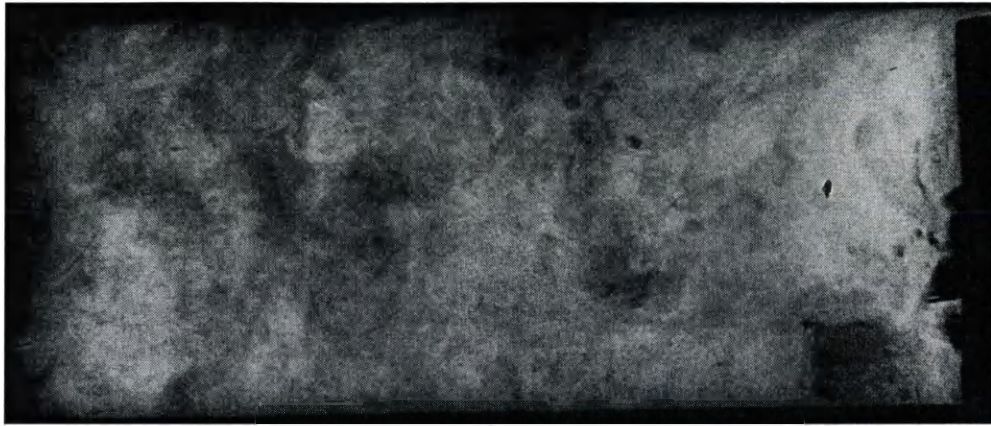
B3●

B2●

B1●



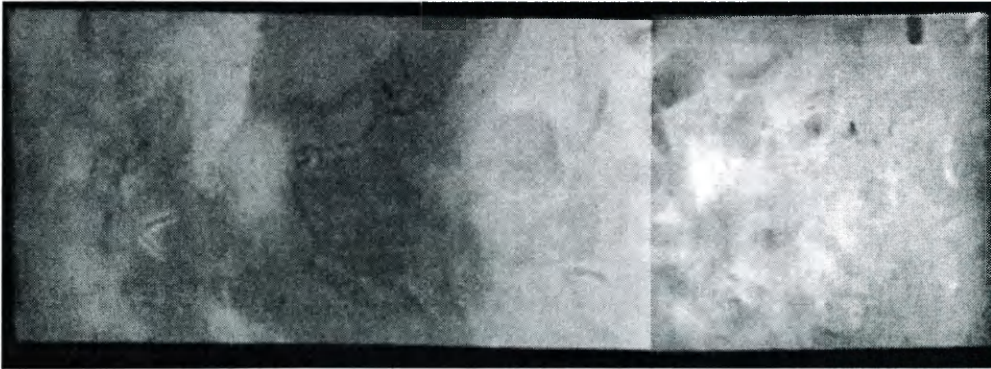
B8 ●●



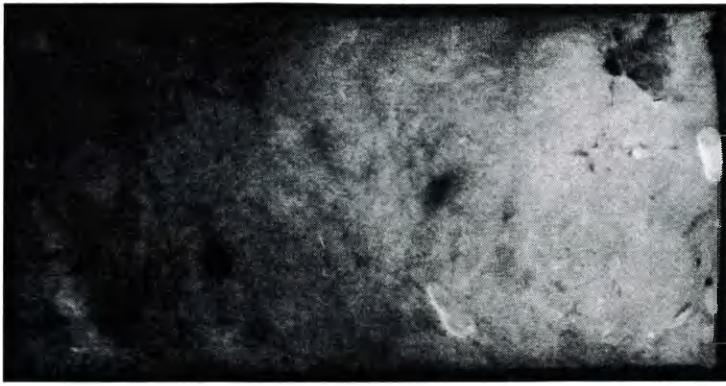
B7 ●●



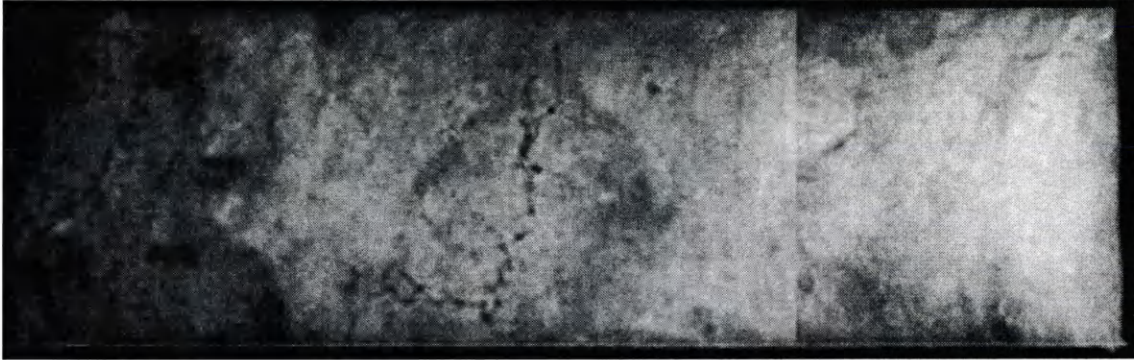
B6 ●



B5 ●●



B12 ●●●●●●



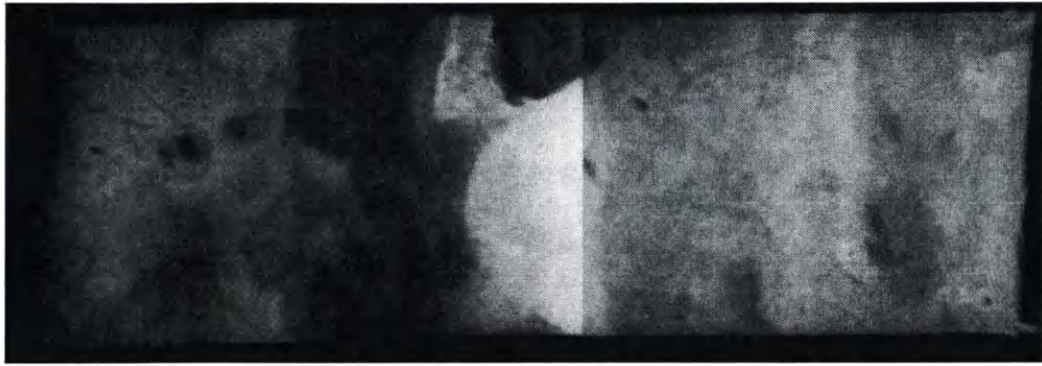
B11 ●●



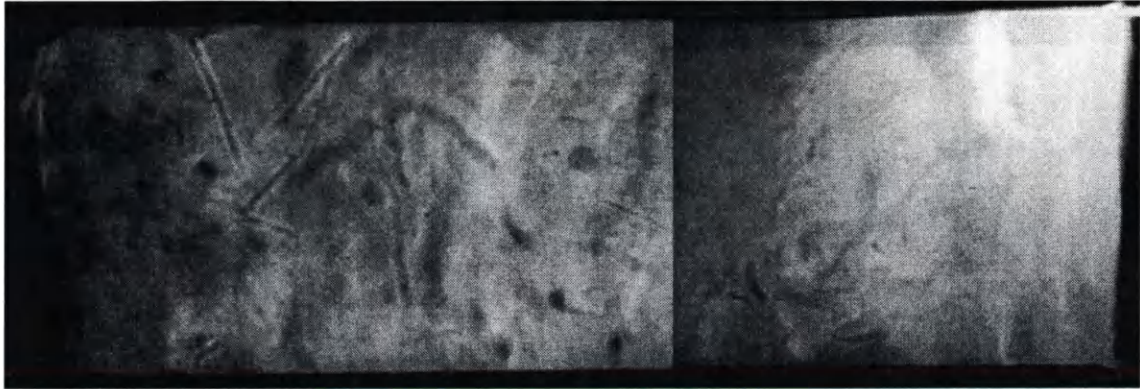
B10 ●●●



B9 ●●●



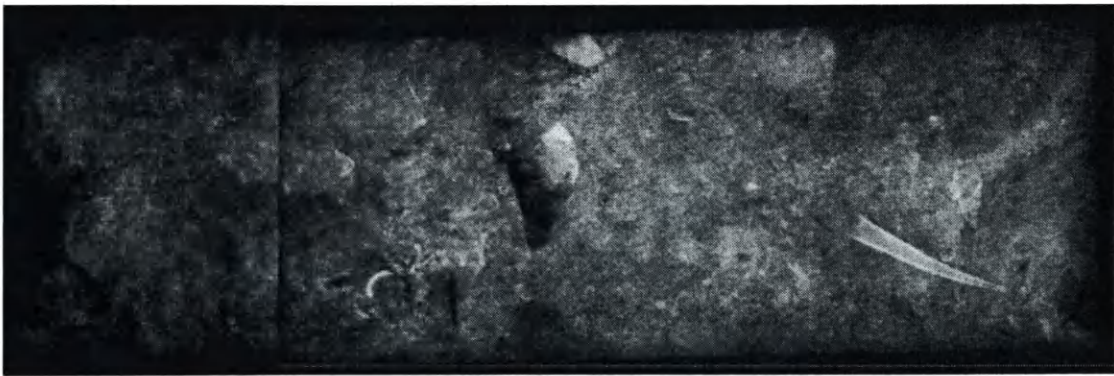
B16●●●●



B15●●



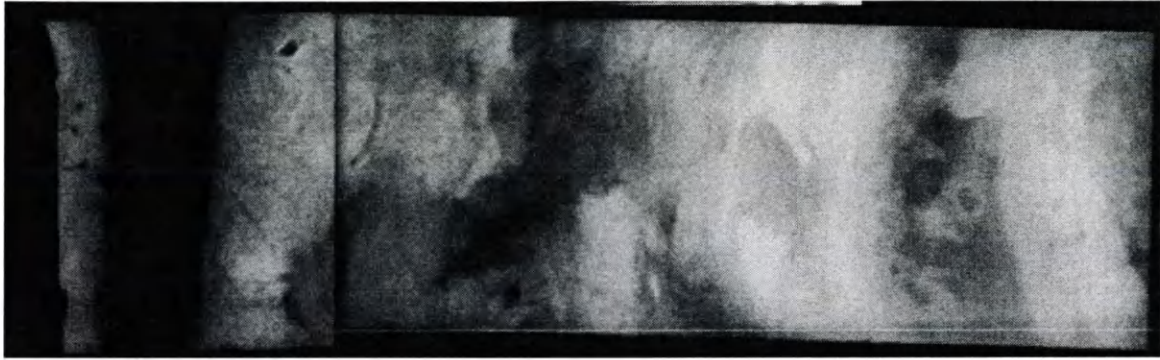
B14●●



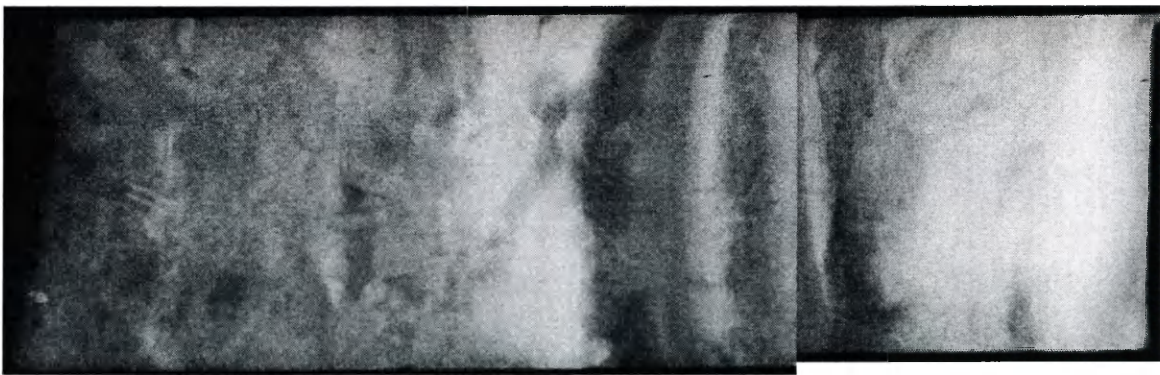
B13●●●●●



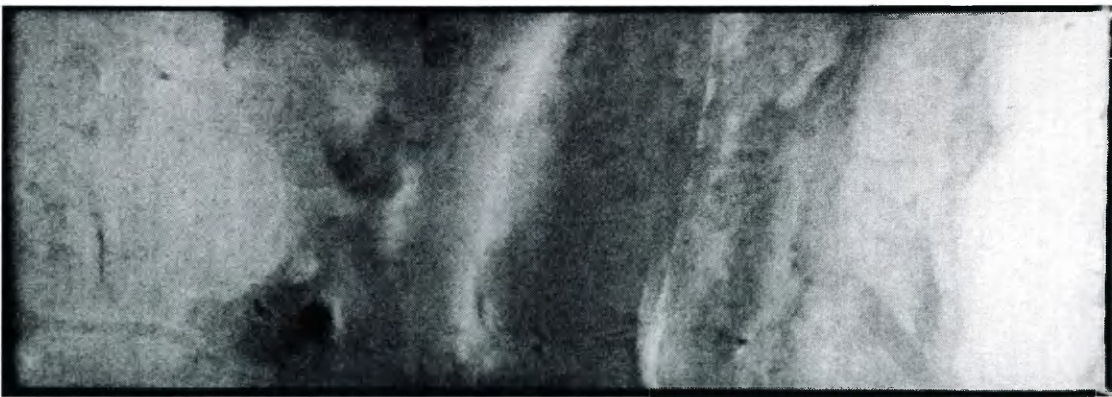
B20●



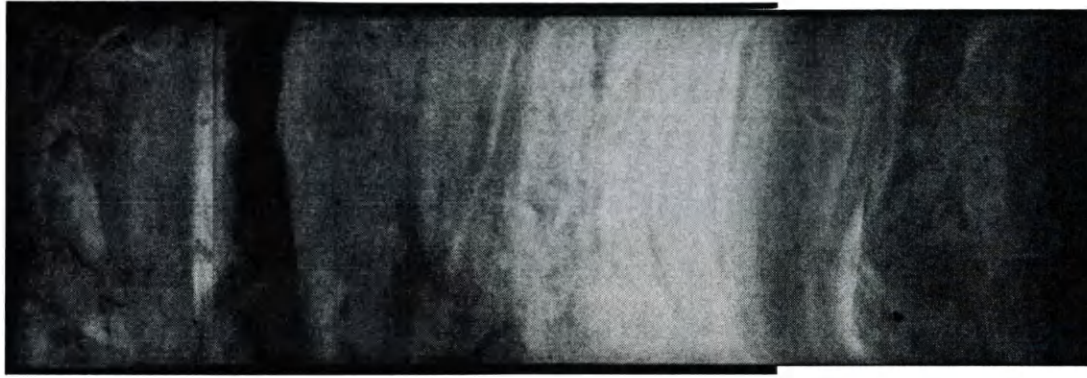
B19●●●●



B18●●●●



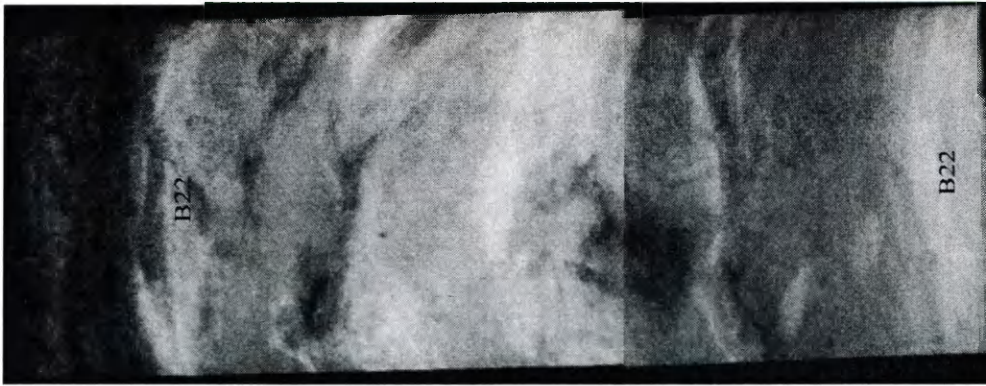
B17●●●●



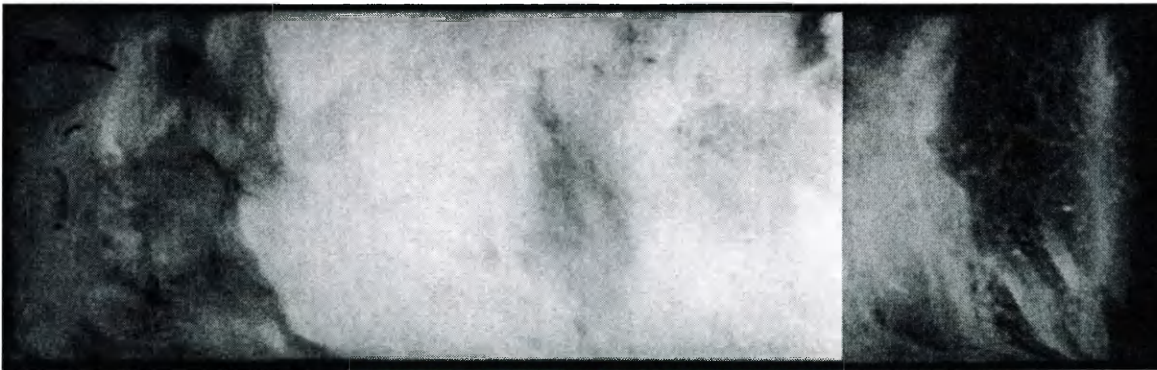
B24 ●



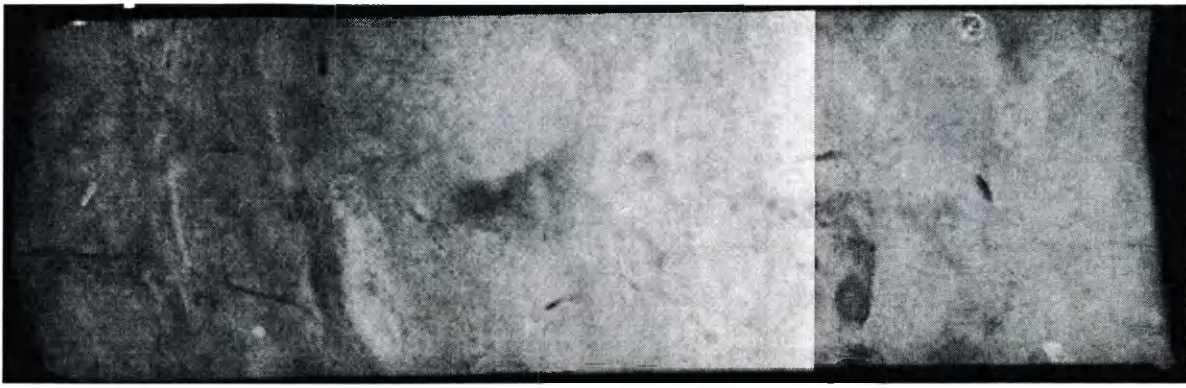
B23 ●



B22 ●



B21 ●



B28 ●●



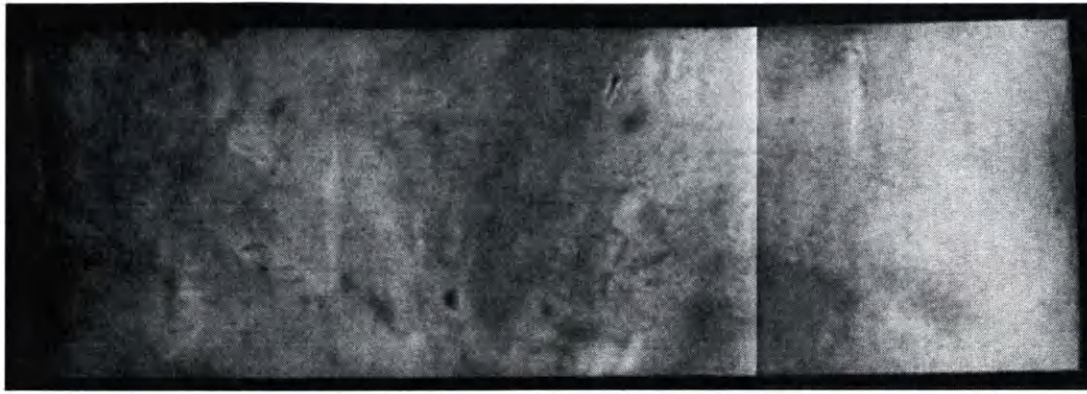
B27 ●●



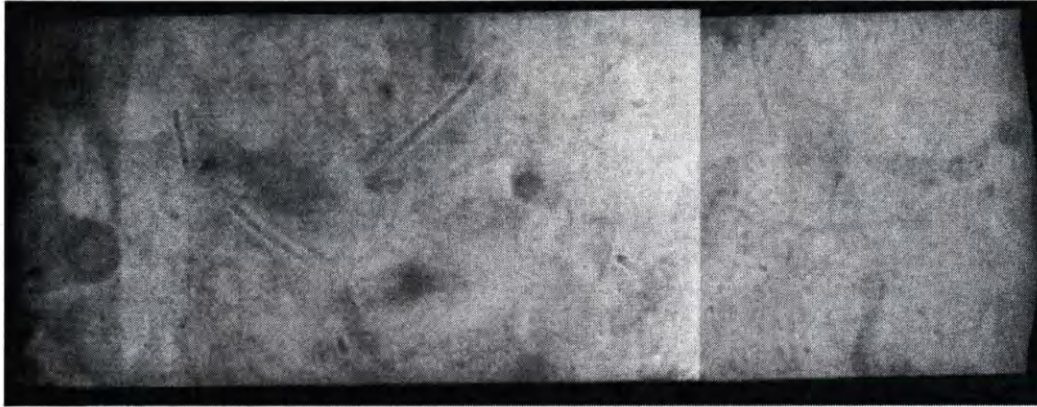
B26 ●●●



B25 ●



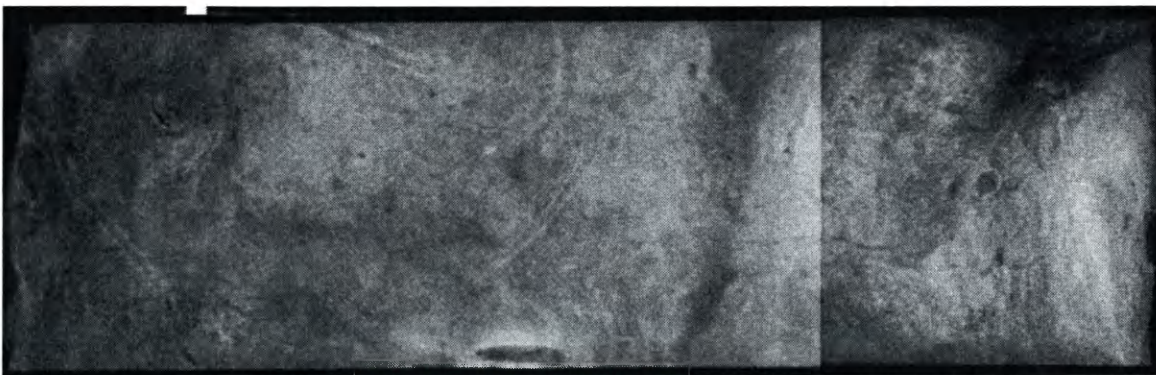
B33



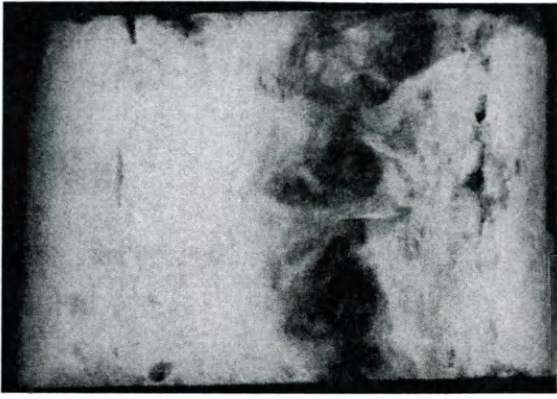
B32



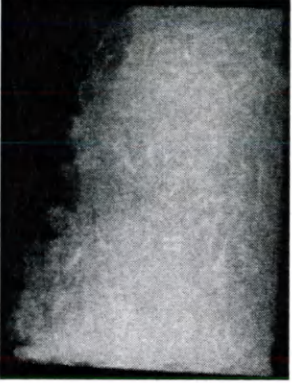
B30



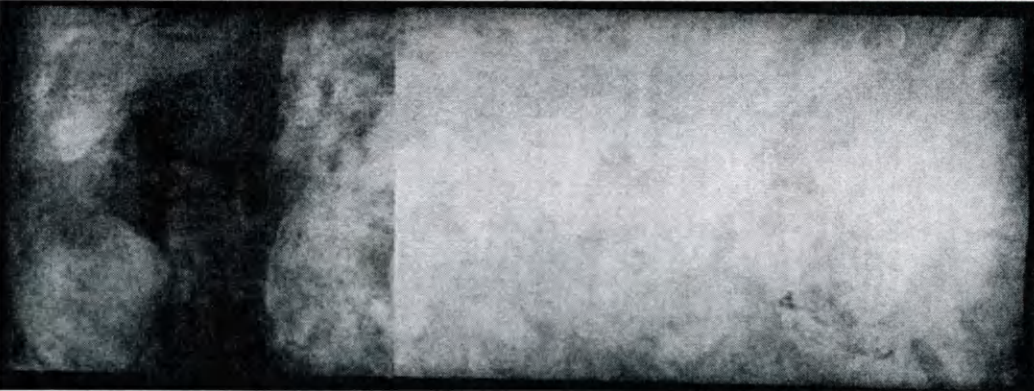
B29



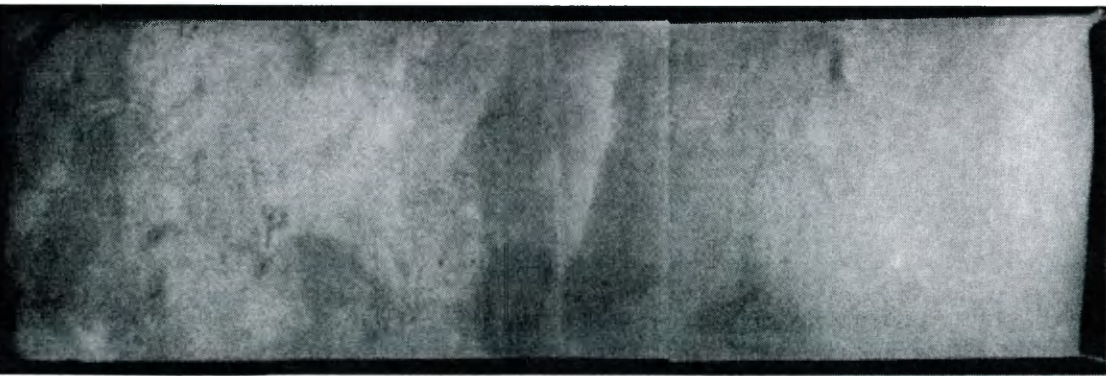
B37●●



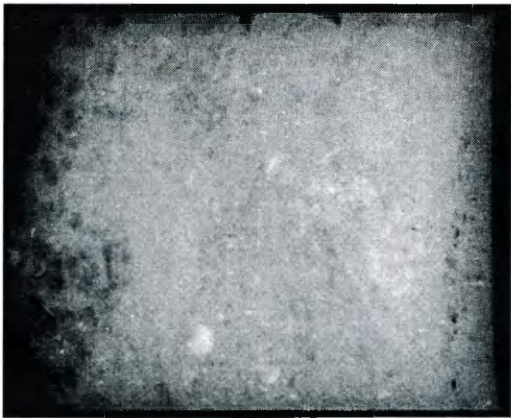
B36●●●●●



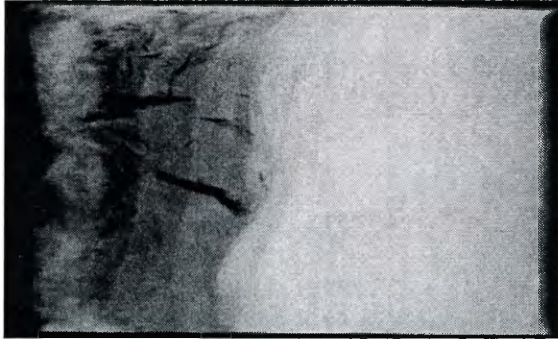
B35●●●



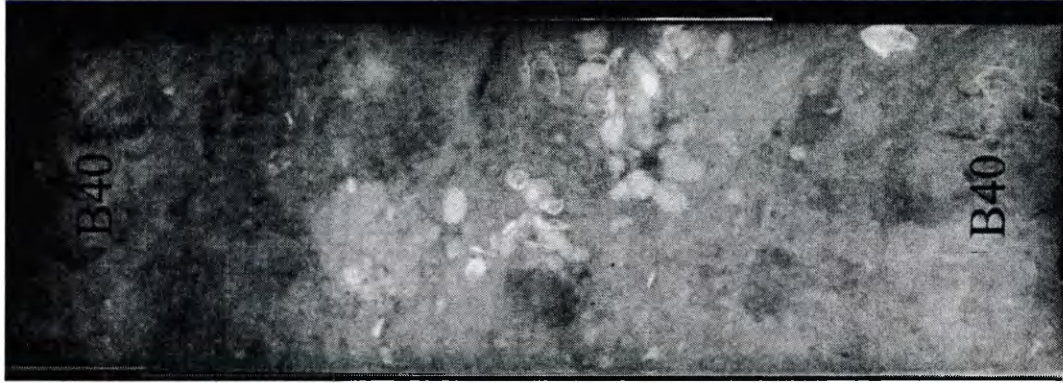
B34●●●



B38 ●●●●●



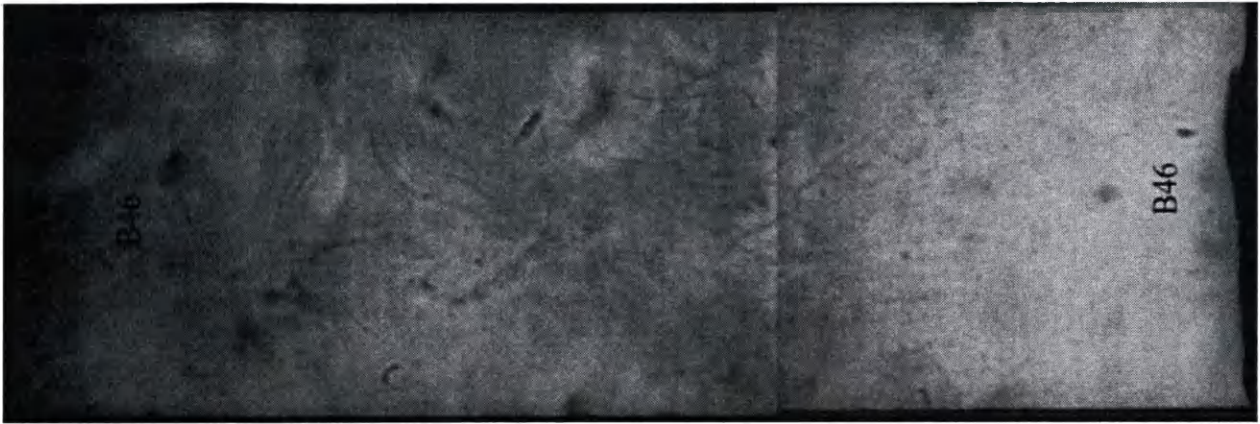
B39 ●●●●●



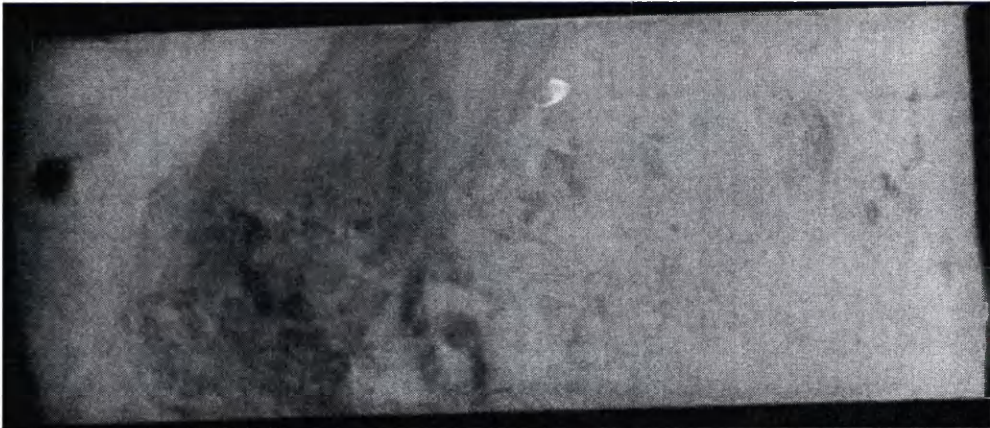
B40 ●●●●●



B41 ●●



B46



B45



B44



B42



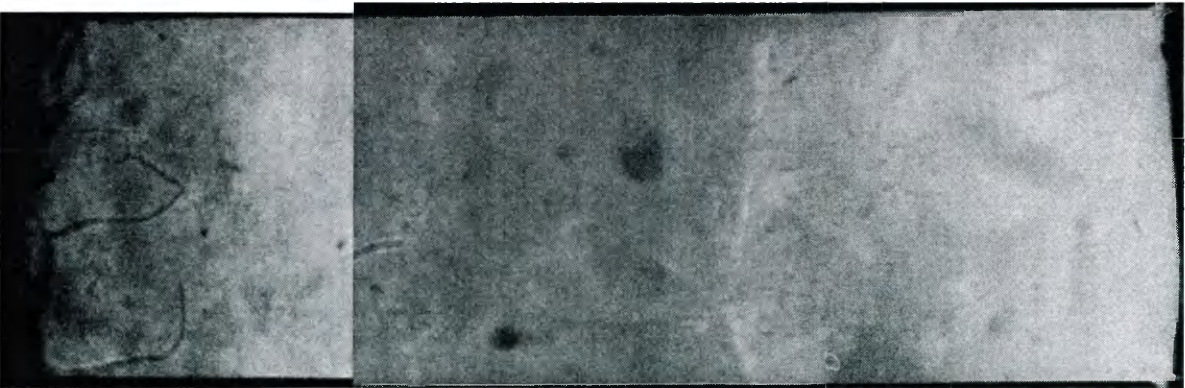
B50 ●●●●●



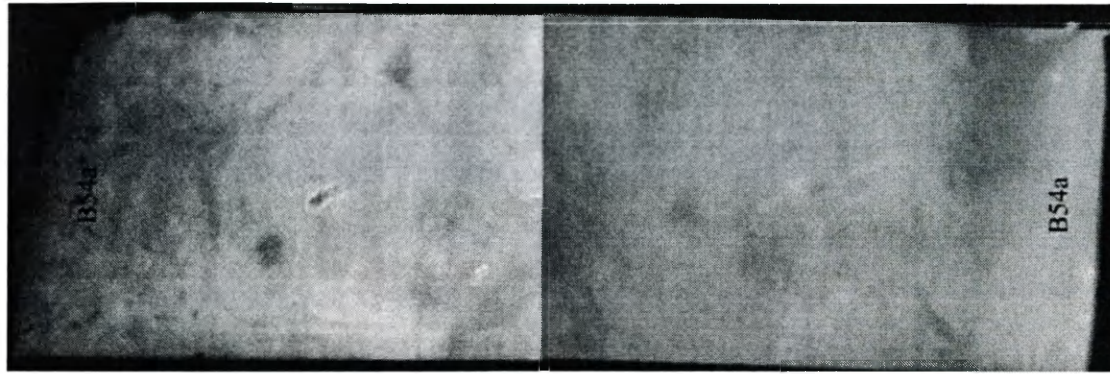
B49 ●●●



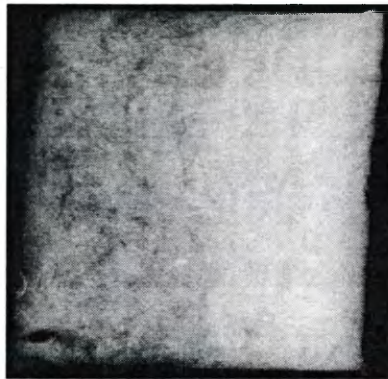
B48 ●●●



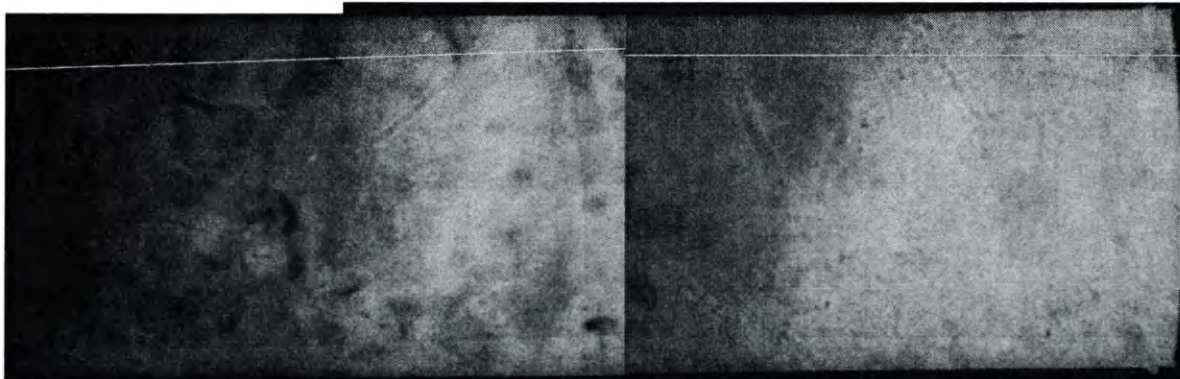
B47 ●●●●●



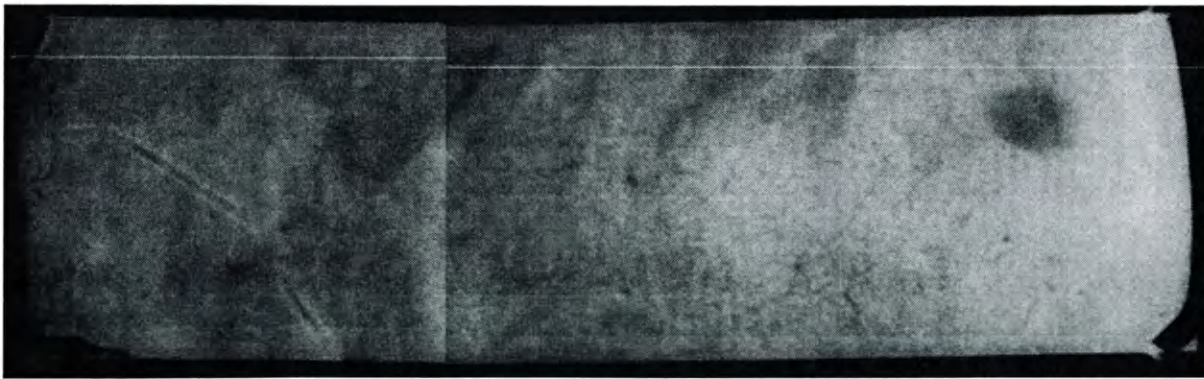
B54A ●●



B53 ●●●●



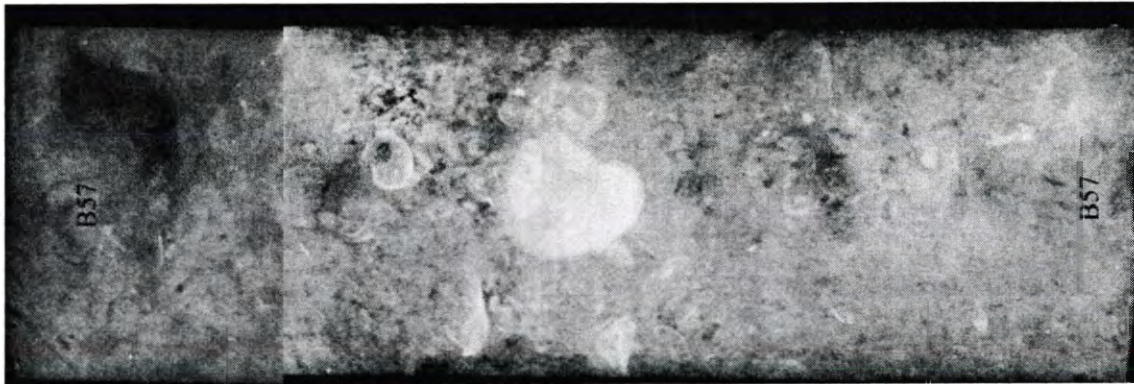
B52 ●●



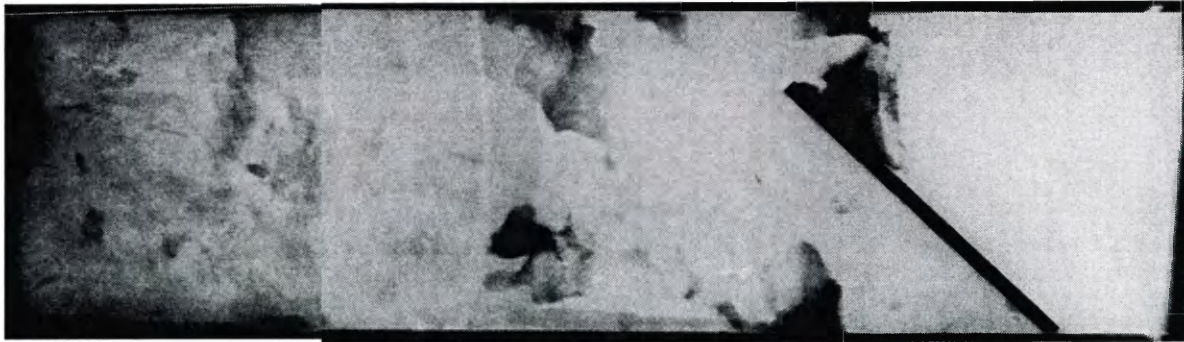
B51 ●●



B58●●●●●



B57●●●●●



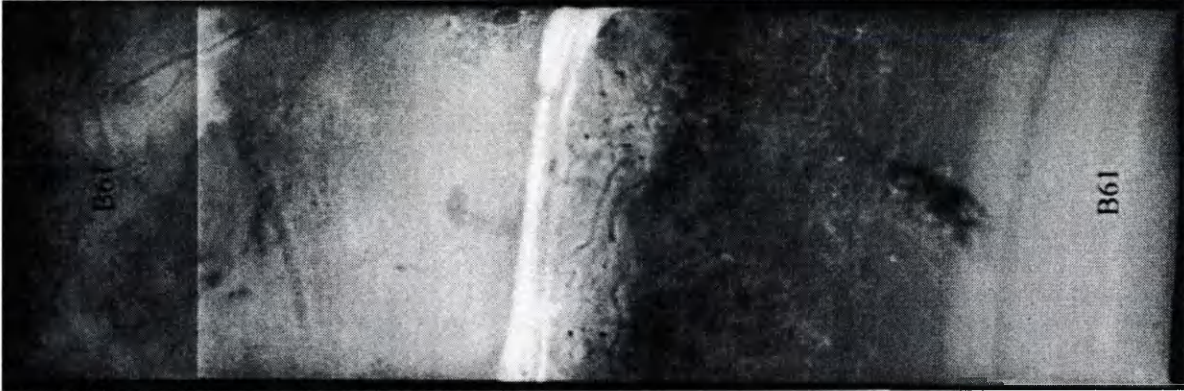
B56●●●●●



B55●●●



B62 ●●



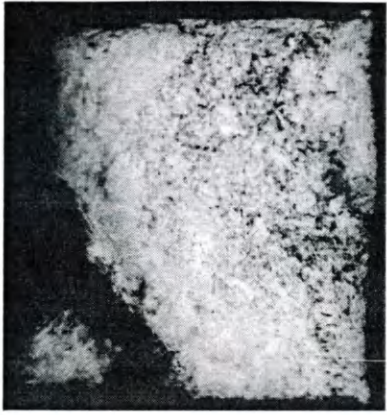
B61 ●●●



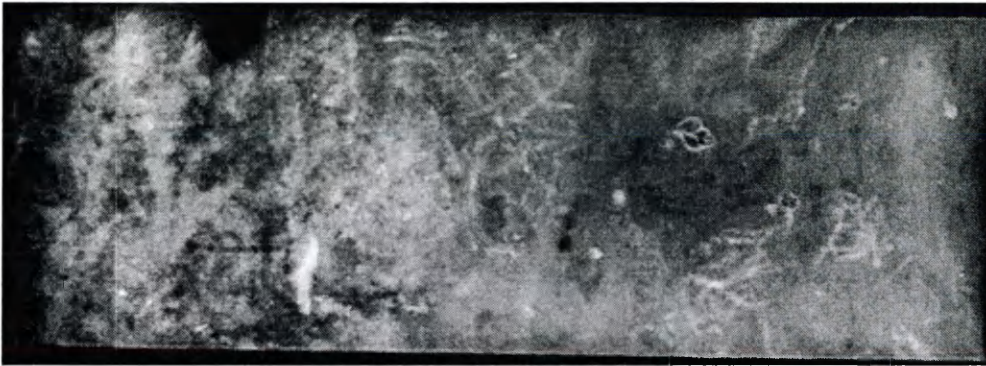
B60 ●●●●



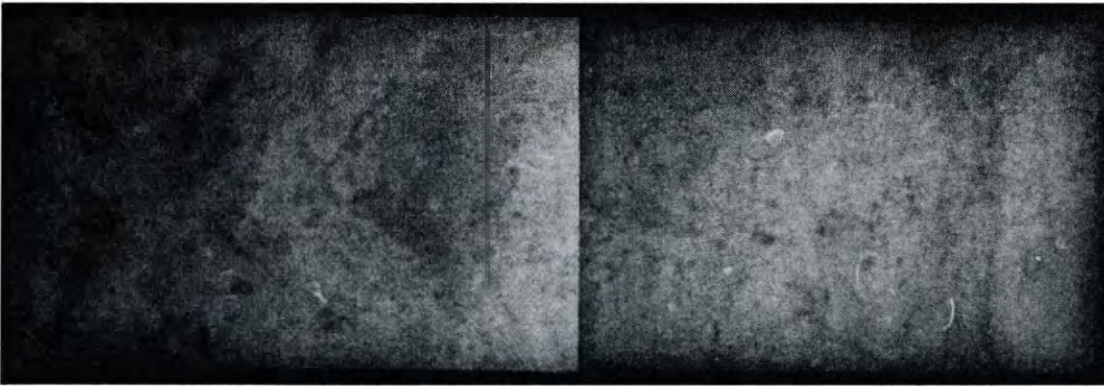
B59 ●●



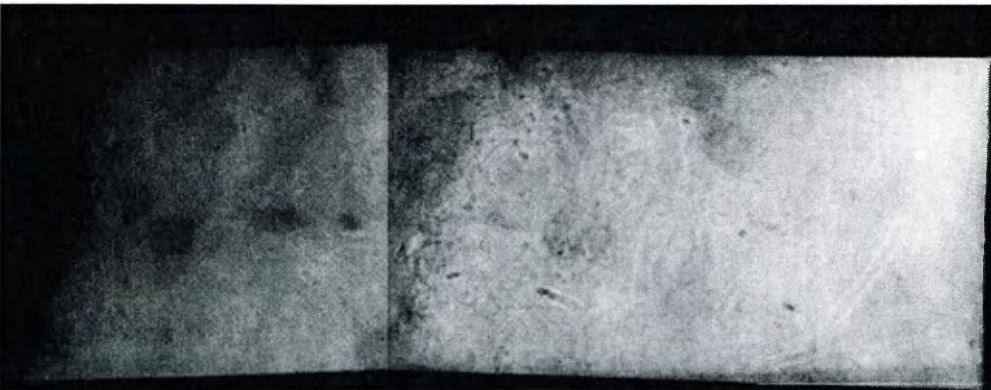
B70●●●●●



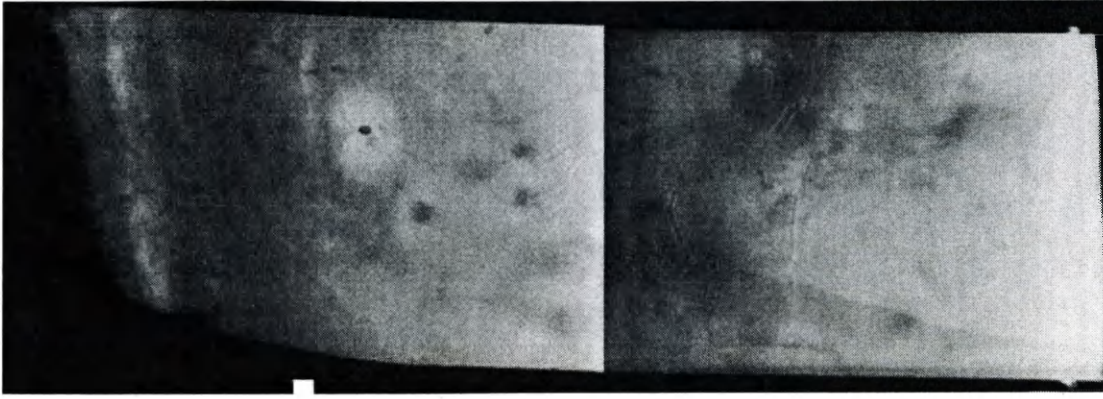
B67●●



B66●●



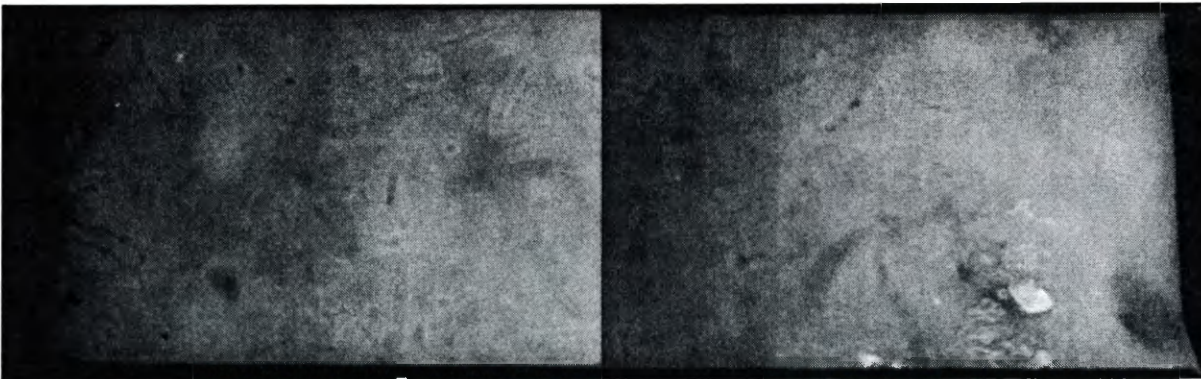
B63●●



B75 ●●●●●●



B73 ●●



B72 ●●

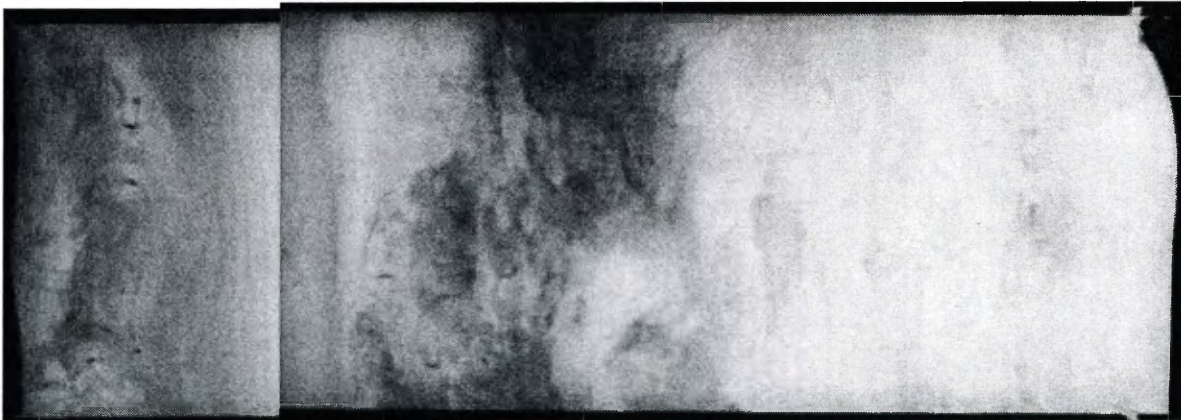


B71 ●●



B76 ••

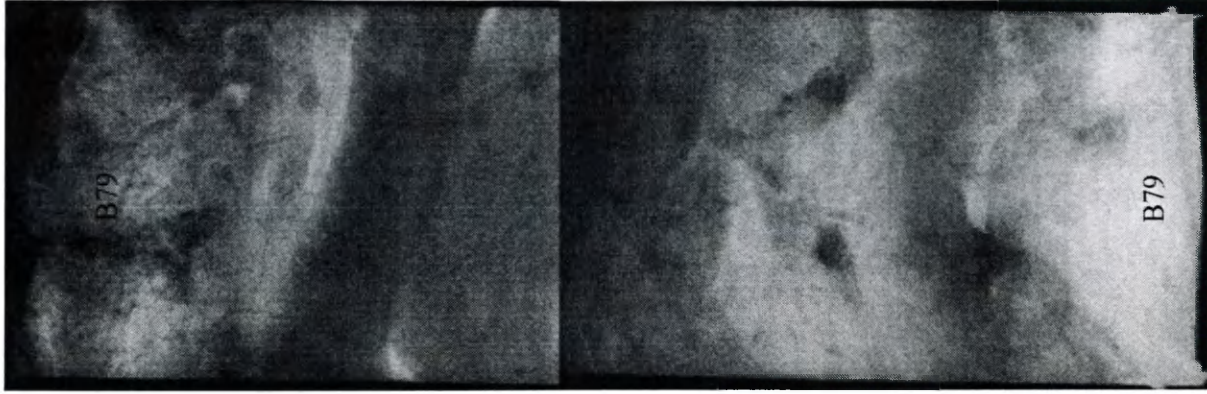
- missing bottom half of X-radiograph.



B77 ••••



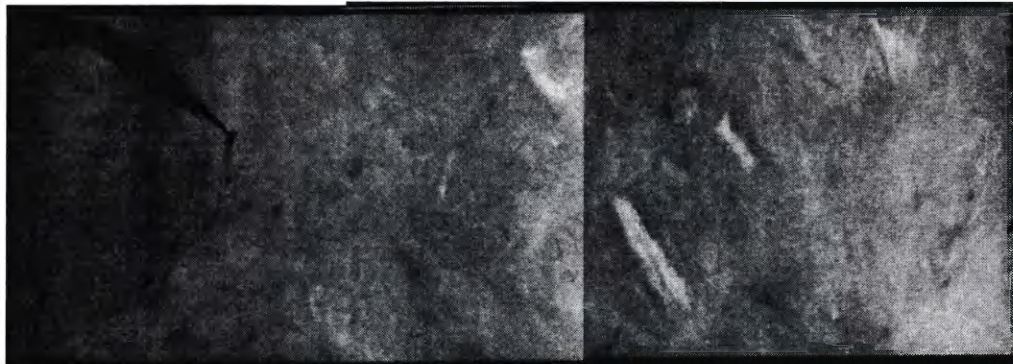
B78 ••••



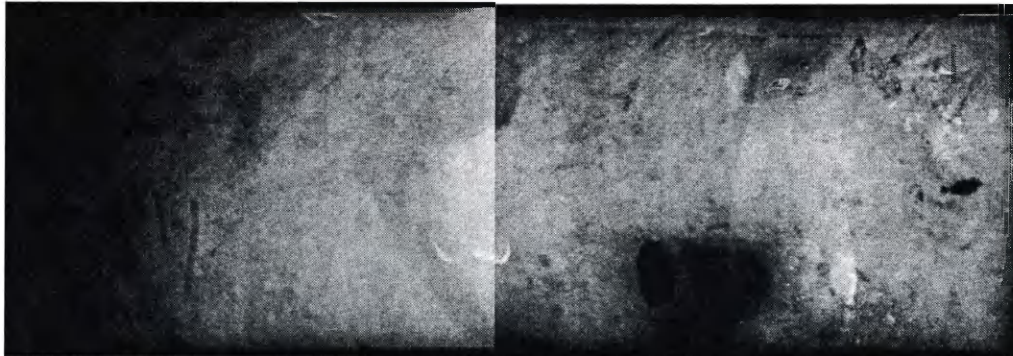
B79 ••••



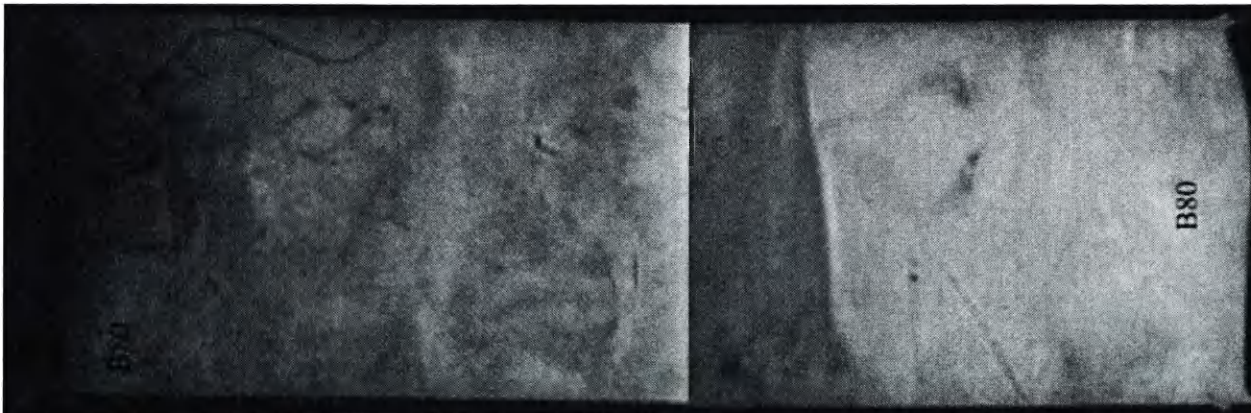
B83 ●●



B82 ●●●●●●

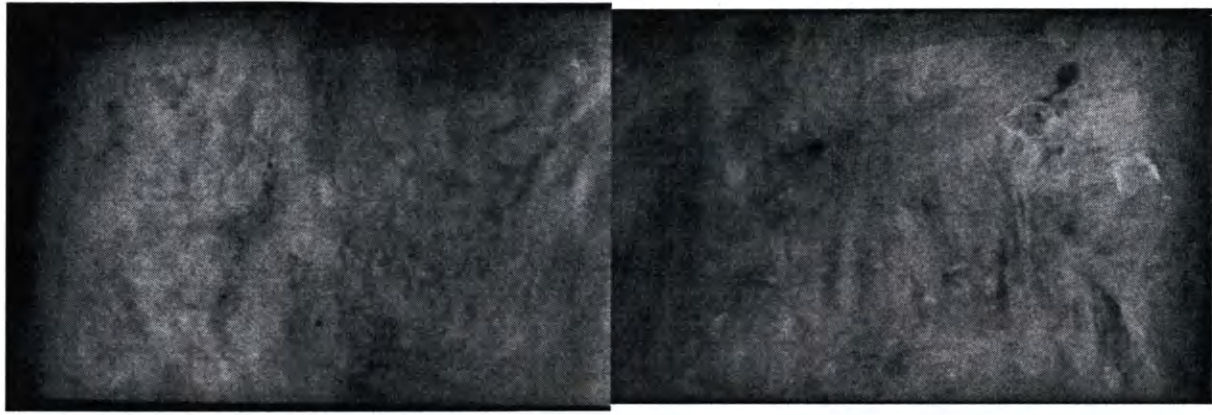


B81 ●●●●●

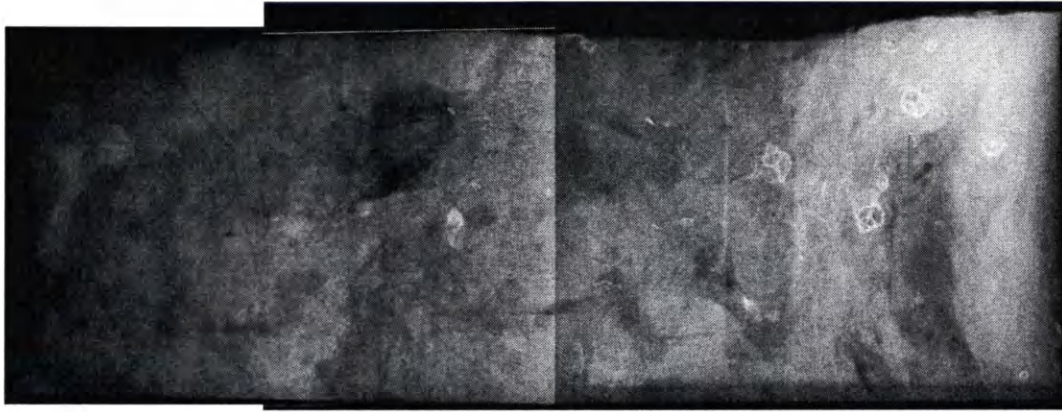


B80

B80 ●●●



B87●●



B86●●



B85●●



B84●●

APPENDIX C

Box Core ⁷Be Data

Box Core	Depth (cm)	Activity (dpm g ⁻¹)	dpm g ⁻¹ error	Dry Bulk Density (g cc ⁻¹)	Activity * BD	Inventory (dpm cm ⁻²)
1	0-1	0.074	.02	1.489	0.110	
	1-2	0.044	.03	1.514	0.067	
	2-3	0.000		1.629	0.000	0.177
2	0-1	0.000	.01	1.295	0.000	
	1-2	0.000		1.620	0.000	
	2-3	0.000		1.648	0.000	0.000
3	0-1	0.000	.02	1.442	0.000	
	1-2	0.000		1.284	0.000	
	2-3	0.000		1.436	0.000	0.000
4	0-1	0.905	.03	1.041	0.942	
	1-2	0.249	.02	1.134	0.282	
	2-3	0.000		1.167	0.000	1.225
5	0-1	0.868	.03	1.139	0.989	
	1-2	0.368	.02	1.157	0.426	
	2-3	0.331	.01	1.094	0.362	1.776
6	0-1	0.517	.03	1.344	0.695	
	1-2	0.159	.02	1.744	0.277	
	2-3	0.000		1.830	0.000	0.972
7	0-1	0.053	.01	1.292	0.068	
	1-2	0.292	.06	1.299	0.379	
	2-3	0.000		1.323	0.000	0.448
8	0-1	0.423	.02	1.032	0.436	
	1-2	0.389	.02	1.149	0.447	
	2-3	0.689	.01	1.211	0.834	
	3-4	0.883	.03	1.262	1.114	
	4-5	0.027		1.262	0.034	2.866
9	0-1	1.380	.03	0.990	1.363	
	1-2	0.274	.02	1.046	0.287	
	2-3	0.000		1.132	0.000	1.649
10	0-1	0.463	.02	1.148	0.532	
	1-2	0.020	.01	1.261	0.025	
	2-3	0.000		1.321	0.000	0.557
11	0-1	0.205	.02	1.182	0.242	
	1-2	0.000		1.189	0.000	
	2-3	0.000		1.243	0.000	0.242
12	0-1	0.450	.03	1.208	0.544	
	1-2	0.000	.02	1.291	0.000	
	2-3	0.000		1.304	0.000	0.544
13	0-1	0.522	.03	1.134	0.592	
	1-2	0.059	.01	1.211	0.071	
	2-3	0.000		1.308	0.000	0.663
14	0-1	0.099	.01	0.890	0.088	

Box Core	Depth (cm)	Activity (dpm/g)	dpm g ⁻¹ error	Dry Bulk Density (BD) (g/cc)	Activity * BD	Inventory (dpm/cm ²)
	1-2	0.000		0.955	0.000	
	2-3	0.000		1.012	0.000	0.088
15	0-1	0.000	.01	1.038	0.000	
	1-2	0.000		0.982	0.000	
	2-3	0.000		1.007	0.000	0.000
16	0-1	0.369	.02	0.858	0.316	
	1-2	0.626	.02	0.877	0.549	
	2-3	0.000		0.916	0.000	0.866
17	0-1	0.300	.02	0.946	0.284	
	1-2	0.000	.01	1.063	0.000	
	2-3	0.000		1.079	0.000	0.284
18	0-1	0.662	.02	0.770	0.510	
	1-2	0.071	.01	0.792	0.056	
	2-3	0.000		0.895	0.000	0.566
19	0-1	0.401	.02	0.850	0.341	
	1-2	0.093	.02	1.103	0.103	
	2-3	0.000		1.168	0.000	0.443
20	0-1	0.255	.02	1.065	0.272	
	1-2	0.201	.02	1.006	0.202	
	2-3	0.000		0.915	0.000	0.474
21	0-1	0.648	.02	0.949	0.615	
	1-2	0.637	.02	0.987	0.629	
	2-3	0.441	.01	1.076	0.475	1.718
22	0-1	0.489	.02	0.788	0.385	
	1-2	0.215	.01	0.848	0.182	
	2-3	0.000		0.763	0.000	0.568
23	0-1	0.933	.03	0.844	0.787	
	1-2	0.129	.02	0.745	0.096	
	2-3	0.000		0.833	0.000	0.884
24	0-1	0.476	.03	1.168	0.556	
	1-2	0.223	.02	1.199	0.267	
	2-3	0.164	.02	1.168	0.191	1.015
25	0-1	0.030	.01	1.336	0.040	
	1-2	0.000		1.403	0.000	
	2-3	0.000		1.483	0.000	0.040
26	0-1	0.274	.03	0.976	0.267	
	1-2	0.495	.02	0.963	0.477	
	2-3	0.046	.02	1.154	0.053	0.797
27	0-1	0.445	.03	0.958	0.426	
	1-2	0.241	.02	0.968	0.233	
	2-3	0.000		1.003	0.000	0.659
28	0-1	0.167	.02	0.967	0.162	
	1-2	0.000		1.023	0.000	
	2-3	0.000		0.997	0.000	0.162
29	0-1	0.521	.02	0.846	0.441	
	1-2	0.480	.02	0.878	0.422	
	2-3	0.286	.01	0.894	0.256	1.118

Box Core	Depth (cm)	Activity (dpm/g)	dpm g ⁻¹ error	Dry Bulk Density (BD) (g/cc)	Activity * BD	Inventory (dpm/cm ²)
30	0-1	0.000	.01	0.607	0.000	
	1-2	0.000		0.760	0.000	
	2-3	0.000		0.803	0.000	0.000
31	0-1	0.069	.02	1.676	0.116	
	1-2	0.000		1.719	0.000	
	2-3	0.000		1.721	0.000	0.116
32	0-1	0.650	.02	1.189	0.773	
	1-2	0.433	.02	1.286	0.557	
	2-3	0.000		1.284	0.000	1.330
33	0-1	1.670	.04	0.992	1.653	
	1-2	0.781	.03	1.092	0.852	
	2-3	0.309	.01	1.096	0.339	2.844
34	0-1	0.807	.03	1.282	1.034	
	1-2	0.367	.03	1.229	0.451	
	2-3	0.539	.01	1.260	0.679	2.164
35	0-1	0.494	.02	1.361	0.672	
	1-2	0.025	.01	1.394	0.035	
	2-3	0.000		1.280	0.000	0.707
36	0-1	0.092	.02	1.027	0.094	
	1-2	0.000		1.027	0.000	
	2-3	0.000		1.027	0.000	0.094
37	0-1	0.265	.02	1.504	0.399	
	1-2	0.000		1.521	0.000	
	2-3	0.000		1.536	0.000	0.399
39	0-1	0.187	.02	1.027	0.192	
	1-2	0.000		1.027	0.000	
	2-3	0.000		1.027	0.000	0.192
40	0-1	0.665	.04	1.245	0.828	
	1-2	0.019	.03	1.282	0.024	
	2-3	0.000		1.323	0.000	0.852
41	0-1	0.269	.02	0.807	0.217	
	1-2	0.000		0.872	0.000	
	2-3	0.000		0.879	0.000	0.217
44	0-1	0.533	.03	0.962	0.513	
	1-2	0.331	.02	0.984	0.326	
	2-3	0.000		1.089	0.000	0.839
45	0-1	0.557	.04	1.348	0.751	
	1-2	0.311	.04	1.386	0.431	
	2-3	0.000		1.473	0.000	1.182
46	0-1	0.425	.02	0.911	0.387	
	1-2	0.000		0.902	0.000	
	2-3	0.000		0.938	0.000	0.387
47	0-1	1.720	.03	0.888	1.529	
	1-2	0.801	.02	0.958	0.768	
	2-3	0.000		0.963	0.000	2.296
48	0-1	0.000	.02	1.027	0.000	
	1-2	0.000		1.027	0.000	

Box Core	Depth (cm)	Activity (dpm/g)	dpm g ⁻¹ error	Dry Bulk Density (BD) (g/cc)	Activity * BD	Inventory (dpm/cm ²)
	2-3	0.000		1.027	0.000	0.000
49	0-1	0.115	.02	1.027	0.118	
	1-2	0.000		1.027	0.000	
	2-3	0.000		1.027	0.000	0.118
50	0-1	0.045	.02	1.027	0.046	
	1-2	0.000		1.027	0.000	
	2-3	0.000		1.027	0.000	0.046
51	0-1	0.812	.02	0.962	0.781	
	1-2	1.490	.03	0.967	1.436	
	2-3	0.390	.02	1.026	0.400	2.617
52	0-1	0.779	.04	0.811	0.632	
	1-2	0.649	.01	0.868	0.563	
	2-3	0.110		0.950	0.104	1.299
53	0-1	0.142	.02	1.380	0.196	
	1-2	0.119	.01	1.268	0.151	
	2-3	0.000		1.253	0.000	0.347
54A	0-1	0.141	.02	0.618	0.087	
	1-2	0.000		0.759	0.000	
	2-3	0.000		0.814	0.000	0.087
54B	0-1	0.231	.02	1.192	0.275	
	1-2	0.097	.01	1.212	0.118	
	2-3	0.570	.03	1.215	0.692	
	3-4	0.378	.02	1.225	0.462	1.548
55	0-1	1.270	.03	1.394	1.770	
	1-2	0.087	.02	1.344	0.117	
	2-3	0.000		1.420	0.000	1.886
56	0-1	0.277	.02	1.159	0.321	
	1-2	0.501	.02	1.162	0.582	
	2-3	0.000		1.326	0.000	
	3-4	0.154	.02	1.344	0.207	1.110
57	0-1	0.863	.03	1.063	0.917	
	1-2	0.555	.02	1.247	0.692	
	2-3	0.134	.02	1.335	0.179	1.788
58	0-1	0.000	.02	1.027	0.000	
	1-2	0.000		1.027	0.000	
	2-3	0.000		1.027	0.000	0.000
59	0-1	0.345	.02	0.736	0.254	
	1-2	0.000		0.733	0.000	
	2-3	0.000		0.831	0.000	0.254
60	0-1	2.710	.03	0.871	2.357	
	1-2	0.385	.02	0.819	0.315	
	2-3	0.000		0.824	0.000	2.672
61	0-1	0.961	.04	0.805	0.774	
	1-2	0.249	.01	0.962	0.240	
	2-3	0.000		0.988	0.000	1.013
62	0-1	0.149	.02	1.027	0.153	
	1-2	0.000		1.027	0.000	

Box Core	Depth (cm)	Activity (dpm/g)	dpm g ⁻¹ error	Dry Bulk Density (BD) (g/cc)	Activity * BD	Inventory (dpm/cm ²)
	2-3	0.000		1.027	0.000	0.153
63	0-1	0.730	.02	0.843	0.616	
	1-2	0.796	.03	0.957	0.762	
	2-3	0.267	.01	0.981	0.262	1.640
66	0-1	1.310	.03	1.169	1.535	
	1-2	0.269	.02	1.235	0.332	
	2-3	0.000		1.325	0.000	1.867
67	0-1	0.281	.02	1.066	0.300	
	1-2	0.000		1.128	0.000	
	2-3	0.000		1.256	0.000	0.300
69	0-1	0.025	.01	1.355	0.034	
	1-2	0.000		1.523	0.000	
	2-3	0.000		1.607	0.000	0.034
70	0-1	0.413	.03	1.027	0.424	
	1-2	0.215	.02	1.027	0.221	
	2-3	0.151	.01	1.027	0.155	0.800
71	0-1	1.770	.03	0.834	1.471	
	1-2	0.401	.01	0.842	0.338	
	2-3	0.000		0.867	0.000	1.809
72	0-1	0.562	.03	0.801	0.450	
	1-2	0.000	.03	0.912	0.000	
	2-3	0.000		0.899	0.000	0.450
73	0-1	0.030	.01	0.921	0.028	
	1-2	0.000		0.916	0.000	
	2-3	0.000		0.988	0.000	0.028
74	0-1	0.011	.01	2.031	0.022	
	1-2	0.000		2.043	0.000	
	2-3	0.000		1.849	0.000	0.022
75	0-1	1.150	.04	0.664	0.763	
	1-2	0.683	.02	0.689	0.471	
	2-3	0.000		0.809	0.000	1.234
76	0-1	0.807	.02	0.575	0.464	
	1-2	0.089	.01	0.688	0.061	
	2-3	0.000		0.796	0.000	0.525
77	0-1	0.721	.03	1.027	0.740	
	1-2	0.483	.02	1.027	0.496	
	2-3	0.598	.02	1.027	0.614	
	3-4	0.778	.02	1.027	0.799	
	4-5	0.639		1.027	0.656	3.306
78	0-1	0.324	.03	0.805	0.261	
	1-2	0.151	.02	1.048	0.158	
	2-3	0.000		1.126	0.000	0.419
79	0-1	0.484	.02	0.818	0.396	
	1-2	0.016	.01	0.898	0.014	
	2-3	0.000		0.941	0.000	0.410
80	0-1	0.937	.02	0.956	0.896	
	1-2	0.245	.02	0.959	0.235	

Box Core	Depth (cm)	Activity (dpm/g)	dpm g ⁻¹ error	Dry Bulk Density (BD) (g/cc)	Activity * BD	Inventory (dpm/cm ²)
81	2-3	0.000		1.014	0.000	1.130
	0-1	0.055	.02	1.062	0.058	
	1-2	0.000		1.121	0.000	
82	2-3	0.000		1.234	0.000	0.058
	0-1	0.765	.02	0.686	0.525	
	1-2	0.246	.01	0.771	0.190	
83	2-3	0.000		0.767	0.000	0.714
	0-1	1.280	.03	1.099	1.402	
	1-2	0.261	.03	1.123	0.293	
84	2-3	0.000		1.120	0.000	1.695
	0-1	0.879	.02	0.872	0.766	
	1-2	0.653	.02	0.824	0.538	
	2-3	0.733	.02	0.898	0.658	
85	3-4	0.778	.01	0.887	0.689	2.652
	0-1	1.080	.04	1.148	1.242	
	1-2	0.546	.02	1.148	0.627	
	2-3	0.660	.02	1.178	0.778	
86	3-4	0.194	.01	1.220	0.237	2.884
	0-1	0.984	.03	1.008	0.992	
	1-2	0.739	.03	1.081	0.799	
	2-3	0.384	.02	1.048	0.403	
87	0-1	0.509	.03	1.325	0.674	2.193
	1-2	0.089	.02	1.340	0.119	
	2-3	0.000		1.344	0.000	

VITA

Lila Eve Rose

Born in Portchester, New York on February 23, 1981 in a snowstorm. Attended Pennington-Grimes Elementary School in Mt. Vernon, N.Y., where she grew up. Was a Daisy, a Brownie and a Cadet in Girl Scouts. Graduated from Pelham Memorial High School in 1999. Received a B.A. in Geology and English Language and Literature from Smith College in 2003. Her Highest Honors thesis was entitled “Stress Bands in Belizean Patch Reef Corals: Their Use as Paleoclimate Indicators.” She entered the M.S. program at VIMS in 2004 and has traveled to New Zealand several times for research cruises and conferences.